HELLENIC REPUBLIC

UNIVERSITY OF IOANNINA

POLYTECHNIC SCHOOL

DEPARTMENT OF MATERIALS SCIENCE AND ENGINEERING

MASTER STUDY PROGRAMM

"Master of Science (MSc) in Technologies of Advanced Materials"

MASTER THESIS

Georvasili Stefanie

TITLE OF MASTER THESIS

"Computational modeling using finite elements of the thigh bone during gait"

IOANNINA, 2020

ΕΛΛΗΝΙΚΗ ΔΗΜΟΚΡΑΤΙΑ

ΠΑΝΕΠΙΣΤΗΜΙΟ ΙΩΑΝΝΙΝΩΝ

ΠΟΛΥΤΕΧΝΙΚΗ ΣΧΟΛΗ

ΤΜΗΜΑ ΜΗΧΑΝΙΚΩΝ ΕΠΙΣΤΗΜΗΣ ΥΛΙΚΩΝ

ΠΡΟΓΡΑΜΜΑ ΜΕΤΑΠΤΥΧΙΑΚΩΝ ΣΠΟΥΔΩΝ

«ΠΡΟΗΓΜΕΝΑ ΥΛΙΚΑ»

ΜΕΤΑΠΤΥΧΙΑΚΗ ΔΙΑΤΡΙΒΗ

Γεωρβασίλη Στεφανία

ΤΙΤΛΟΣ ΜΕΤΑΠΤΥΧΙΑΚΗΣ ΔΙΑΤΡΙΒΗΣ

"Μοντελοποίηση με πεπερασμένα στοιχεία της συμπεριφοράς μηριαίου οστού κατά τη διάρκεια βάδισης "

ΙΩΑΝΝΙΝΑ, 2020

Η παρούσα Μεταπτυχιακή Διατριβή εκπονήθηκε στο πλαίσιο των σπουδών για την απόκτηση του Μεταπτυχιακού Διπλώματος Ειδίκευσης στην εξειδίκευση:

Μοντελοποίηση με πεπερασμένα στοιχεία της συμπεριφοράς μηριαίου οστού κατά τη διάρκεια βάδισης

που απονέμει το Τμήμα Μηχανικών Επιστήμης Υλικών του Πανεπιστημίου Ιωαννίνων.

Εγκρίθηκε την 30/10/2020 από την εξεταστική επιτροπή:

ΟΝΟΜΑΤΕΠΩΝΥΜΟ   **ΒΑΘΜΙΔΑ**

1. Δημήτριος Φωτιάδης, Καθηγητής του ΤΜΕΥ της Πολυτεχνικής Σχολής του Παν/μίου Ιωαννίνων, **Επιβλέπων**

2. Λεωνίδας Γεργίδης, Αναπληρωτής καθηγητής του ΤΜΕΥ της Πολυτεχνικής Σχολής του Παν/μίου Ιωαννίνων

3. Αιμίλιος Πάκος, Επίκουρος καθηγητής του τμήματος Ιατρικής της Ιατρικής Σχολής του Παν/μίου Ιωαννίνων

ΥΠΕΥΘΥΝΗ ΔΗΛΩΣΗ

"Δηλώνω υπεύθυνα ότι η παρούσα διατριβή εκπονήθηκε κάτω από τους διεθνείς ηθικούς και ακαδημαϊκούς κανόνες δεοντολογίας και προστασίας της πνευματικής ιδιοκτησίας. Σύμφωνα με τους κανόνες αυτούς, δεν έχω προβεί σε ιδιοποίηση ξένου επιστημονικού έργου και έχω πλήρως αναφέρει τις πηγές που χρησιμοποίησα στην εργασία αυτή."

(Υπογραφή υποψηφίου)

Acknowledgements

First of all, I would like to thank my family, who all these years support my dreams and my effort. My parents deserve special thanks for their unlimited support and encouraging. I would also like to thank my sister and brother who is next to me and helped me in every step in my life.

I would like to cordially thank my supervisor Prof. Dimitrios I. Fotiadis, Dept. of Materials Science and Engineering, University of Ioannina for his trust, his support and great assistance in order to complete this thesis.

 I would also like to thank Prof. Pakos Emilios, Dept. of Medical, University of Ioannina, Dr Gkiatas Ioannis, Dept. of Medical, University of Ioannina, for the collaboration and support.

What is more, I would like to sincerely thank   Dr Potsika Vasiliki , Dept. of Materials Science and Engineering, University of Ioannina , for inspiration, guidance and continuous support. I had an excellent collaboration with her and provided me with data and knowledge to accomplish this work.

In addition, I would like to refer to the support of Dimitrios Dimopoulos, Dept. of Medical, University of Ioannina in the gait cycle part that I needed his help.

Furthermore, I would like to thank Grigori Kwtoula for the excellent cooperation, friendship and support in demanding working conditions. Whenever I needed him he was in a good mood to help me.

Summary

Total hip arthroplasty is a common surgical procedure to replace the femoral head. It has been successfully applied around the world since the mid-1950s.

In the present study, a patient's total hip arthroplasty implant is examined. The integration of the endoprosthesis in the femur has been simulated in the Ansys computer program, which uses the finite element method.

Technological development in the field of computers provides the appropriate tools for the analysis and prediction of the effect of prosthetic bones from an industrial point of view. The study focuses on the application of time-varying loads. The analysis is done with the finite element method and the results concern the development of trends and deformations of Von Mises from the imposed loads in different daily activities.

Chapter 1 analyzes the physiology of the femur as well as its internal structure, to better understand the distribution of tendons within the bone and the function of the hip in general.

Chapter 2 deals with total hip arthroplasty, its development and the diseases that lead to it, but also the risks that lurk. There are also different types of implants, in terms of the materials used and the way they are fixed, with or without the use of cement.

Chapter 3 analyzes the strengths and strains of the femur in daily activities. There is also a brief reference to the definition of voltage, deformation and Hooke's law, the Von Mises criterion is also presented. Finally, the gait cycle and the "stress shielding" phenomenon observed after the operation are described, where the implant receives the loads during gait, preventing the proper development of the bone.

Chapter 4 introduces the concept of biomechanics and the theory of finite elements. In addition, a detailed report is made on bone biomechanics.

Chapter 5 refers to the state of the art, a level of development reached at any particular time as a result of the common methodologies employed at the time.

Chapter 6 includes the methodology followed within the ANSYS computer program to achieve the measurements. The materials used for the three-dimensional geometries are also presented. Then the processing and creation of the appropriate grid for the performance of results is analyzed as realistically as possible. Then the boundary conditions are determined, ie the drop points and the application points of the force.

Chapter 7 και 8 presents and compares the relevant results obtained from the simulation of femoral ligaments through the ANSYS Workbench software. These results relate to the maximum Von Mises trends but also the deformations that develop in the implant and the bone and strain. Thus, the overall conclusions of the analysis are extracted and suggestions are made for further study of the system.

In conclusion, the results of the numerical solution of the load give satisfactory answers to the activities that cause possible material failure, as the areas of the implant and bone where the maximum stresses and deformations occur under load-changing conditions are identified in different daily activities.

Περίληψη

Η ολική αρθροπλαστική ισχίου είναι μια κοινή χειρουργική διαδικασία για την αντικατάσταση της μηριαίας κεφαλής. Εφαρμόστηκε με επιτυχία σε όλο τον κόσμο από τα μέσα της δεκαετίας του 1950.

Στην παρούσα διατριβή, εξετάζεται ένα εμφύτευμα ολικής αρθροπλαστικής ισχίου ασθενούς. Η ενσωμάτωση της ενδοπρόθεσης στο μηρό έχει προσομοιωθεί στο πρόγραμμα υπολογιστών Ansys, το οποίο χρησιμοποιεί τη μέθοδο των πεπερασμένων στοιχείων.

 Η τεχνολογική ανάπτυξη στον τομέα των υπολογιστών παρέχει τα κατάλληλα εργαλεία για την ανάλυση και την πρόβλεψη της επίδρασης των προσθετικών οστών από βιομηχανική άποψη. Η μελέτη επικεντρώνεται στην εφαρμογή μεταβαλλόμενων με το χρόνο φορτίων . Η ανάλυση γίνεται με τη μέθοδο των πεπερασμένων στοιχείων και τα αποτελέσματα αφορούν την ανάπτυξη τάσεων και παραμορφώσεων Von Mises από τα επιβληθέντα φορτία σε διαφορετικές καθημερινές δραστηριότητες.

Το Κεφάλαιο 1 αναλύει τη φυσιολογία του μηρού καθώς και την εσωτερική δομή του, για να κατανοήσει καλύτερα την κατανομή των τενόντων μέσα στα οστά και τη λειτουργία του ισχίου γενικά.

Το Κεφάλαιο 2 ασχολείται με την ολική αρθροπλαστική του ισχίου, την ανάπτυξή του και τις ασθένειες που την οδηγούν, αλλά και τους κινδύνους που κρύβονται. Υπάρχουν επίσης διαφορετικοί τύποι εμφυτευμάτων, όσον αφορά τα υλικά που χρησιμοποιούνται και τον τρόπο στερέωσής τους, με ή χωρίς τη χρήση τσιμέντου.

Το κεφάλαιο 3 αναλύει τις δυνάμεις και τα στελέχη του μηριαίου οστού στις καθημερινές δραστηριότητες Υπάρχει επίσης μια σύντομη αναφορά στον ορισμό της τάσης, της παραμόρφωσης και του νόμου του Hooke, παρουσιάζεται επίσης το κριτήριο του Von Mises. Τέλος, περιγράφεται ο κύκλος βάδισης και το φαινόμενο "θωράκιση από το στρες" που παρατηρούνται μετά τη χειρουργική επέμβαση, όπου το εμφύτευμα δέχεται τα φορτία κατά τη διάρκεια του βηματισμού, εμποδίζοντας την ορθή ανάπτυξη του οστού.

Το Κεφάλαιο 4 εισάγει την έννοια της βιομηχανικής και τη θεωρία των πεπερασμένων στοιχείων. Επιπλέον, γίνεται λεπτομερής αναφορά για τη βιομηχανική των οστών.

Το Κεφάλαιο 5 αναφέρεται στην κατάσταση της τέχνης, ένα επίπεδο ανάπτυξης που επιτυγχάνεται ανά πάσα στιγμή ως αποτέλεσμα των κοινών μεθοδολογιών που εφαρμόστηκαν τότε.

Το Κεφάλαιο 6 περιλαμβάνει τη μεθοδολογία που ακολουθείται στο πρόγραμμα υπολογιστή ANSYS για την επίτευξη των μετρήσεων. Παρουσιάζονται επίσης τα υλικά που χρησιμοποιούνται για τις τρισδιάστατες γεωμετρίες. Στη συνέχεια, η επεξεργασία και η δημιουργία του κατάλληλου πλέγματος για την απόδοση των αποτελεσμάτων αναλύεται όσο το δυνατόν πιο ρεαλιστικά. Στη συνέχεια καθορίζονται οι οριακές συνθήκες, δηλαδή τα σημεία πτώσης και τα σημεία εφαρμογής της δύναμης.

Το Κεφάλαιο 7 και 8 παρουσιάζει και συγκρίνει τα σχετικά αποτελέσματα που προκύπτουν από την προσομοίωση των μηριαίων συνδέσμων μέσω του λογισμικού ANSYS Workbench. Αυτά τα αποτελέσματα σχετίζονται με τις μέγιστες τάσεις Von Mises αλλά και με τις παραμορφώσεις που αναπτύσσονται στο εμφύτευμα και στα οστά και στο στέλεχος. Έτσι, εξάγονται τα συνολικά συμπεράσματα της ανάλυσης και γίνονται προτάσεις για περαιτέρω μελέτη του συστήματος.

Συμπερασματικά, τα αποτελέσματα της αριθμητικής λύσης του φορτίου δίνουν ικανοποιητικές απαντήσεις για τις δραστηριότητες που προκαλούν πιθανή αστοχία των υλικών, καθώς οι περιοχές του εμφυτεύματος και του οστού όπου εμφανίζονται οι μέγιστες τάσεις και παραμορφώσεις σε συνθήκες μεταβαλλόμενου με το χρόνο φορτίου αναφοράς προσδιορίζονται σε διαφορετικές καθημερινές δραστηριότητες.

Table of Contents

List of figures

List of tables

Introduction

The importance of implants in the science of medicine is enormous. Implants are artificial devices that in many cases, not only help better function, or support natural tissues, but also completely replace them. A number of applications can be enumerated in almost all tissues of which the human body is composed and in which implant additions are found.

Total hip arthroplasty is a surgical procedure that is required in patients with a damaged hip joint. The upper part of the femur, the head, which is damaged, is initially removed, based on previous calculations. Then with special rasps it is created by the tunnel surgeon to place the first part of the endoprosthesis, the sterile. If lesions appear in the pelvis, i.e. in the acetabular, then the damaged bone is removed with special rasps.

  The reasons that can lead to partial or total destruction of this joint are many. The hip joint, detailed in Chapter 1, includes the femoral head, which moves inside the pelvic acetabular. Both the femoral head and the acetabular are covered at the points that touch the cartilage layer. The cartilage does not contain nerves or blood vessels and is used on the one hand as a layer to absorb the vibrations of the joint and on the other hand, due to its smooth surface, as a material for smoothing the coefficient of friction between the two surfaces. Surgery is mainly aimed at restoring most patients' movements, who can now enjoy painless activities. The success of the operation depends to a large extent on the appropriate choice of implant. Its shape and construction material should facilitate greater range of motion and no pain.

1 Physiology of hip and femur

Hip joint is one of the most important joints for body weight transfer and gait activities. It is also one of the strongest load-bearing joints, as it supports the body in an upright position and helps to rotate and bend the foot. It is the main link between the lower bones with the pelvis and skeleton. It is a triaxial hinge and thus allows movements at all levels, but extremely stable and therefore difficult to dislocate.

1.1 Long Bone Structure and Function

The bones make up the skeleton providing support to the body, protecting the interior organs and the ability to move through the traction of muscles, joints and tendons. Bones also play a key role in the body's metabolism by participating in calcium homeostasis. The human skeleton is made up of more than 200 bones which can be classified according to their shape and size, short, flat and sesamoid (irregular). Long bones are mainly characterized by large limb bones, femur, tibia, arm, buttock, ulna, but also smaller bones, such as metacarpals and phalanxes. The geometry of the long bones is described by the tubular shaft called diaphysis, medullar canal, upper and lower limbs (epiphyses) and the intermediate regions of transcription that associate diaphysis with epiphyses (Figure 1.1).

1.1.1 Macroscopic Recommendation

Long bones consist of the periosteum, bone tissue, bone marrow, vessels and nerves. The periosteum is a thin film located on the outer surface of the bone and consists of two layers, the outer or fibroelastic and the inner or osteogenic. The outer layer contains vessels and nerves and serves to attract muscle and tendons, while the inner one contains osteoblastic cells, the osteoblasts (Ε.Δ.Κατρίτση,et al., 1954).

Bone tissue is architecturally distinguished in two forms, the cortical and compact bone, and cancellous and trabecular bone bone. The diaphysis consists of cortical bone, while inside it surface (subdural area) spongy bone is found, the epiphysis consist of spongy bone and the metaphysis regions include both forms of bone tissue. 80% of long bones comprise cortical bone, although the percentage this varies considerably between the long bones.
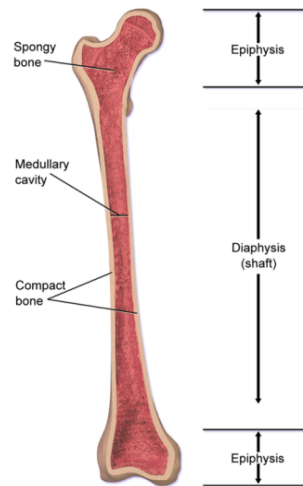
Figure 1-1: Geometrical characteristics of long bone.

The cortical bone is composed of lamellae systems that form its horseshoe structure (Figure 1.2). They are distinguished in (a) outside or peripherally and in or perianal pedals (circumferential lamellae or lamellar bone) forming continuous layers of thickness 150 - 300 µm tangential to the respective peristalsis and endos surfaces, and (b) in Harvesian systems or osteons (Figure 1.3). The osteons form the bulk of the cortical bone forming cylinders along the longitudinal axis of bone extended by the Harvesian canals (Whedon,et. al., 2017).
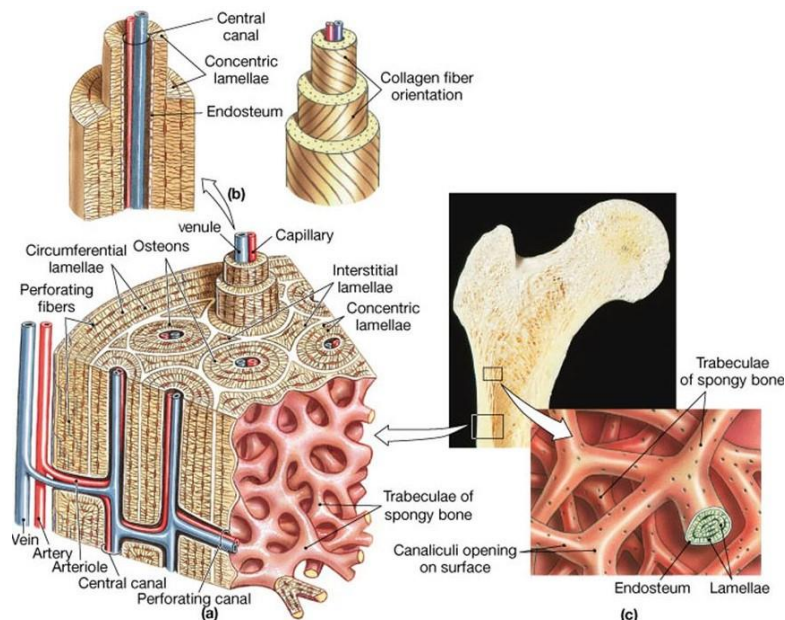
Figure 1-2: Cortical and trabecular bone structure.

The shape of the osteons is circular or ellipsoid with diameter of 100 - 300 µm and length of about 10 mm, in which they are wound about 3 - 8 petals of 3 - 7 µm thick

each. The Harvesian canals have an average diameter of 50 - 100 µm that extend toward the medullar lumen and contain vessels and nerves. Tubes (canaliculi) pass through each osteon which contains small cavities (lacunae). The Volkmann (Volkmann canals) tubes are oblique or transverse to the Harvesian canals, which are also angiophores, but differ in that their walls are not concentric but irregularly, and their role is to anesthetize the intestinal tubes. The thin layer between neighboring osteons is called the cement line and the gap between the osteons is supplemented by interstitial lamellae which come from osteons residues. The rows of gaps (pores) inserted by Harvesian canals, Volkmann tubes (diameter 20 µm) and tubes and cavities (diameter 0.2 µm) determine the intracortical porosity.

The structure of trabecular bone is described as a network of small, interconnected rods (50 - 300 µm in diameter) called trabeculae, with long distance between successive units. The trabeculae consist of pedals (Fig. 1.2) and may contain few in number small canals (canaliculi) and cavities (lacunae), just as in solid bone. The porosity of trabecular bone is mainly determined by the gaps between beams and varies according to anatomical position and type of bone from 50% - 95%. Due to the contiguous and indistinguishable presence of one or the other form of bone tissue, solid bone is defined as this with a porosity of less than 30%. Bone vessels start from the periosteum, mainly feeding on the outer layers and from the carotid artery that enters the bone mass from the trunk and branching into an ascending and descending branch (Figure 1.2). The nerves are located in the periosteum and accompany the carotid artery inside it bone.

1.1.2   Microscopic Recommendation

Bone tissue comprises 35% of the organic portion and 65% of the inorganic portion. The organic portion comprises the cells (2%) and the organic matrix (98%). (Ε.Δ.Κατρίτση,et. al,1954). Cells of bone tissue are:

Osteoblasts: Osteoblasts are derived from mesenchymal cells and are osteoblastic cells that produce the organic matrix. Osteoblasts are created in the periosteum and bone marrow layer.

Osteoclasts: Osteoclasts are derived from precursors of bone marrow. Osteoclasts have as their primary function bone degradation.

Osteocytes: Osteocytes are mature cells derived from osteoblasts enclosed by osteoblastic bone matrix. They are in the bone cavities (lacunae) and communicate with each other through the canaliculi. These cells are active elements of bone and are involved in bone deconstruction and remodeling.

The main constituent of the organic matrix is type I collagen (90%) and is produced most of it by osteoblasts. The collagen molecules self-organize into fibrils, 300 nm in length and 1.23 nm in diameter (Figure 1 .3). Their tertiary structure is characterized by a periodicity of 67 nm and gaps of 40 nm between the ends of the molecules. The collagen fibers are mainly located in the osteons and arranged parallel to each other. Their tertiary structure is characterized by a periodicity of 67 nm and gaps of 40 nm

between the ends of the molecules. The collagen fibers are mainly located in the osteons and arranged parallel to each other. Their directionality varies from pedal to pedal of the same osteon following a helical shape (Figures 1.2 and 1.3). Therefore, in each pedal the fiber direction can be longitude nal (i.e. 12 parallel to the long axis of the osteon), transverse (perpendicular to the axis) or oblique (forming an angle with the axis). The remaining 10% of the foundation consists of a small percentage of type V collagen and also a small molecular size non-collagen proteins such as proteoglycans and osteocalcin. About half of it produced by the osteoblast organic matrix diffuses into the extracellular fluid.

The inorganic matrix of bone is mainly composed of crystalline hydroxyapatite. This element is initially deposited on the organic bone substrate in the form of calcium phosphates which are then transformed into hydroxyapatite crystals. The mature crystals are disc-shaped and occupy the space between the collagen fiber gaps, arranged approximately parallel to the fibers (Figure 1.3). To a lesser extent the inorganic portion contains calcium carbonates (8- 10%), magnesium phosphate, fluoride and calcium chloride. (Whedon,et al., 2017)

The bone microstructure is a custom structure that determines the mechanical behavior of the bone in the mechanical environment. The organic part gives shape to the bone and contributes to its strength and stiffness in compressive loading, while the inorganic part determines the tensile behavior. When the organic part is removed, the bones become particularly brittle, and with the removal of the inorganic part the bones become extremely flexible and can be distorted or bent without fracture.
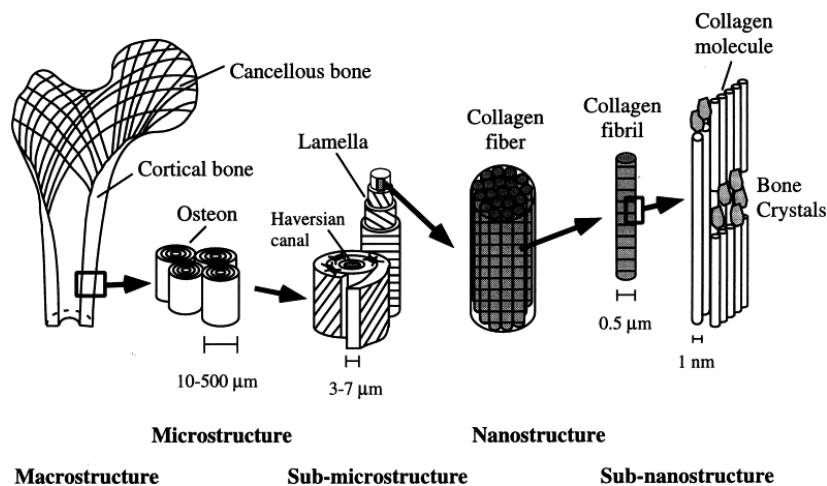
Figure 1-3: Hierarchical bone structure

Equally important in the mechanical behavior of the bone is the hierarchical organization and proper orientation of its bearing elements. The bone is a heterogeneous and anisotropic material. The anisotropy of the cortical bone is determined by the orientation of the osteons, and the spongy bone by that of the trabecular system. Also, the porous nature of the cortex, though limited to that of the spongy bone, contributes to

its anisotropic properties, which in combination with biological fluids that fill in the gaps, influence the propagation of mechanical elastic waves.

The mechanical strength of the bone has been adjusted so that with minimal material it exhibits optimum behavior in the directions of maximum loads. The bones in throughout life there is a constant degradation and rebuilding to adapt to new conditions that evolve over time. Although to a certain extent the bone structure is genetically controlled, it is shown to be further modified through remodeling processes in accordance with its Wolff's law.

1.2   Hip joint

Hip bone or anonymous bone consists of three parts: the iliac bone, the hip bone, and the pubic bone, which are distinct from one another in a young person but unite in the adult. The union of the three segments occurs in and around a large, cup-shaped, arthritic cavity, the acetabular, located near the medial and outer surface of the bone. The two anonymous bones left and right are joined together in front of the pubic symphysis and behind the sacral bone forming the pelvis. (Jones,et.al, 2019)

The hip joint exhibits three degrees of freedom of movement. Normal range of motion includes 0°-140° flexion, 0°-15° extension, 0°-45° abduction, 0°-30° extension, 0°-40° turn out and turn into 0°-50°. In the hip region there is a complex synergy between large and small muscle groups. Hip motion muscles are divided into five categories according to their orientation around the hip joint: in the category of extensor muscles, which includes the major gluteus and the tendons of the foot, in the category of swivel muscles, which include the in and out of the thyroid, the superior and inferior twin muscles, the anterior and quadriceps muscle. Category of muscle attachments, including the pectoralis muscles, the short, long and long muscles: in the class of flexor muscles, characterized by the iliac musculature, which is a combination of three maximal and minimum muscles c iliac muscles, the category of abductors, comprising the mesogloutiaio and minor gluteal muscle.
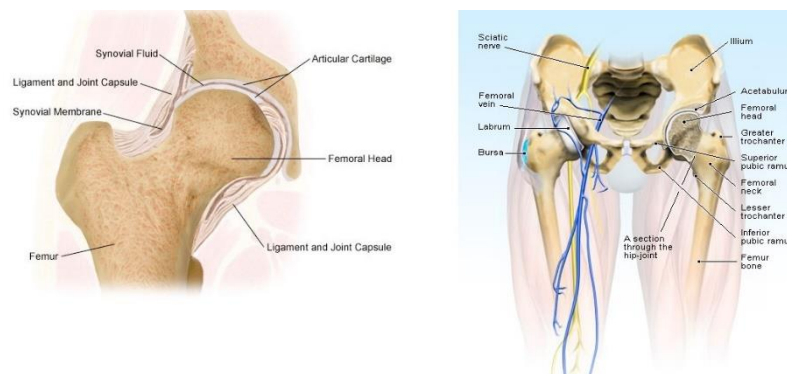
Figure 1-4: Anatomy of hips

Blood supply to the hip joint is made by the intra-peripheral femoral artery and the external peripheral femoral artery, which are branches of the deep femoral artery. The

deep femoral artery is in turn a branch of the femoral artery. There is also a small contribution from a small artery to the small ligament of the femoral head, which is a branch of the anterior portion of the thyroid. The blood supply to this artery becomes very important in order to avoid vascular necrosis of the femoral head when the blood supply from the in and out of the periventricular femoral artery is interrupted.
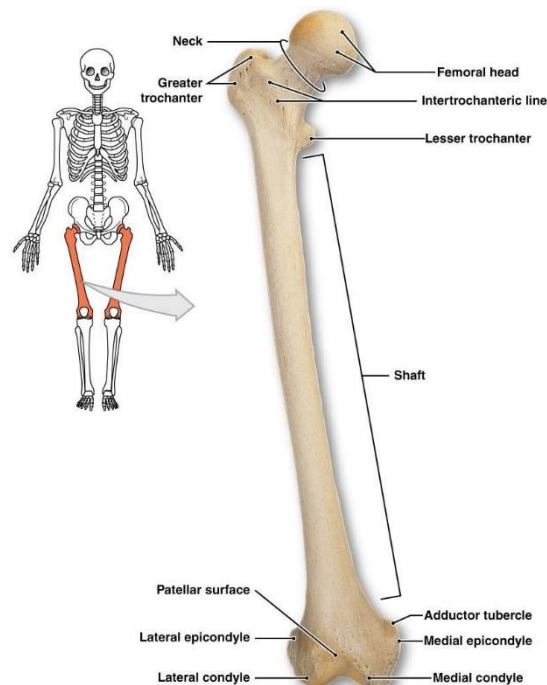
Figure 1-5: Hip joint

1.3   Thigh bone anatomy

The femur is the longest bone in the human body and can hold up to 30 times the weight of an adult. In its upright posture it is not vertical, but it tilts gradually downward and inward to bring the knee joint closer to the body's gravity line. The upper part of the bone consists of the head, which is articulated with the anterior bone, the neck and the two trochanter, the greater and the lesser .The greater trochanter projects upward and serves as a point of departure for muscles that act as abductors and outbound rotors. The lesser trochanter is smaller and conical in shape, extending backward and inward to the femur, just below the neck joint. The thigh bone is long and triangular in shape. In the upright posture, the femur is not vertical, but it tilts downward and inward in order to bring the knee joint closer to the body's gravity line. The lower part has two vertebrae that articulate with the knee joint.
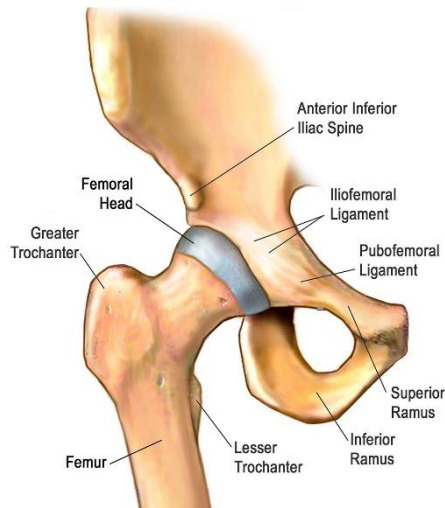
Figure 1-6: Upper extremity of the femur

The head is spherically shaped. Heading upward, inward and slightly forward. Most of its curvature is upward and forward. Its surface is smooth and covered with glass cartilage except for an oval cavity, the well. The well is located downward and behind the center of the head and fastens with the femoral head attachment.

The neck has a flat pyramid shape. The neck connects the head to the bone. The middle axis of the neck forms a large angle (90°-135°) with that of the diaphysis. The angle is larger in infancy and decreases continuously during human development. In the average adult human, the neck forms a 125° angle with diaphysis, but this varies inversely with the size of the pelvis and the height of each person. It is shorter in short than in long bones and when the basin is wide. After a person has fully developed, the angle is usually not subject to change, even in old age. Also, the femoral neck forms an angle of 25 degrees to the frontal plane. Finally, the hip joint capsule overlaps the head and neck of the femur and fastens to the base of the neck. (Kapandji, 1995)

Trochanters are protruding bone sections that provide muscle activity that rotates the thigh on its axis.

The greater trochanter is a large, abnormal, quadrilateral overhang, located at the junction of the neck with the upper part of the diaphysis. It has two surfaces and four borders. The side-out surface, square in shape, is wide, rough, convex, and is characterized by a diagonal pit, which serves to insert the tendon of the medial gluteus muscle. Beneath and behind this diagonal pit is a bag inserted between the bone and the tendon of the maxillary gluteus. The mid-middle surface, smaller than the lateral surface, has at its base a deep cavity, the trochanteric cavity, for insertion of the outer thyroid tendon and above and in front of it a pit for insertion of the inner thyroid and twin muscle. The upper border is thick and abnormal and is characterized by a pit for insertion of the opiate muscle, muscle located in the gluteal area of the lower leg. The lower border corresponds to the line joining the trotter base to the lateral surface of the

diaphysis and is characterized by a protruding crust for inserting the upper portion of the outer wide muscle. The anterior border allows insertion into the lateral portion of the minimal gluteus muscle. Finally, the rear border protrudes a lot.

The lesser trochanter is a conical protrusion, which varies in size to different individuals. It protrudes at the lower and back of the femoral neck base. From the top of it three separate borders extend. The tip of the trochanter is tracheal and the tendon of the maxillary tendon is inserted.

The variable-sized protrusion present at the joint of the upper part of the neck with the greater trochanter is called the femur. It's the meeting point of 5 muscles: the minimal gluteus, the outer broad muscle, the inner thyroid and the upper and lower twin muscles. (Jones,et al., 2019).

2   Total hip arthroplasty

Hip arthroplasty is classified into four main categories. Replacement of the femoral shaft alone, replacement of the acetabular cavity, replacement of the head surface in the femur and total hip arthroplasty covering the first two, which will be analyzed in this thesis.

The incidence of hip arthroplasty increases rapidly, directly with increasing age. It is an internationally accepted and safe solution for the relief of diseases and injuries, causing pain in the damaged joint, and the restoration of normal movement. For the success and longevity of a total arthroplasty, the proper placement of the prosthesis is essential to allow immediate mobilization of the patient, full direct loading, and normal joint movement. The function of total arthroplasty should be similar to normal articulation (Knight, et al., 2011).

Figure 2-1: Replacement of the head surface in the femur and total hip arthroplasty

2.1   History and evolution of total hip arthroplasty

Total hip arthroplasty (OA) as a current form, i.e. of cup prosthesis and the femoral stem is a result of many years of efforts, that the object had the restoration of the damaged joint, in order to restore functionality, but mostly be removed the pain. Historical evolution of total arthroplasty passed through various stages. Precursor and one of the first steps was to imioliki arthroplasty i.e. replacing the single element within the joint, usually the femoral head (Houcke, et al., 2017).

The Scales (1967) in an article about the development of THR delivers the German Gluck in 1890 the first attempt imiolikis hip replacement in which the femoral head is replaced by a spherical head of ivory, stabilized femoral neck screw.
In 1939 the Bohlman manufactured metallic head chrome-cobalt which adapts to a rivet Smith-Petersen. The intention he used successfully in three patients (Bohlman, 1952).A little later the Austin Moore and Harold Bohlman, an the article of Bone and Journal Joint Surgery 1943 entitled Metal hip Joint, describe the case of a patient with giant cell tumor of the upper end of the femur. The tumor was removed and in its place was placed femoral prosthesis Vitale 12 inches in length, the proximal end of the bearing ball head fitted in the acetabular and eyes for fixation of muscles. The distal portion has a pipe shape and penetrated surrounding the remaining portion of the femur. This first artificial metal joint worked for two years with no problems until the patient died of other causes.

The 1946 brothers Judet Paris using the homonymous prosthesis, consisting of a head and femoral stem (stem) of acrylic, which is placed in the intertrochanteric region. The stent was modified by themselves, with metal reinforcement femoral stem , and later the whole intent was constructed in failure because of the problems presented in support of the femoral stem.
Great progress in the development of THR performed when Austin Moor used his experience gained with Bohlman and built intraluminal prosthesis femoral stem this time. The Moore correctly believed the invention in that the endoluminal femoral stem gives greater mechanical support from a shaft placed in intertrochanteric region. So in 1950 for the first time puts the intention of a patient (Moore A., 1963), demonstrating that it was the right solution to support the femoral prosthesis.
The Moore then was slotted so as to reduce the one hand the weight and on the other to be fitted bone grafts for better integration and fixation of the prosthesis to the femur.
At about the same time the Smith-Petersen publishes his experience of the intention cup (Smith-Petersen, 1948).The inspiration for the hip cup (cup arthroplasty) started accidentally when he observed that fibrous connective tissue developed by way of pocket around an inactive material, glass, penetrated after injury.

The placement of inactive materials, such viskaloeides, pyrex, bakelite and vitallium end, suitably shaped between the joint surfaces of the hip patient, was the rationale for generating reactive tissue around them. Such joint replacement, so-called Smith Petersen Cup Arthroplasty of vitallium , remained stable method for the treatment of the reconstruction of the hip patient for many years.
The problems encountered by the hip cup, consisting in need meticulous surgical technique, a long period kinesitherapy bench and subsequently progressive loading of the limb. The results were not as expected and sometimes mobility hip disappointing. The femoral head is absorbed gradually and often a large percentage of

them needed reoperation due to failure. It reported that only half of the cases were successful in pain and mobility, and yet, the process was not able to correct severe anatomical abnormalities (Steinberg, et al., 1982).

Inevitable were all developments which occurred until 1950 matured tripped the concept of combining the two methods, i.e. the imiolikis arthroplasty with femoral prosthesis and the cup arthroplasty. There by replaced at the same time and both articular surfaces of the hip. The result of this combination has been the creation of the first total hip replacement.

In 1951 they began efforts McKee and Farrar culminating in five years in the homonymous total hip. This consists of a femoral endoprosthesis formula Tompson and cup of chromium-cobalt bearing projections which is wedged in the acetabular.

In this final form the same researchers arrived after two other efforts. The first 1951 when placed in the femoral endoprosthesis with a modified rivet Mckee bearing ball head of stainless steel in combination with a metal cup in the acetabular . The second, later, when Tompson formula intention used femoral cup by color-cobalt screw in the acetabular. (GK Mckee, 1982).

In the early 1950 by Sir John Charnely in Writington began experimenting with the use of polytetraflouroethylainiou (Teflon), an inactive low friction material, which is believed can function as "synthetic articular cartilage." Thus placed two minutes in cups thickness of said material in the acetabular and the femoral head is preformed.

The initial results were very impressive. However but soon they started to show failures as necrosis of the femoral head and the cup loosening. The failure led to the abandonment of this intention and the use of another consisting of two elements. The acetabular is replaced with a Teflon cup and the femoral head endoprosthesis femoral stainless steel. Both fixed to the bone with cement methylmetharyliko (J. Charnely, 1961).

In Charneley must orthopedic too much for his contribution to the construction of a total hip arthroplasty.

Like the Swiss Maurice Muller respectively presented promising results with the same name cementitious THR.

The fact that the total hip fastened with cement which is implicated in bone destruction (thermal necrosis, foreign body reaction etc.) Led various researchers to biological fixation solution. This aims to stabilize the prosthesis to bone tissue growth, so as not to interfere anything between bone prosthesis.

In 1960 Ring use the same name total hip, which consisted of femoral Moor formula intention cobalt-chromium and cup of the same material. The cup sterneotan pelvic screw-addition and was placed in a valgus. This intention was used successfully for several years.

The Ring then amended the total and the latest models contain the same basic concept ie without cement solidification, but with cup of polthylainiou. This avoids the problem of high friction coefficient, metal on metal and the creation of shavings which are implicated in the relaxation.

By the same rationale used in ceramic for construction of both the cup and the femoral head. The total ceramic arthroplasty was first proposed in 1934 by Rocker but only used in 1970 by Bontin (Lampiris, 1987).

The disadvantage was the high rate of relaxation, because it did not guarantee stability in twisting forces.

In conclusion on how stabilization, total hip two groups can be distinguished. Those which are fixed to bone biologically i.e. growth of new osseous tissue between the prosthesis and bone and are secured with cement.

In the last decade the trend of using increasingly cement less total hip is evident. The design change in geometry of the intentions and the use of new materials has resulted in a direct primary support to the bone and therefore the immediate weight bearing. Postoperative long-term patient follow-up (follow up) has shown excellent results in 15 years with very little relaxation rates. (Makris, 2003)

Those elements that characterize a successful OA as Mckee wrote in 1970 and applied to date are:

1. Passive materials.
2 . A satisfactory design intent (design).
3. Stabilization of the prosthesis to the bone.
4. Proper surgical technique.
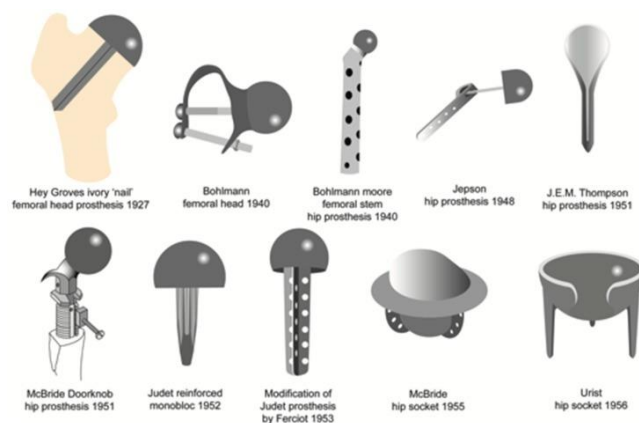
Figure 2-2: Evolution of the prostheses design.

2.2   Conditions and symptoms leading to total hip arthroplasty

Those who have had cartilage damage in one or more of their compartments because of osteoarthritis (idiopathic or post-traumatic), inflammatory arthritis (rheumatoid, psoriatic, etc.), vascular necrosis are in need of total hip replacement. However, over 95% of total arthroplasty is performed due to osteoarthritis, a condition that is constantly increasing with the increase in life expectancy.

The most common first symptom is pain, which is usually accompanied by swelling of the joint and then with complete lack of mobility. (U. States, 2019)

Irritations and aches in the hip can be caused by either an external blow or a disease that affects the body. External factors that cause severe hip joint problems are falls and fractures of the upper thigh bone.

Figure 2-3: Fractures of the hip joint

The most common form of arthritis is osteoarthritis, also known as degenerative arthritis or degenerative joint disease, deteriorating joint function by reducing articular cartilage as well as hypochondria. When bone surfaces are not adequately protected with cartilage, the bones may be exposed and damaged. Pain due to pain reduces hip movements resulting in peripheral muscle atrophy and loosening of joints.
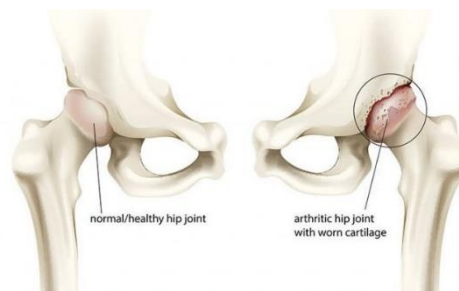
Figure 2-4: Arthritis of the hip joint

Congenital dislocation of the femoral head is a hereditary condition; a child is born with an unstable hip due to the abnormal formation of the hip joint in the early stages of fetal development. Over the years, the problems of dysfunctional joints become more severe as the person with the disease crumbles
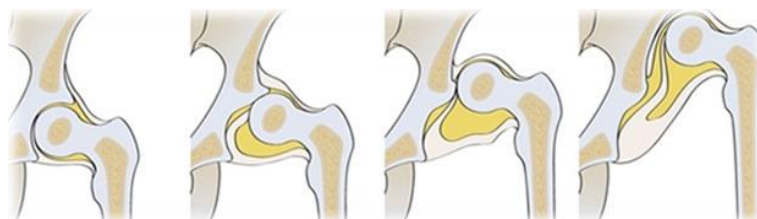
Figure 2-5: Congenital dislocation of the femoral head

Osteonecrosis of the hip is caused by a disorder of the femoral head that results in cell death. The bone in the head of the femur is dead and gradually settles down. Cartilage covering the femoral head disintegrates and collapses resulting in arthritis.

Figure 2-6: Osteonecrosis of the hip joint

Total hip arthroplasty resolves the problems reported by replacing the problematic area of the femur, the head, with an appropriate stent structure and material for normal hip movement and use.

2.3   Complications in total hip arthroplasty

As with all surgeries, there are potential risks and complications and some recovery time is required. Some of the potential complications that any total hip arthroplasty can have are: pain, bone or ligament fractures, vascular or nerve damage, transient or permanent nerve damage, imbalance, prosthesis, thrombi that can migrate heart or lungs, delayed healing of surgical incision, deep inflammation, superficial inflammation, early wear of the prosthesis which may require new surgery.

Some people may develop blood clots in the deep veins of the foot that cause pain or swelling of the foot. This is due to the change in blood flow and its ability to clot after surgery. There are a variety of ways to prevent them, such as adhesives, specific foot exercises, and inoculated medicines. A small minority of blood clots, especially those of the thigh veins, can detach and travel through the blood vessels to the lungs, where they can adhere. This can cause sudden shortness of breath, chest pain or even collapse. However, it is usually possible to treat with anticoagulants and oxygen therapy. (surgeons, 2019)

Hip dislocation occurs when the femur head is not located in the acetabular. It is a rare but serious injury, often associated with hip fracture or pelvic fracture. When this occurs during the procedure, the hip should be placed under anesthesia again. If the hip continues to dislocate, further surgery or a support may be needed to stabilize it. Even after you have started walking without support it is important to follow a muscle strengthening program to help stabilize the hip and improve its functionality.

To reduce the risk of postoperative infections, appropriate selection of antibiotics administered prior to surgery will be necessary. Special clean-air surgeries are also used to pump them through, and antibiotics should probably be given a short sequence at the time of surgery. However, in-depth infection can occur in about 1 in 100 cases. The infection can be treated, but the new hip joint usually needs to be removed until the infection has passed. The new hip members are then implanted 6-12 weeks later.

The most common cause of hip fracture failure is when the artificial hip relaxes. This can happen at any time, but it is more common after 10-15 years. It usually causes pain, and the hip can become unstable. Relaxation is usually associated with thinning of the bone around the implant, which makes the bone more prone to fractures. A fracture around the implant can usually be managed through surgery or even a recurrence.

Therefore, many problems that patients face after hip replacement surgery are the result of osteolysis. Osteolysis is the reduction in bone mass due to the body's reaction to thin pieces of polyethylene that wear out over time. The above reaction causes inflammation and results in bone resorption and loosening of the implant or even fracture. As a countermeasure to the above, the use of ceramics in the implant system has been adopted to reduce polymer wear over time.

Many times even though the limbs are equal, after surgery they look different and in addition the patient feels them differently. The leg, which is replaced by the femur, may increase or decrease in length during surgery, with the increase being the most common. If the edges are really the same, the feeling of unevenness disappears within the first month. Otherwise, high-heeled shoes are used until a second replacement operation is performed. The reason for the above is mainly the wrong choice of implant. Typically the wrong choice is the incorrect length of the femoral portion of the implant and the diameter of the head chosen to be greater than the diameter of the acetabular.

2.4   Stent geometry

In total hip arthroplasty, the geometry of the stent to be used plays an important role in the proper stress distribution and postoperative functionality of the prosthetic joint. The parameters of the stent geometry are the length and diameter of the sternum, the diameter of the head, the diameter and the angle of the neck. Depending on the geometry of the femur, the type and extent of hip disease and the age of the patient, the length of the sternum, the position of the neck base, the material of construction and the geometry of the stent surface are selected. As a result, optimal support for the femoral prosthesis, proper loading of the bone to avoid loose bone atrophy, and ease of implant insertion during surgery.

Femur

The femur consists of the sternum and neck of the stent. The ideal geometry of the shaft in a total hip arthroplasty is the same as the intact and normal femur. The femur is the

stent, without the head and is divided into the neck and the main stem. Each of them plays a different but important role in supporting the hip and is made of different material morphology, which changes the physical, chemical and mechanical properties of the femur. In an ideal replacement, the femur should have exactly the same geometry and angle as the intact femur. The most common materials used for the main strain are Ti6Al4V and CoCr, titanium alloy used in the present thesis.

The head

The femoral head is spherical in shape and forms the upper part of the femoral head. Its role is to enclose the acetate in the correct dimensions and at the right angle to move it in three dimensions and minimize dislocation. They are usually made of ceramic such as alumina or metal such as Ti6Al4V. It is mechanically immobilized to the main shaft on a conical overhang usually by means of PMMA for welding. It has been experimentally shown that the difference in its geometry offers different properties throughout the stent. If the head is smaller than the acetabular cross-section and is not precisely enclosed, there is a very high risk of detachment, although in the above case a greater range of motion is observed.

Acupuncture implant

The acetabular region is replaced by a similar morphology intent, the choice of which material is determined according to the material of the femoral head and the age of the patient. It consists of two parts: One is concave in shape and mechanically immobilized in the patient's pelvis and is always metallic. The second part plays the role of cartilage replacement and can be metallic, ceramic or even polymer.

Figure 2-7: Different types of stents

2.5   Materials of stents

Four main types of bearings are studied and applied in THA: metal-on-polyethylene (MoP), metal-on-metal (MoM), ceramic-on-ceramic (CoC), and ceramic-on-polyethylene (CoP). Recently, hybrid combinations were introduced such as ceramic heads and metallic inserts (CoM). Many factors influence the choice between these types of bearing, such as the implant cost, age and activity level of the patient,

complications during surgery, etc. MoM articulations were introduced first in 1950, by McKee and Farrar, leading to unsatisfactory results as two out of three implants were removed after 1 year due to loosening and the third removed for fracture. After many improvements of the bearings, they were reintroduced in 1960, when the wear rate ranged from 1 to 5 mm^3 per year (which was roughly 20 times lower than that registered for metal on polyethylene). MoM articulations were used for both total hip replacements and hip resurfacing (HR), which have the advantage of preserving the femoral head and neck, resulting in a less invasive operation and a lower dislocation rate. When, during the 2000s, the issues of metal debris came to light, the MoM replacements were almost stopped completely. In the early middle 2000s, these implants were used in more than one out of five cases in the UK and up to one-third in the US. Today, they are used in less than 1% of the total surgical operations. MoM articulations have been used again in the last two decades, thanks to the appearance of new surface finishing techniques that improve their wear resistance. On the other hand, MoM bearings aim to ensure high wear resistance, good manufacturability and low friction torque. However, even if lower wear volume is associated with such implants, very small particles are produced. The amount of metal ions present in the serum and their potential toxic effects both locally and systemically are a cause for concern. Moreover, polishing wear, promoted by wear debris, produced by the abrasive action of carbides, has been shown in retrieved Co-Cr alloy hip implants (Merola,et. al, 2019).

Up to the middle of the 1990s, the most widespread hip implant was MoP couples that worked well in older and less active patients. Two relevant problems were still a concern: aseptic loosening as result of inadequate initial fixation caused by particle-induced osteolysis around the implant and hip dislocation.

In the 80's, when aseptic loosening and osteolysis arose as main issues in metal-on-polymers hip implants, the firsts CoC couples were launched, starting with alumina and zirconia .Zirconia ceramics have been introduced for orthopedic implants as a secondary ceramic material along with alumina for several years. Major advantages of ceramics for THA are their hardness, scratch resistance, and the inert nature of debris. These characteristics promote the use of CoC bearings, and the inert nature of the wear debris result in them being the best choice for young patients. On the other hand, their use is expensive, and implants require an excellent surgical insertion to preclude chipping of contact surfaces.

The introduction of an innovative hybrid hard-on-hard bearing ceramic head and metallic insert claimed to reduce ion release and wear particle production and possibly the breakage of the ceramic insert rim. In in vitro studies on CoM hip implants, smaller particles and lower wear have been found.

Nowadays hip joint prostheses are made with metals, ceramics and plastic materials. Most used are titanium alloys, stainless steel, special high-strength alloys, alumina, zirconia, zirconia toughened alumina (ZTA), and UHMWPE. Usually, stems and necks are composed of metals, whereas femoral heads can be both metal and ceramic, and the acetabular can be made of metals, ceramics or polymers. There are several combinations that can be realized by using these materials with the aim of coupling with the fewest concerns and the highest long-term success odds.

Hereafter, we present an overall evaluation of biomaterials (polymers, metals, ceramics) for THA.

2.5.1 Polymers

Polymer materials were the first choice for low friction hip replacements, as proven by Charnely. Highly stable polymeric systems such as PTFE, UHMWPE or polyetheretherketone (PEEK) have been investigated due to their excellent mechanical properties and their high wear resistance (Beer, et. al, 1992). Nevertheless, when implanted, acetabular cups made of polyethylene generate debris that is attacked by the body's immune system. This leads to bone loss, also known as osteolysis; furthermore, since the debris accumulates in the area close to the implant, the bone loss leads to loosening of the implant stem. This results in the needs of a revision, namely, another surgery. Revision for loosening is four times higher than the next leading reason (dislocation at 13.6%) and is more severe in young patients.

2.5.1.1 PTFE

PTFE has a high thermal stability; it is hydrophobic, stable in most types of chemical environments, and generally considered to be inert in the body. It was used by Charnley in his firsts THA, but exhibited two main drawbacks, which were found only after implantation in 300 patients. The material had a very high wear rate, equal to 0.5 mm per month, and PTFE produced voluminous masses of amorphous material due to the vast number of foreign-body giant cells. Furthermore, this debris elicited an intense foreign-body reaction that Charnley verified by injecting two specimens of finely divided PTFE into his own thigh.

Charnley tried to use a composite material based on PTFE reinforced with glass fibers (known as Fluorosint), finding poor performance in vivo, despite its fine behavior in vitro. The composite, after one year of implantation, developed a pasty surface that could be easily worn away. Plus, the filler acted abrasively and lapped the metal counter-face. Moreover, this composite material showed a higher rate of infection (20%) and loosening (57%) than the other materials employed.

2.5.1.2 UHMWPE

Charnley introduced UHMWPE in 1962, urged by the failure of PTFE as a bearing material and sustained by the promising behavior in laboratory tests . The polymer is characterized by its excellent wear resistance, low friction and high impact strength. It is created by the polymerization of ethylene, and it is one of the simplest polymers. Its chemical formula is $(-C_2H_4-)_n$, where n is the degree of polymerization, being the number of repeating units along the chain. The average degree of n is a minimum of 36,000, having a molecular weight of at least 1 million g/mole as defined by the standard (Merola,et. al, 2019).

During the 1980s and early 1990s, aseptic loosening and osteolysis emerged as major problems in the orthopedic field, and these problems were perceived to limit the lifespan of joint replacements. To limit the wear particle concentration and improve the overall mechanical characteristics, efforts have been made to improve the overall characteristics of UHMWPE for hip implants. In the 90s, scientists were able to correlate changes in the physical properties of the UHMWPE with the in vivo degradation of mechanical behaviors.

In the recent years, a different approach was developed to stabilize polyethylene. Blending vitamin E with polymers was firstly meant as a hygienically safe stabilization, Tocopherol compounds were proposed as a stabilizer for polyolefin in the 1980s .In 1994, Brach del Prever et al. introduced UHMWPE blended with vitamin E for a prosthetic implant. In 2007, the first vitamin E-diffused, irradiated UHMWPE hip implant was clinically introduced in the United States (Biomet Inc., Warsaw, IN, USA). The blending led to the interruption of the oxidation cycle by decreasing the reactivity of the radical species, giving origin to a third generation of polyethylene. If vitamin E-stabilized, irradiated UHMWPE undergoes accelerated aging at high temperatures and/or in the presence of pure oxygen, it will be oxidatively more stable than gamma-sterilized or high-dose irradiated UHMWPE. In vitro studies supported the hypothesis that vitamin E-blending would enhance the oxidative stability of XLPEs. There are also some drawbacks in the procedure: increasing the concentration of vitamin E in the blend is not viable, the obstacle of cross-linking in the presence of vitamin E prescribes the use of a lower concentration. Therefore, a balance is needed to obtain elevate cross-linking density and high oxidative stability (Beer, et. al, 1992).

2.5.1.3   PEEK

Polyether-ether-ketone (PEEK) is a well-known biocompatible polymer used in orthopedic applications. It has been considered as an alternative joint arthroplasty bearing material due to its favorable mechanical properties and the biocompatibility of its wear debris. PEEK had been used as biomaterials, in particular in the spine, since the 1980s due to its structure that confers outstanding chemical resistance, inertness, and thermal stability for in vivo conditions. In 1998, Wang and coworkers tested acetabular cups made of PEEK on a hip simulator for 10 million cycles. They observed a reduction in the wear rate of almost two orders of magnitude in comparison to a conventional UHMWPE/metal or UHMWPE/ceramic couple. However, despite the good promises deriving from in vitro, low contact stress situations, when in high contact stress environments, there are questions about the suitability of this material as acetabular cups or knee tibial components. No clinical data of its use are available.

2.5.2   Metals

Metallic materials have wide applications in the medical and bioengineering fields and are widespread as orthopedic implants components. The most common traditional metals used for THA are stainless steels, titanium alloys (Ti6Al4V) and mainly cobalt-chromium-molybdenum alloys. The latter have good corrosion resistance compared to other metals, and high toughness, high wear resistance and higher hardness than other metals and polymers.
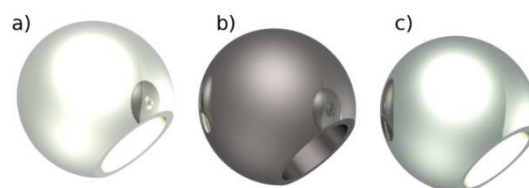
Figure 2-8: Metal femoral heads: (**a**) stainless-steel; (**b**) Oxinium (**c**) CoCrMo.

2.5.2.1 Cobalt Chromium Molybdenum Alloys

MoM articulation is typically produced from cobalt-chromium-molybdenum (CoCrMo) alloys. CoCrMo alloys are composed of 58.9–69.5% Co, 27.0–30% Cr, 5.0–7.0% Mo, and small amount of other elements (Mn, Si, Ni, Fe and C). These metallic alloys can be divided in 2 categories: high-carbon alloys (carbon content >0.20%) and low-carbon alloys (carbon content <0.08%). In addition, metallic alloys can be manufactured using 2 different techniques such as casting and forging; the grain size of the forged alloy is typically less than 10 μm, whereas the grain size of the cast material ranges from 30 to 1000 μm. Intensive studies were done on the metallurgy for CoCrMo alloys with carbon; nevertheless, there is no complete phase diagram. This is mainly due to the complex phases existing in the system. Various carbide species, such as $M_{23}C_6$, and M_6C can take place based on the heat treatment . The differences in the microstructure of the carbides, their chemical composition, and nano-hardness are related to wear performances. (Beer, et. al, 1992)

Cobalt and chromium are both present in the environment and in food. They are necessary to human beings as trace elements in the body but are toxic when highly concentrated. Patients with Co-Cr metal-on-metal pairings are exposed to wear with release of cobalt and chromium into the synovial fluid. These are capable of migrating to the blood before being expelled through the urine. There is poor knowledge on the effects of circulating Co and Cr; they may affect mainly biological and cellular functions with potential effects on the immune system, mutagenesis, and carcinogenesis. In patients with metal-on-metal hip implant, elevated levels of circulating Co and Cr ions may be generated, and there is a positive linear correlation with a lymphocytic reactivity.

2.5.2.2 Other Metal Alloys

Metallic materials have high module of elasticity, which limits stress distribution from implant to bone. Therefore, new metallic components have been developed with lower elastic modulus and higher corrosion and wear resistance. There is continuous research for new metallic alloys for application in hip prostheses to obtain a better biocompatibility along with superior mechanical properties. Still, it is mandatory to find a compromise between the many optimal characteristics desired for an implant material. Co-Cr-Mo alloys have low chemical inertness but high wear resistance, whereas stainless steel alloys have low strength and ductility. Zirconium (Zr) and tantalum (Ta) are refractory metals—due to their great chemical stability and elevate melting point—and are very resistant to corrosion, due to the stability of the oxide layer. As vanadium is a relatively toxic metal, some attempts were made to replace it in the widespread Ti-6Al-4V alloys. To improve biocompatibility and mechanical resistance, this Ti-6Al-4V alloy was replaced with iron (Fe) or niobium (Nb), realizing the improved alloys Ti-5Al-2.5Fe and Ti-6Al-7Nb. These alloys with respect to the traditional Ti-6Al-4V have greater dynamic hardness and lower elastic module, allowing a better implant/bone stress distribution. A new class of titanium alloys introduced into the orthopedic field uses molybdenum in concentration greater than 10%. Its presence stabilizes the β-phase at room temperature; these are referred to as β-Ti alloys. Having 20% less elastic

modulus, they behave closer to real bones and have better shaping possibilities. Femoral stems made of a β titanium alloy have been used as part of modular hip replacements since the early 2000's but were recalled in 2011 by the US Food & Drug Administration (FDA) due to elevated levels of wear debris. Yang and Hutchinson found that the dry wear behavior of a β titanium alloy (TMZF (Ti-12Mo-6Zr-2Fe (wt. %)) is very similar to that of Ti64, whereas their behavior is completely different in simulated body fluid, where the wear of TMZF is significantly accelerated. Another recently introduced metal material is the oxidized zirconium (Oxinium, by Smith & Nephew), with a metal core and abrasion-resistant ceramic surface. The niobium alloy of zirconium has proven to decrease the UHMWPE wear rate and particle production considerably (Merola,et. al, 2019).

The revision rate of large head metal-on-metal and resurfacing hips is significantly higher than that of conventional total hip replacements. The revision of these bearings has been linked to high wear as a consequence of edge loading, which happens when the head-cup contact patch extends over the cup rim. Underwood et al. highlighted that using hip implants with low clearance, having more conformal contact and so a larger contact patch, increases the risk of edge loading and therefore intense wear.

2.5.3 Ceramics

The word ceramics derives from Greek, *keramos*, meaning potter or pottery. Ceramics were defined by Kingery as "the art and science of making and using solid articles, which have, as their essential component, and are composed in large part of, inorganic nonmetallic materials". It is likely to say that a ceramic is whatever material is neither a metal, a semiconductor nor a polymer. Ceramics are used to build engineering components when wear resistance, hardness, strength and heat resistance are required. Ceramics were also defined as "the materials of the future", as they are derived from sand that is about 25% of the earth's crust as compared to 1% for all metals. In the lasts decades, ceramic materials have exhibited great appealing and diffusion thanks to their chemical and physical characteristics, attracting the interest of biomedical scientists and companies . Ceramic materials were introduced in the THA more than twenty years ago to overcome the major issue of polyethylene wear.

2.5.3.1 Alumina

Alumina was introduced in THA implants in 1971, when Boutin realized alumina-on-alumina hip coupling, leading to good clinical results. Alumina ceramic has been one of the main ceramics to be used in THA, relying on its good tribological properties, meaning a favorable frictional behavior and a high wear resistance. On the other hand, it has weaker mechanical resistance than other materials. It showed good performances in compression, but weak resistance to tensile stresses . Alumina ceramics have been used in clinical applications for their tribological properties due to their hardness. Among the ceramics, alumina is probably the most commonly used material.

The alumina used for hip replacements was different from the first generation of the material used for industrial applications. In particular, the first generation of alumina showed poor microstructure with low density, scarce purity, and large grain size. This

generation of alumina was unsuited for biomedical use. The continuous efforts performed in this field allowed researchers to purify and improve this process, leading to an alumina for medical use, commercially known as Biolox. The ISO 6474 standard, introduced in 1980, aimed to improve the quality of alumina for THA and to decrease the fracture occurrence. Alumina performance is related to different aspects, such as the density, the purity and the grain size. The last one, in particular, influences the wear rate, as it decreases with smaller grain size. In the 90's alumina hip implants were improved with the arrival of Biolox forte on the market, which could rely on innovations in the production process to furnish much better mechanical characteristics. It was realized using improved raw material, with smaller gain size, low level of impurities and sintered in air.

Recently, concerns have been raised because of some clinical reports on the presence of audible noise in some ceramic-on-ceramic THA patients. The so-called "clicks" or "grinds" have been described after THA, regardless of whether metal-on-polyethylene, metal-on-metal, or ceramic-on-ceramic bearings were used. The "squeak" appears to be limited, however, to hard-bearing couples. It is probably related to implant design or cup orientation and the exact etiology of squeaking is the object of debates; there is neither a specific definition for post-surgery squeaking nor a universal categorization for the sound.

2.5.3.2   Zirconia

Zirconia has high toughness and good mechanical properties; among all the monolithic ceramics, it has outstanding crack resistance, these are the main reasons that made zirconia a very widespread alternative to alumina for THA. Firsts attempts were focused on magnesia partially stabilized zirconia (MgPSZ), that did not satisfy the wear resistance requirements, Therefore, further developments were focused on yttrium stabilizing oxide (Y-TZP), a ceramic that is completely formed by submicron-sized grains, representing the current standard for clinical application.

With respect to metals, Y-TZP shows superior wettability properties that allows for fluid film formation between the articulating surfaces of an implant. Even if in clinical practice the Y-TZP femoral heads were only coupled with UHMWPE cups, tests performed on Y-TZP vs. alumina returned positive results. From the wide investigation campaign on the wear performance of UHMWPE vs. zirconia, there is a general agreement on the fact that the wear is not higher than UHMWPE vs. alumina. Discrepancies in results derive mostly from the differences in the bulk materials used in laboratories, in their finishes, testing procedures etc. There is great concern in the orthopedic community regarding the future of Zirconia as prosthesis. The market has decreased more than 90% between 2001 and 2002 (corresponding with the recall and abandon of Prozyr, by Saint Gobain). More than 600000 femoral heads used in Y-TZP have been implanted worldwide, mostly in EU and US. The debate on the Y-TZP future is due to its pros and cons; it exhibits the best mechanical properties (resistance to crack propagation) but is prone to aging in the presence of water.

Zirconia manufacturers tried to shrink this problem, claiming that it was limited under in vivo conditions until 2001 when around 400 femoral heads failed in a short period. This event was related to accelerate ageing affecting two batches of Prozyr. Even if the reason was identified to be processed controlled, this event led to catastrophic impact on the use of the Y-TZP, pushing some surgeons to go back to other solutions. The ageing problem and the Prozyr event are still an issue, and further efforts are required to gain

confidence from the orthopedic society. In this way, the future seems to be based on the combination of zirconia and alumina to obtain advanced composites.

2.5.3.3 Zirconia Toughened Alumina

In the second half of the 1970s, a new class of ceramic-based composite materials developed. This new composite material was realized by introducing up to 25% wt. of zirconia into an alumina matrix; this composite material is known as zirconia toughened alumina (ZTA). The addition of a fraction of zirconia to alumina results in a composite material of increased toughness. In the 2000s, the first ZTA material introduced in a clinic was a composite known under the trade name of Biolox Delta.

This material provides elevate resistance to the onset of cracking and to crack propagation. This ZTA composite combines the best characteristics of both alumina and zirconia: the strength and toughness of alumina and the excellent wear resistance, chemical and hydrothermal stability of the alumina. This combination is realized through the uniform distribution of nano-sized particles of yttrium-stabilized tetragonal zirconia (Y-TZP) in the alumina matrix. A small percentage of chromium oxide (Cr_2O_3) is added to counterbalance the hardness reduction caused by the zirconia presence. Strontium oxide (SrO) is added to the material, during the sintering process, to form strontium aluminate ($SrAl_{12-x}Cr_xO_{19}$) platelets. These flat and elongated crystals dissipate cracks energy and limit their advance, as it would require extra energy for the crack to overtake the crystal. The final composite is a mixture of roughly 75% alumina, 25% zirconia, and less than 1% chromium oxide and strontium oxide. Deville et al. found that Alumina Y-TZP composites exhibit significant ageing, but this process was far slower than usually observed in Y-TZP ceramics, which is ascribable to the presence of the alumina. On the other side, the presence of zirconia aggregates was recognized as the main cause of ageing sensitivity. Realizing an optimal dispersion at acid pH can avoid the formation of zirconia aggregates, but as soon as the percolation threshold level is exceeded, ageing cannot be avoided.

2.6 Stent application

Of the various bone diseases that a patient undergoing total hip arthroplasty may have, poor bone quality results. Its poor quality affects the choice of stent as well as the type of its solidification. For stabilization, the surgeon will apply the stent to the femur using either stabilization with cement, without cement or a combination of them.

2.6.1 Stabilization with cement

The first researcher and surgeon to use cement for "better stabilization" was the German Gluck in a total knee arthroplasty in 1890. However, Charnley introduced and made widely known the use of bone cement, PMMA, to stabilize articular stent in the knee, in the 1950s. Although bone cement implantation involves two interfaces, bone-cement and stent-cement, the basis for a robust implant is that of bone-cement. This method is highly dependent on the surgeon if during the operation he is required to properly apply the implant in combination with the cement and bone. The cement-bone interlocking at the microscopic level allows for immediate and almost complete loading of the leg.

Acrylic cement is a standard material for stabilizing the femoral prosthesis within the spinal canal and its quality has been greatly improved with a view to long-term survival of the materials. When using cement, the stems should occupy about 80% of the cross-section of the spinal cord, so that the cement covers - perimeter of the stylet - about 4 mm in the proximal portion of the spinal cord and 2 mm in the peripheral. Central placement of the shaft in the spinal cord reduces the chance of creating localized areas with a thin cement casing that can fragment and cause loosening of the prosthesis.

Cobalt-chromium alloy strains are preferred because they exhibit a higher modulus of elasticity, which leads to a reduction in the stresses applied to the cement housing within the proximal portion of the medullar lumen. The cement is more resistant to compression loads, weaker to voltage loads and weakened by the effects of repeated, cyclic loads. Fatigue begins at stress points inside the cement housing, especially in areas where the cement layer is thin and the femur is in contact with bone (Vaishya, et. al, 2013).

Cement-stabilized femoral prostheses fail to a lesser degree than cement-stabilized acetabular cups, because the strains receive greater compression forces. Men, who are more active, report higher rates of failure than women.

Figure 2-9: Stabilization with cement

2.6.2   Stabilization without cement
In recent decades implants have been designed that do not require cement for bone application. Early failure of cement stents in fixing them was common. Their failure was in specific areas where there was bone destruction. The cause of the failure was initially thought to be caused by infection but the course was attributed to local inflammation caused by cement.

These stents are generally larger and longer than those that use cement. Most implants that do not use cement for implantation have a rough texture or porous surface that allows bone to be created on that surface. Since stabilization is based on bone growth on

the stent, it takes longer for post-operative recovery. They are also not used in a patient with osteoporosis.

The main advantage of biological stabilization of the cementless stent is that it is permanent. It has been assumed that when the stent placement is stable from the outset it does not change over time.

Another advantage of cementless stents is that there is no bone loss even in the face of relaxation, unlike cements that use cement.

Fractures of the femur have been a fairly common phenomenon in total hip arthroplasty that does not use cement in stent implantation, although most are not harmful, although it is a major disadvantage. Another problem with cementless implantation is the orientation of the head in the design of the stents whose implantation is achieved by means of wires.

3 Loading and straining of the femur

3.1   Types of mechanical loading of the femur

During daily activity and under conditions of increased mechanical stress, the femur receives force and torque action. The mechanical behavior of the femur depends on its strength, geometrical characteristics, age, as well as on its type, speed and frequency of loading. Forces and torques act on the bone in different directions and cause different types of loads such as their tensile, compressive, bending, torsion and / or combinations. (Δ.Ι.Γουλες,et.al, 2005)

Tensile

Applying tensile stress to the femur results in the development of symmetrical internal stresses and deformities. Its maximum values appear at a level perpendicular to that applied by the tensile forces, so the type of fracture that occurs in tensile is transverse. Under the influence of these forces, the bone first forms a neck and eventually fails. Microscopically, the reason for the tensile fractures is due to the removal of the cement lines from the bones. The bones that are most prone to tensile fractures are those that have a higher percentage of porosity inside.

Compression

When compressive forces are applied to the bone, the result is the development of symmetrical internal stresses and deformities. Under the influence of these forces, the bone is shortened and enlarged. Application of compressive loads can cause fracture in the upper third of the femur, which is mainly composed of spongy bone.

Shear

When applying shear forces, loads are exerted parallel to one of the longitudinal axes of the bone. At the same time, internal shear stresses and deformations develop, the direction of which forms, with the bone surface, initially at right angles and then at acute angles as loads continue to apply. Fractures of shear stresses occur in the femoral condyle of the bone.

Bending

The bending forces cause the bone to bend around a neutral axis, so there is a combination of tensile and compressive forces on either side of this axis. Fractures to the femur due to bending often occur because the cortex is less resistant to stretching, the fracture line starts from the area where the tension-causing forces are applied. Small bending forces can cause the cortical bone to rupture to the side opposite the fracture. The tensile failure proceeds transversely to the bone and the neutral axis of displacement, and bending fractures are generally lateral or transverse, or may have a butterfly fragment.

Torsion

The application of torsional forces to the bone tends to rotate it around an axis, while inside it rotational torqueses are developed. Torsion forces are exerted when one end of the bone is stationary and the other end is forced to rotate. Shear stresses and deformations are also developed at planes perpendicular to the axis of rotation, as well as compressive and shear stresses and deformations at planes diagonal to the same axis. This kind of mechanical load causes spiral fractures in the bone.
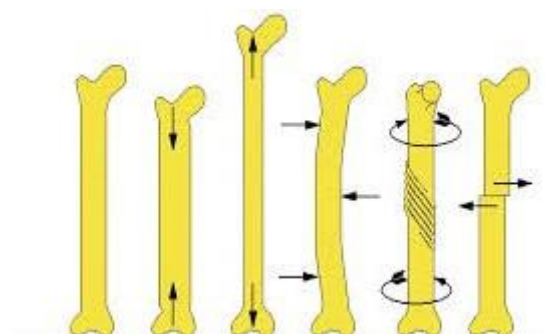
Figure 3-1: Types of mechanical loading of the femur (calmness, compression, tensile, bending, torsion, shear)

In general, in clinical practice most fractures are caused by a combination of stresses. Charging of the femur is done dynamically, with the application of varying forces, such as walking. In a few cases the charging is constant, such as standing up. The femur when strained at a high rate of load application is stiffer, more durable and absorbs more energy before being fractured.

Bone strength depends on the type of charge and its direction. The compressive strength is greater than the tensile strength for both load directions, whereas, for the longitudinal loading condition, the compressive strength is almost three times the shear strength.

3.2   Definitions of stress and strain

All materials have a specific property called a flexibility measure. When forces are applied to a structure, it is deformed. When this deformation does not exceed a certain limit then the construction tends to return to its original shape or its original volume after these forces have ceased to be applied. There is a wide variety of structures in nature. The perfect elastic structure is one where when the forces exerted on it are completely returned to its original shape and its original volume, the perfect plastic structure is that when the forces are removed the structure remains completely deformed. No structure is fully elastic or plastic, all exhibiting the properties of elasticity and plasticity to varying degrees. (Enderle, et. al, 2005)

For the analysis of the deformation of a structure, we consider an elemental cube of this structure that can be deformed in all directions shown in the figure. The force exerted, which causes the deformation, creates internal forces whose measure and direction are not homogeneous but depend on the external force, the shape of the structure and the mechanical properties of the material. These internal forces are the stress and the strain.

Stress is the force applied to a material, divided by the material's cross-sectional area:

$$\sigma = \frac{F}{A_0},\qquad\qquad (3.1)$$

where σ = stress (N/m^2, Pa), F = force (N), A_0 = original cross-sectional area (m^2)

Strain is the deformation or displacement of material that results from an applied stress:

$$\varepsilon = \frac{L - L_0}{L_0},\qquad\qquad (3.2)$$

where ε = strain ,L = length after load is applied (mm),L_0 = original length (mm). Strain has no dimensions, it is just a number. The most common way to analyze the relationship between stress and strain for a particular material is with a stress-strain diagram. The stress-strain diagram provides valuable information about how much force a material can withstand before permanent deformation or failure occurs.
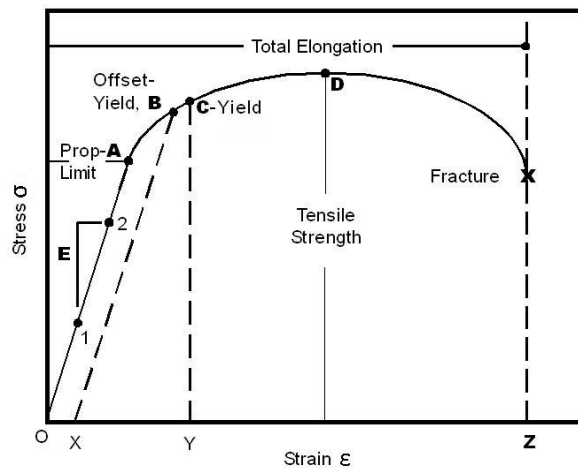
Figure 3-2: A stress-strain diagram

3.3   Hooke's Law

Many materials exhibit a proportional relationship between stress and strain up to certain point, referred to as the proportional limit, shown here as point "A."(Figure 3.2) This stress-strain relationship is known as Hooke's Law, and in this region, the slope of the stress-strain curve is referred to as the modulus of elasticity (aka Young's modulus), denoted E.

$$E = \frac{\sigma}{\varepsilon}\qquad\qquad (3.3)$$

The modulus of elasticity is essentially a measure of stiffness and is one of the factors used to calculate a material's deflection under load. (Δ.Ι.ΓΟΥΛΕΣ, 2005)

3.4 Maximum Rotational Energy Criterion (Von Mises)

The maximum rotational energy criterion formulated by Von Misses in 1913, considers that a ductile metal material will suffer a plastic leak if satisfied the following condition:

$$\frac{\sqrt{2}}{2}[(\sigma_1 - \sigma_2)^2 + (\sigma_2 - \sigma_3)^2 + (\sigma_3 - \sigma_1)^2]^{1/2} \geq \sigma_0, \qquad (3.4)$$

where σ1, σ2 and σ3 are the main strains(three-dimensional intensities) and as σ_0 the material leakage threshold in single axial tensile.

It is worth noting that the Von Misses criterion shows that plastic leakage does not it depends on any single right or shear stress, but on the contrary it is a function of the differences of the main stresses, i.e. the maximum shear stresses. The criterion provides reasonable predictions for isotropic materials and does not give satisfactory results for anisotropic and viscoelastic materials.

3.5 Analysis of human gait

Step analysis is a major and important chapter of biomedical science because it deals with the analysis of forces and moments that develop in the joints and bones during gait. It also examines how the gaiters, muscles and joints work. Since even the slightest pain causes changes in walking, it is understandable that step analysis contributes to the diagnosis and treatment of lower extremity diseases.

A step cycle is defined as the set of movements and events that occur between two successful contacts of the same lower limb with the ground. The step can be divided into two main phases: posture and swing. During the posture phase one of the lower extremities remains in contact with the ground, while during the swing phase it is moved forward. In a healthy step, a complete step cycle consists of seven stages. The stance phase consists of three stages and includes as the first stage (initial contact) the heel-to-ground contact, as the second stage (middle position) the full support of the tread on the ground and as the third stage (boundary position) the finger's withdrawal. The swing phase comprises four stages, the first of which is the stepping of the toe which is common to both phases, the initial swing phase, the passage of the foot. floating lower limb the perpendicular plane to the ground (mid-swing), while the fourth stage comprises the lower extremity to full extent (marginal swing), shortly before its next (initial) contact with the ground, which marks the end of a complete step cycle . The distance between the middle posture of one lower leg and the middle posture of the other lower leg - in a step circle, is defined as a step. Swing-stop rotation creates two more subcategories of the cycle.

One subcategory in which body support is left at one lower extremity and another in which body support is assumed by both lower extremities. In a healthy treadmill and at normal walking speed, the stopping phase occupies 61% of the total cycle time, while

the swing phase occupies the remaining 39%. Circle events tend to be reported in percentages, e.g. during the cycle at 10% and 50% the support of the body takes place with the involvement of both ends and its duration is 20% of the cycle. At the beginning of the stop phase and at the end of the swing phase the initial-end contact duration is 12% and one of the lower limbs remains in full contact with the ground for 60% of the cycle, with the remaining 28% raise the heel with only the front of the lower limb in contact with the ground. The length of a regular step cycle varies depending on height, or weight, but on average is given at 1100msec. The hip muscles are also responsible for the movements of the lower limbs and the hip.
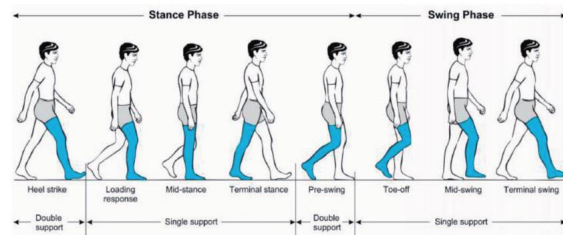
Figure 3-3: Human gait cycle

3.6   Stress shielding

During the walk, various loads are applied to the head of the femur, which creates stress on it. The phenomenon of "stress shielding" occurs when the stent is inserted into the femur and participates in the acceptance of loads and stresses. This results in a decrease in the stresses on the bone thus preventing proper growth.

A normal femur, without the stent, carries all the loads that are distributed, through the neck, from its head to the diaphragm and the rest of the bone. The upper part of the bone receives fewer loads, as a large load is created around the stent. Under Wolff's law, when the bone is loaded, it develops the proper structure to withstand it. In places where higher stresses and higher loads occur, there is more bone mass, whereas in places where lower stresses and smaller loads occur, bone mass is reduced. This may lead to the failure of the stent due to relaxation. Most research on this phenomenon studies the tendencies that develop in the femur with a built-in stent compared to the tendencies that develop in normal femur. Using the finite element model of the femur, the stresses are measured. Then taking into account the changing trends with the introduction of the stent in the bone it is possible to compare with other models.
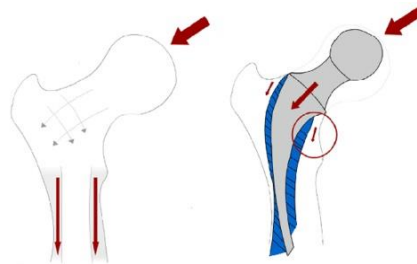
Figure 3-4: Stress-shielding-mechanism

4 Biomechanics and Finite Element Method

4.1 Biomechanics

Biomechanics is perhaps the oldest field of biomedical technology with references reaching as far as ancient Greece. The word 'biomechanics' was first used in the decade 1970 to describe every application of engineering science to biology and medicine. In ancient times the father of biomechanics was considered to be the Aristotle.

Biomechanics is the science that aims to represent living organisms with mechanical models. This representation may be related to the function of a cell, a tissue or even an entire cell organization. For this reason it is crucial for biomechanics to study the morphology and functions of biological materials and then to measure their mechanical properties and represent them with mechanical models. (Houcke,et. al, 2017)The ultimate goal of biomechanics is to develop materials and systems that support the mechanical properties of organisms. There is no need for the materials and systems that will used to be biological. It can be any materials as long as it meets the operating requirements of the organization.

4.2 Biomechanics of bones

Bones are the connective tissues of the skeleton and from a biomechanical point of view we are treated microscopically as a complex biphasic material, with one phase cells (organic part) and as a second phase salts and hydroxy-apatite (inorganic part). Their role is to provide the coherence required for static support of the body, movement and protection of internal organs. In its construction, the bone has a hierarchical structure and has the unique property of adapting (Wolff's law), that is, it is rebuilt and healed in such a way as to increase its resistance to mechanical load imposition. This is why bones do not have the same mechanical properties in all directions when loading on them, a phenomenon called material anisotropy (Maquet,et. al, 1985).
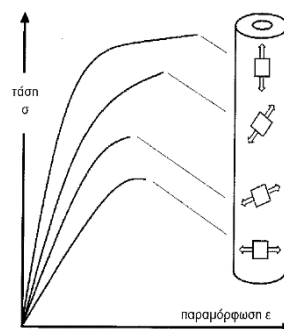
Figure 4-1: Strain-stress diagram for different angles in the femur (Wolff's law)

Although the relationship between mechanical load and mechanical properties is not similar in all living organisms, maximum bone strength is observed in the direction

most frequently loaded daily, e.g. in the femur, maximum strength is found in the vertical axis which, by imposing body weight and walking cycles, is strained daily by a much greater proportion than other bone axes.

Structurally and functionally, the bone is distinguished into a spongy interior and a compact exterior, which makes the material extremely durable in relation to its weight. In their chemical composition these two phases have no differences, but they differ significantly in their mechanical properties. The spongy bone due to its porosity is more ductile as a material but less resistant to tension. It consists of small bone needles projecting toward the center of the bone. These needles have been observed to be oriented in the direction of the external loads, so as to provide the greatest resistance with the lowest weight for each bone. On the contrary, compact bone is more durable but at the same time brittle.

Solid bone is usually found on the outer walls of the diaphragm and on the smooth outer surfaces of all bones. The thickness of the compact bone varies from bone to bone, depending on the requirements of the mechanical load exerted on it and the strength it is expected to have. It is this combination of solid and porous that gives the bone its good mechanical properties. In elongated bones, such as the thigh bone, we can generally distinguish the areas of the epiphysis and the area of the diaphragm. The pituitary gland is located at the end of the bone and is usually protected by a thin layer of vitreous tissue, the cartilage. The pituitary gland is the area of bone that contacts other bones and connects with them through the joints. Between the two parts of the pituitary gland lies the axis of the elongated bone called the diaphysis. The diaphragm has the structure of a hollow tube and in its cavity lays the bone marrow.

Generally, this cavity does not exist in flat bones and in very small bones of a complex shape.
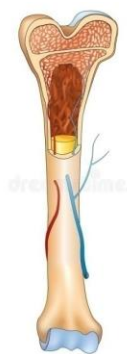
Figure 4-2: Internal structure of femur

The two main properties that are systematically studied in bone are its strength and stiffness. To study these two properties, the bone has to be subjected to a number of stresses. Bone, like most materials, has a leakage limit between the elastic and plastic area, although its plastic deformation prior to failure is much smaller than that of

metals. In addition, the behavior of this composite material depends on the speed of deformation.
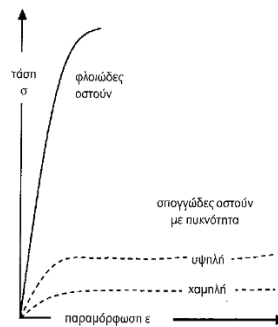
Figure 4-3: A typical stress-strain diagram for both types of bone

4.3 Historical evolution of the Finite Element Method

The Finite Element Method (FEM) derives from the requirements for resolving complex resilience and structural analysis problems in aeronautical and structural engineering. It is an evolution of the Native methods. The initial development of the method is traced back to the 1940s and the work of Alexander Hrennikoff and Richard Courant. A key common feature of this groundbreaking work is the discretization of a continuous space into a set of discrete spaces. In the 1960s and 1970s, FEM appeared in problems of elasticity, fluidity, heat transfer and nonlinear problems. At the same time, NASTRAN, the premier commercial building analysis program with the FEM, appears. In the 1980s, FEM is widely used by engineers, in universities and small businesses, due to the development of personal computers. The availability of a graphical interface for easier model development and presentation of results contributes to its dissemination FEM. In the 1990s, the method is applied to complex fluid mechanics problems, coupled multidisciplinary analysis, and large-scale problem solving on parallel computers. Completing the method in CAD (Computer Aided Design) and CAM (Computer Aided Manufacturing) environments is almost perfect. Nowadays, there are a plethora of construction analysis programs with (IBM) such as ABAQUS, ADINA, ALGOR, ANSYS, COSMOS / M, DYTRAN, MARC, NISA, LS-DYNA3D, LUSAS, MSC / NASTRAN, SOLVIA and others.

4.4 Finite Element Method - Description of the method

The Finite Element Method (FEM) is a method of approximate and arithmetic problem solving of continuous mechanical, fluid mechanics, arbitrary geometry field problems, boundary conditions and loads. It is used to find approximate solutions to some differential equations as well as to integral equations (Rapp, 2017). The approximate solution is based on the total elimination of the differential equation, solid-state problems, or the reduction of partial differential equations to an approximate system of ordinary differential equations, which is solved using standard numerical techniques

such as the Euler method and the Runge-Kutta method. The method is based on a combination of variable methods and local approaches applied to a finite element to solve the problem. Repeating local discretization in the rest of the medium entails discretization of the problem and approximation by linear algebra techniques. By discretion we mean the approach of a physical system, which has an infinite number of degrees of freedom, from a substitute model, which has a finite number of degrees of freedom.

The analysis with FEM is achieved using a computer, where differential equation systems are solved. These differential equations characterize the behavior of each structure. A fundamental step in analyzing and studying a structure with FEM is to segment the structure into a finite number of parts, called elements. The functions used within each element are simple, usually some polynomial expressions. These elements are linked together at specific points, called nodes. The set of nodes and elements after segmentation is the grid of the analysis.

Each node, depending on the type of construction, is characterized by some possible displacements called degrees of freedom of the node. In the case of two-dimensional analysis of a structure, a node may be displaced by and rotated about each of the x, y axes, while in the case of three dimensions the additional possible displacements are those of the z axis. In a three-dimensional construction, each point, and thus each node, has three degrees of freedom, while in two-dimensional construction it has two degrees and in the nets one. In bending structures to determine the position of the element the arrow is not sufficient, but the inclination is also required. So, for example, within each node have three degrees of freedom, which are the displacements along the x, y axis, and the turning of the node around the z axis. Knowledge of all nodes and degrees of freedom makes it possible to calculate the total possible displacements for the entire construction. Particular attention should be paid to how to support the under-construction of the structure, as it, depending on its type, blocks some degrees of freedom.
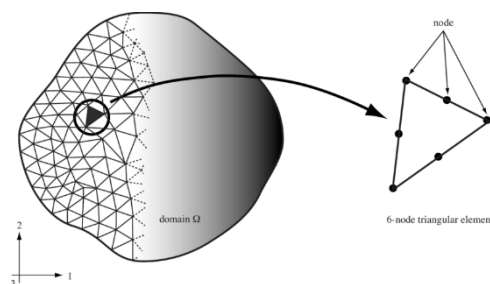
Figure 4-4: Finite-element discretization

Each finite element does not cease to have the same elastic behavior as the original body. The advantage of this subdivision is that the element is finite in size and simpler in form. These properties allow for an approximate study of the element's intensity.

Therefore, knowing the displacements of the nodes of an element, it can be used to calculate the displacements of each point of the element. The next step is to calculate the strains and then the stresses. With these elements, one can apply the Energy Theorems (Principles of Possible Works), which give equations that determine the unknown node displacements, where no total number of nodes of construction and the number of degrees of freedom of each node.

Advantages of the Finite Element Method are:

 i) The interpolation functions are simpler.

 ii) Completions are made in each element separately, so in simple cases, the result is easily read in detail, while in the more complex one numerical integration can be used.

 (iii) The analysis and study of a construction by this method is advantageous over other methods because it enables the user to vary the dimensions and applied forces of the construction concerned and to monitor stresses and strains at regular intervals.

4.5   Formulations-type of finite elements
A key initial model concern is the selection of appropriate finite elements with the appropriate number of nodes.

The following are the most common finite elements, which break down the structures to be studied (Rapp, 2017).

• One-dimensional straight or curved (1D), which have physical properties such as axial, flexural and torsional stiffness. This type of element is ideal for modeling rods, beams, wires, nets, frames. Straight elements usually have two nodes, one at each end, while curved elements require at least three nodes.

• Two-dimensional (2D) elements for bending action (plates, shells) and / or membrane action (flat stress, flat strain). They can have a variety of shapes, such as flat or curved triangles and squares. Nodes are usually placed at the corners of the element. If greater accuracy is required, additional nodes may be positioned along the edges of the element or even within the element.

•Tore-shaped elements for axisymmetric problems, such as thin and thick plates, shells, solids. The cross-section of these elements is the same as in the preceding types: one-dimensional for thin plates and shells and two-dimensional for solid, thick plates and shells.

 • 3D elements for modeling 3D solids, such as machine parts. Otherwise called volume data. Common data formats are tetrahedrons and hexahedrons. The nodes are placed on the tops and possibly inside the element.
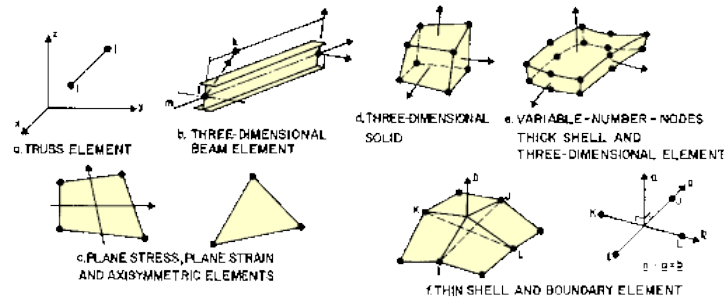
Figure 4-5: Finite elements

Elements may have physical properties such as thickness, coefficient of thermal expansion, density, elasticity, shear and Poisson's ratio. When modeling constructions it is possible to use a combination of all these elements, provided that the individual elements are compressed. Common nodes have the same degrees of freedom.

Finite elements differ in many ways. For finite element analysis, the most important features are the shape of the element and its degree of interference. The degree of interference of the element refers to the degree of the polynomial that appears in the form's function of the element. The degree of a polynomial is called p, while the dimension of a polynomial is called h. Dimension h is usually the diameter of the smaller circle, or smaller sphere, in the case of a three-dimensional element, which surrounds the element (outlined circle). Each element has dimension h and degree p.

The multitude of elements that must be used to solve a particular problem is a result of the engineer's judgment. The general rule of thumb is that the larger the number of nodes and elements or the greater the degree of polynomial of the form function, the more precise the solution of finite elements, and the more expensive the solution.

The multitude of elements that must be used to solve a particular problem is a result of the engineer's judgment. The general rule of thumb is that the larger the number of nodes and elements or the greater the degree of polynomial of the form function, the more precise the solution of finite elements, and the more expensive the solution. For structural analysis, commercial programs typically use finite element matrix analysis, which can be further classified into two basic approaches: the commonly used displacement or stiffness method and force or flexibility method. The finite element software we will use in our analysis is ANSYS.

4.6   The mechanical properties of bone and FE modeling

Bone Mechanical Properties
For general physiological loading conditions the bone material can be considered linear elastic. The constitutive stress–strain relationship shows that bone material behaves in manner similar to that of other engineering materials. Stress–strain curves in tension and compression consist of an initial elastic region, which is nearly linear. This region is followed by yielding and considerable, nonelastic, 'plastic' deformation before a failure. The nonelastic region of the stress–strain curve for the longitudinally oriented specimen

reflects diffuse, irreversible micro damage created throughout the bone structure. Bone tissue that is loaded into this nonelastic region will not return to its original configuration after the load is removed (Kojic,et. al, 2008).

The bone tissue is a two-phase material consisting of collagen and bone mineral, organized in matrix form. Bone mineral (hydroxyapatite) is very rigid and has bigger compression than tensile stiffness. On the other hand, bone collagen has only tensile stiffness. Generally, the bone mineral influence on the mechanical properties of bone tissue is predominant. Hence, bone tissue has bigger compression than tensile stiffness and strength. Also, bone tissue has anisotropic behavior caused by specific micro structural organization. Investigations show that bone tissue is stronger and stiffer in the direction of the osteon orientation than in the perpendicular direction. Because of that, bone stability depends not only on load value, but also on load direction. Elastic modulus and strength of bone tissue are not constant. They are dependent on rate of deformation. Rate of deformation is usually quantified with material strain rate. Because of that, bone tissue is viscoelastic material. Studies in which bone specimens were exposed to loads of different strain rates showed that increasing of strain rate caused increases of the elastic modulus. The elastic modulus of bone tissue is approximately proportional to the strain rate raised to the 0.06 power. Using this relation it can be shown that over a very wide range of strain rates the elastic modulus increases by about a factor of two. Experimental analysis revealed that the apparent density is important for elastic modulus estimation and the following relationship was proposed.

$$E_{axial} = E_c \dot{e}^{0.06} \tag{4.1}$$

Where E_{axial} is the elastic modulus of bone of apparent density ρ, tested at strain rate of $\dot{e}(s^{-1})$ and E_c elastic modulus of bone with an apparent density of ρ_c tested at strain rate of $1.0 s^{-1}$.

With respect to composition and true tissue density, cortical and trabecular bone are very similar. However, their structural organization is very different. The basic difference of cortical and trabecular bone tissue is porosity. Cortical bone porosity ranges from 5 to 30 %, while trabecular bone has porosity from 30 to 90 %. The apparent density of bone tissue for both cortical and trabecular bones shows approximately linear dependence on bone porosity

Finite Element Modeling
The bone structure is usually modeled by 3D finite elements in order to capture the bone geometry, and we here write the dynamic equation of motion for a 3D finite element

$$M^{\,n+1}\ddot{U} +^{n} KU =^{n+1} F^{ext} \tag{4.2}$$

Where M and ^{n}K are the element mass and stiffness matrices, $^{n+1}\ddot{U}$ and U are nodal acceleration and displacement vectors, and $^{n+1}F^{ext}$ is the external nodal force which includes structural external forces and action from the surrounding elements. The equation of motion corresponds to time step 'n', where the left upper indices 'n' and 'n+1' indicate, respectively, start and end of time step. The stiffness matrix ^{n}K can be written as:

$$^{n}K = \int_V B^{Tn}CBdV \tag{4.3}$$

Where B is the strain–displacement matrix and ^{n}C is the constitutive matrix for an isotropic material, the left upper index 'n' is used to show that the axial modulus corresponding to the strain rate $^{n}\dot{e}$ may be used when the rate effects are important.

The derivatives of the interpolation functions are denoted as $N_{K,i} = \partial N_{k}/\partial x_{i}$ and the strain-displacement relation matrix B is defined by these derivatives.

$$B = \begin{bmatrix} N_{1,1} & 0 & 0 & ... & N_{N,1} & 0 & 0 \\ 0 & N_{1,2} & 0 & ... & 0 & N_{N,2} & 0 \\ 0 & 0 & N_{1,3} & ... & 0 & 0 & N_{N,3} \\ N_{1,2} & N_{1,1} & 0 & ... & N_{N,2} & N_{N,1} & 0 \\ 0 & N_{1,3} & N_{1,2} & ... & 0 & N_{N,3} & N_{N,2} \\ N_{1,3} & 0 & N_{1,1} & ... & N_{N,3} & 0 & N_{N,1} \end{bmatrix} \tag{4.4}$$

The constitutive matrix for an isotropic material depends on Young's modulus (E) and Poisson's ratio (v):

$$C = \frac{E(1-v)}{(1+v)(1-2v)} \begin{bmatrix} 1 & \frac{v}{(1-v)} & \frac{v}{(1-v)} & 0 & 0 & 0 \\ \frac{v}{1-v} & 1 & \frac{v}{(1-v)} & 0 & 0 & 0 \\ \frac{v}{1-v} & \frac{v}{1-v} & 1 & 0 & 0 & 0 \\ 0 & 0 & 0 & \frac{1-2v}{2(1-v)} & 0 & 0 \\ 0 & 0 & 0 & 0 & \frac{1-2v}{2(1-v)} & 0 \\ 0 & 0 & 0 & 0 & 0 & \frac{1-2v}{2(1-v)} \end{bmatrix} \tag{4.5}$$

4.7 Description of structural systems

The overall equilibrium equations for linear structure static analysis are (Ansys, 2009):

$$[K]\{u\} = \{F\} \quad \text{Or}$$

$$[K]\{u\} = \{F^{a}\} + \{F^{r}\} \tag{4.6}$$

Where:

$[K] = \sum_{m=1}^{N}[K_{e}]$ =total stiffness matrix

$\{u\}$ =nodal displacement vector
N = number of elements
$[K_{e}]$ =element stiffness matrix

$\{F^{r}\}$ = reaction load vector

$\{F^{a}\}$ =the total applied load vector

4.8   Modeling using the ANSYS program

In general, for the analysis of a construction with commercial software based on FEM, we distinguish the following steps (ansys.com):

➢ First step: Defining geometry
➢ Second step: Selecting the type of finite elements and discretizing the geometry into finite elements.
➢ Third step: Define the mechanical and physical properties of the materials (can be done at an earlier stage) and enforce the boundary conditions.
➢ Fourth step: Choosing the solution and the solution.
➢ Fifth step: Read the results and graphically represent them.

The operation of ANSYS software, like most similar commercial software, consists of three phases:

▪ preprocessing, in which the first three steps are performed
▪ Solving the finite element model
▪ Postprocessing of results
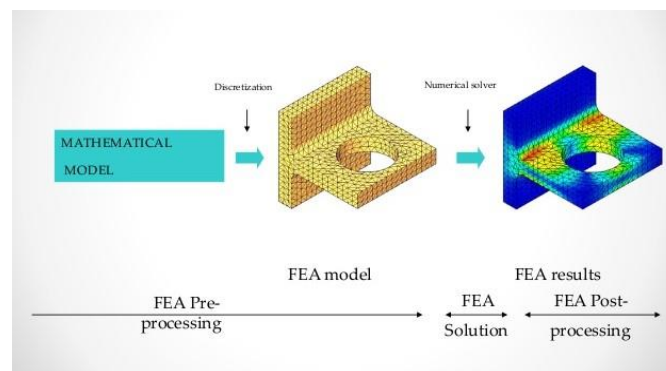
Figure 4-6: Basic Steps in the Finite Element Analysis

More detail:

The initial step in the pretreatment phase, in the so-called ANSYS preprocessor, is to construct the geometry of the object to be simulated. Geometry can be constructed in the ANSYS environment in two ways. In the first way, keypoints are created, after which lines are produced; surfaces are produced, with the final result being the construction of volumes. In the second way they are made directly of volumes or surfaces, either from points without creating lines or giving dimensions. If the geometry is created outside the ANSYS environment, it can be created either in a CAD drawing environment and subsequently imported in the IGES file format or by a standalone preprocessor that provides an input file for the ANSYS environment. This file is called neutral.

Then the type of finite elements is selected. This depends on the resolution to be made, which does not mean that the item cannot be changed later. The mechanical and physical properties of the material are then defined. The properties depend on the specificity of the materials and the type of solution to be performed. Then follows the discretization of the model's geometry. To this end, the options offered by the program are automatic grid creation, element size determination (maximum side or edge size) or line partitions, and subsequent grid creation, and the Smart Size option that adapts the grid to geometry. The latter option shrinks elements in areas of abrupt change of geometry and dilutes them inside tumors or surfaces, where there is no particular need for fine separation.

The final stage of the preprocessor is the imposition of boundary conditions. These can be applied either to geometrical elements (points, lines, surfaces, volumes) or to nodes in the grid.

The choice of solution is tailored to the requirements of the problem. The researcher determines whether the physical phenomenon that is called to simulate relates, for example, to elastic analysis or potential problem, whether it is a static or dynamic problem, and whether it is a linear or non-linear problem. As far as solving is concerned, there are many possibilities that are related to different solving algorithms, which will not give a different result but will require different resolution time.

In the last phase of the software the results are recorded in a new file after the solution. The results can be read in different ways in the program's processor. Two of them are Nodal Solution and Element Solution. In the first, the nodes are given the average value resulting from the finite elements in which they are common, while the second is given a value per finite element. Finally, there is a third way of reading the results with the Element Table option, which normalizes the results by calculating averages.

Finally, it is clarified that a problem is called a linear problem in which if the magnitude of the external actions (forces in our analysis) is doubled, then the magnitude of the result is doubled (the shifts in our analysis). A nonlinear is called a problem that does not apply to the linear ratio. In elastic analysis problems the nonlinearity may be due either to material nonlinearity or to the changing contact between two or more bodies (geometrical nonlinearity). In both cases, the stiffness register is not stable, as opposed to the displacement interference functions.

5   State of the art

There have been several studies on total hip arthroplasty, numerical/ computational or clinical or experimental. If we take a historical look back we will see that others study the intent material with finite elements, others the shape, others the size. Below are some of the most recent studies

In the study (Bennett,et. al, 2008) an analysis of finite elements in six different design endoprosthesis was applied. The analysis was performed with the help of the ANSYS program. The implants received forces between 2.5 and 7 kN. These forces were selected because during the walking cycle, forces are created up to 6-7 times the body weight on the hip joint. Later the results of the finite element analysis were compared between the different models of endoprosthesis with different cross sections. The aim of the interior design is to accept small voltages, small displacements and minimal wear and tear in large stresses.

In this article, the analysis of the stress of endoprosthesis and basic implant designs for the materials under consideration was performed. Then the intentions that had the biggest trends and distortions were optimized to accept lower prices of trends and distortions. The analysis of wear and tear was carried out considering that the endoprosthesis were made of metal with a polymer coating. Common materials such as stainless steel (SS), cobalt-chromium alloy (CoCrMo) and titanium alloy (Ti6Al4V) have also been used. These materials were used because they have great durability and excellent biocompatibility for a long time in the human body.

Over time, the vertical force ranged between 0.0 and 1.4 of body weight. Vertical force exceeds the body weight by about 25% and 75% in the completion of the step, as the force and acceleration have the same direction. Also, the vertical force is zero when the foot is in the suspension phase, which phase accounts for 40% of the foot walking cycle.

The loss of material was also calculated at the point of the joint where the head material (CoCrMo, SS, Ti) comes into contact with its polymer coating and the results are presented in the diagram below.
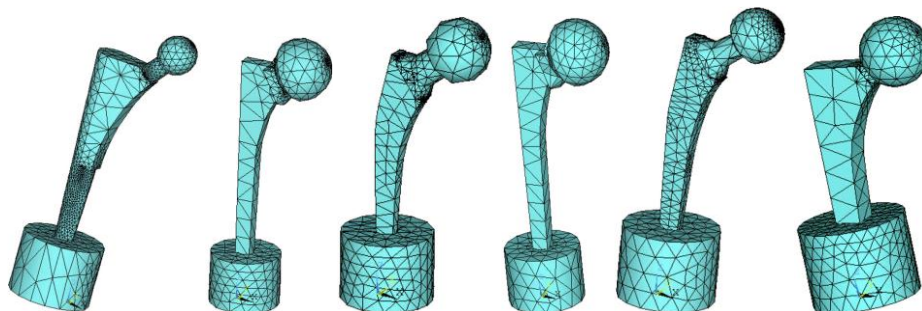
Figure 5-1: Six different endoprosthesis that were used

One head size and neck length was used for analysis. The materials were defined as isotropic and linearly elastic. Then the endoprosthesis 1 and 6 were redesigned with different cross-sections as shown in the figure, where cross-section 1 is the original.
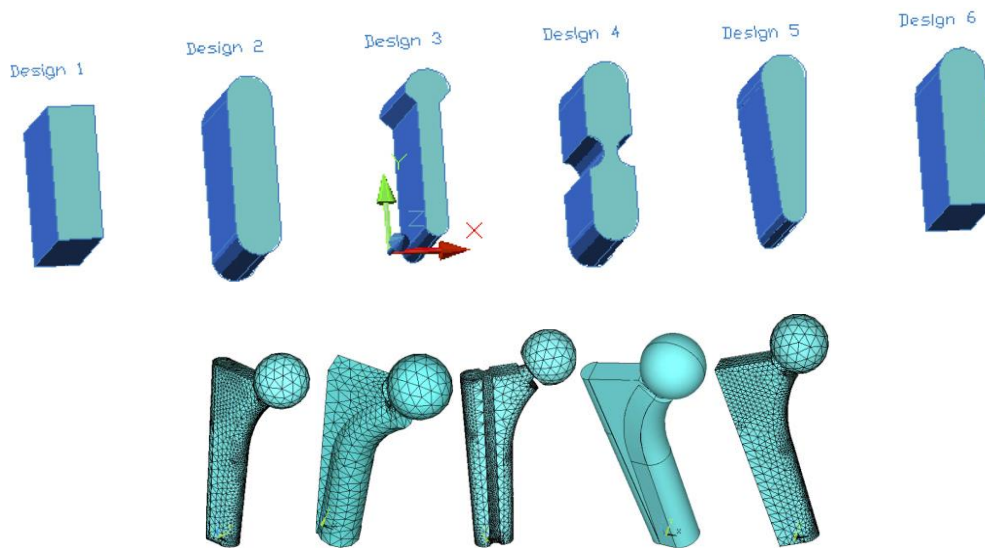
Figure 5-2: The endoprosthesis 1 and 6 were redesigned with different cross-sections.

The forces were applied in the form of pressure, which can be represented by a point force. The part of the endoprosthesis that is embedded in the bone was also defined as thickened.
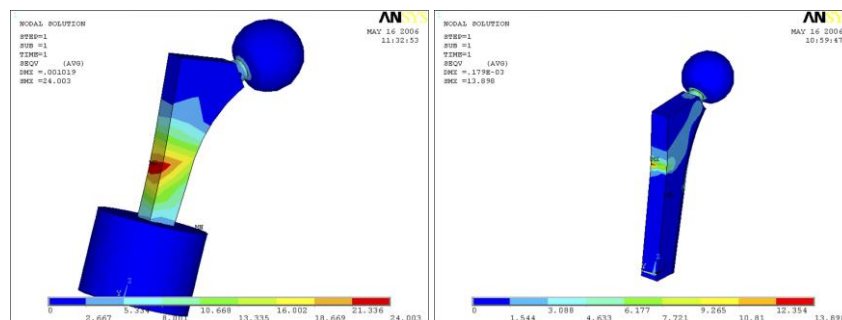
Figure 5-3: Stress that exists at different endoprosthesis.

This study concludes that the rectangular cross section of the Model 6 received three to four times more stresses than the other five cross sections designed. The improved cross-sections of the endoprosthesis had a larger cross-sectional area so there was a significant reduction in the concentration of stresses. Cross section 5 had the lowest voltages. Another cross-section that showed reduced trends was cross-section 6; this cross-section would be the best since the trend values were very low compared to cross-section 1.

The (Saputra,et. al,2013) is an article that investigated the range of motion of the human activities of the Western-style and the Japanese-style using finite element analysis for

THA patient. The Western-style activities consist of picking up, getting up and sitting, while the Japanese-style activities consist of sitting on legs with fully flexed at the knee (seiza), squatting and sitting on legs with fully flexed at the knee (zarei).This study investigated the probability of prosthetic impingement to occur and to calculate the von Mises stress during the activities. The acetabular liner cup positions were varied.
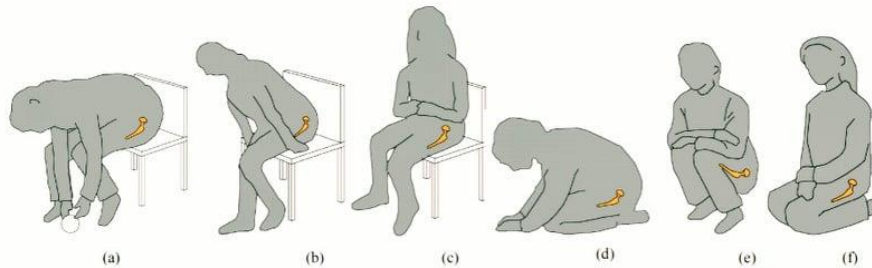
Figure 5-4*:* (a) Picking up an object while sitting on the chair, (b) Getting up from the chair, (c) sitting down on the chair, (d) Bowing while sitting on legs fully flexed at the knee (zarei), (e) squatting, and (f) sitting on legs fully flexed at the knee.

The finite element model of the contact system in the study consists of femoral head, femoral neck and acetabular liner cup. The femoral head and the femoral neck component are assumed to be rigid. The acetabular liner cup component is modeled as an elastic-plastic material with isotropic hardening. Diameter of the femoral head and the femoral neck are 28 mm and 14 mm, respectively. The thickness of the acetabular liner cup is 7 mm. A gap between the femoral head and the acetabular liner cup is 24 µm.
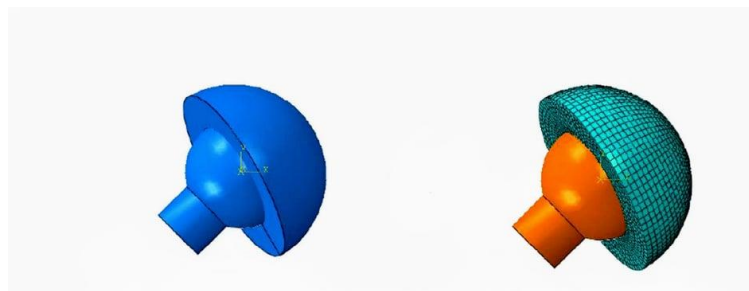
Figure 5-5: Model of the femoral head and the acetabular liner cup

The loads in the x, y and z directions were Fx = 15 N, Fy = 270 N and Fz = -427.5 N, respectively, and were applied on a point at the center of the femoral head. All the degree of freedom at the outer surface of the acetabular liner cup is constrained. The simulation is conducted in two steps: firstly, the load is applied to the center of the femoral head with constraining the rotation of the femoral head is constrained and

secondly, the load at the center of the femoral head is constrained with rotating the femoral head. The range of the rotation is according to the RoM of human activities.

The variation of the angle between inclination and anteversion of the acetabular liner cup is simulated in order to study the possibility of the impingement to occur between the femoral neck and the acetabular liner cup lip. The variations of inclination of the acetabular liner cup are 45º and 60º and the variation of anteversion of the acetabular liner cup are 15º and 30º. The angle of the femoral neck axis line and the femoral stem axis line is 135º. The simulation uses a femoral head diameter of 28 mm.
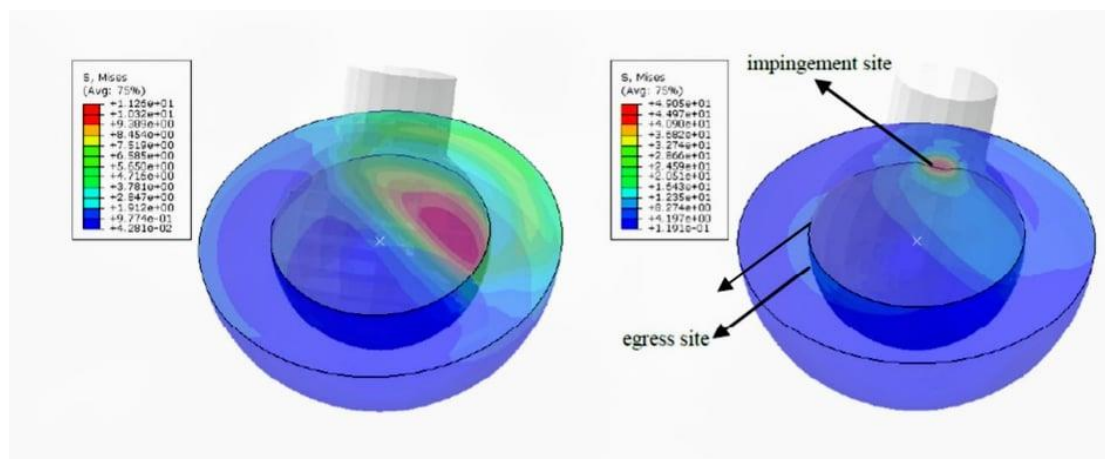
Figure 5-6: The von Mises stress for: getting up activity and picking up activity where the acetabular liner cup position is 45° inclination and 15° anteversion of the Western activity.

Based on the results, it can be stated that most activities in the Western-style and Japanese-style can be performed safely by the THA patients. The impingement and dislocation are predicted to occur at picking up activity in the Western-style activity for the inclination and anteversion combination of the acetabular liner cup of 45º-15º. The seiza activity in the Japanese-style activity is not recommended to be performed for the THA patients because of the safety margin of the internal rotation is less than 10q. The impingement between the femoral neck and the acetabular liner cup lip during a contact situation can be predicted by the finite element simulation. It is demonstrated that the von Mises stress at the impingement position is higher than the yield strength of the material.

Finally, in our study, a three-dimensional patient bone that has undergone total hip arthroplasty was modeled using Solid Edge V19. The bone was analyzed for stresses / forces when cycling, sitting down, standing up, knee bending, walking, stance, stairs up, stairs down and jogging. Stress analysis was performed using Finite Elements Analysis to investigate the behavior of the human femur during these activities.

In the study (Kumar,et. al, 2015) a three-dimensional virtual bone was modeled using Solid Edge V19. The bone was analyzed for stress and strain while walking, standing, running and jumping. Trend analyzes were performed using the ANSYS 14.0 computer program to investigate the behavior of the human femur during these activities. The results were compared with previous studies.

Bone modeling was performed using 3D design software and it was observed that the maximum and minimum voltages are located at designated points, so the bone behaves similarly to that of the beam. This study identifies stresses and deformations in two charging cases: Only with the reaction force from the hip and with all the forces exerted by the muscles, the maximum compression voltage takes place in the middle of the escape and the maximum tensile stress side by side. The bending torque is reduced in case the muscle forces are added to the measurements. Curvature reduces the ability to apply stress to the bone, ie it reduces its mechanical strength. This study does not take into account the strength of the muscles in the bending position.

There are many methods for modeling a femur in which radiographic and axial data are used, but due to a lack of such data, a virtual femoral bone with Solid edge V19 was modeled. Dragos POPA proposed a method of creating a CAD model with the help of dimensions obtained from human femur. The dimensions obtained are divided into six different two-dimensional designs, which can be converted into a single three-dimensional model. The properties of the materials are shown in the table below. Although bone is a clear example of a natural composite material, its properties vary from point to point, but in this study it is considered an isotropic material.

The CAD model is inserted into the ANSYS computer program and the geometry grid is created. For several curved points of the model, grid processing applications were used. The data size was 2.5mm using the sizing application from the grid application menu. Network optimization was performed using pre-selected software options, which increased the quality of the network even more, thus giving better results.

Further marginal conditions were applied, such as: one end being pressed, at the other end a force application of 705N, ie considering the person healthy with a weight of 72 kg, a torque caused by the 10000 N-mm muscle was applied to the case of simple walking.
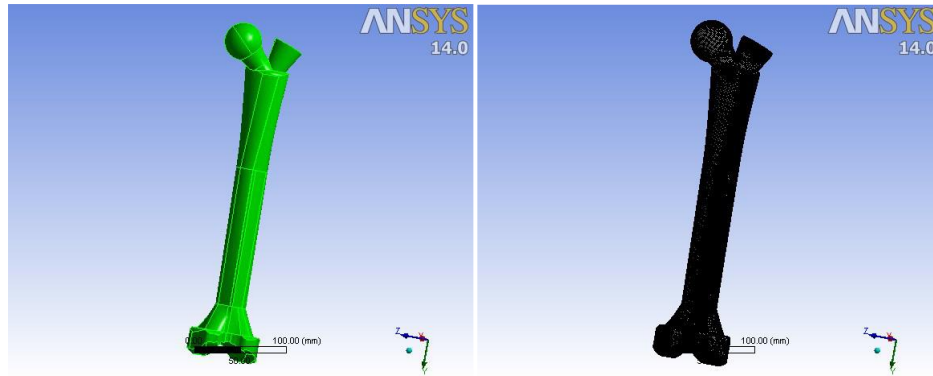
Figure 5-7: Femoral geometry

The SHELL181 element was used to analyze structures with porous characteristics. It has four nodes with six degrees of freedom at each node. It is generally used in applications with large, linear rotation, and / or for large non-linear distortion. Many times SHELL181 is used instead of the SHELL43 element due to the convergence problem as shown in Figure 2.

The results of this study suggest that the femur is loaded during daily activities. Activities include standing, regular walking, running and jumping.
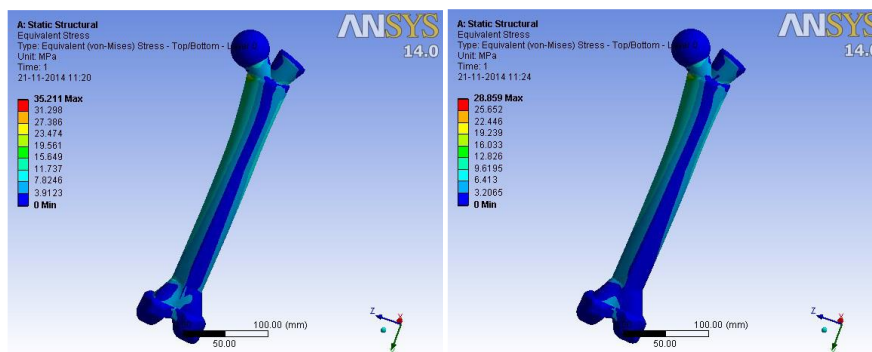
Figure 5-8: Total Stress developed during Walking and Standing
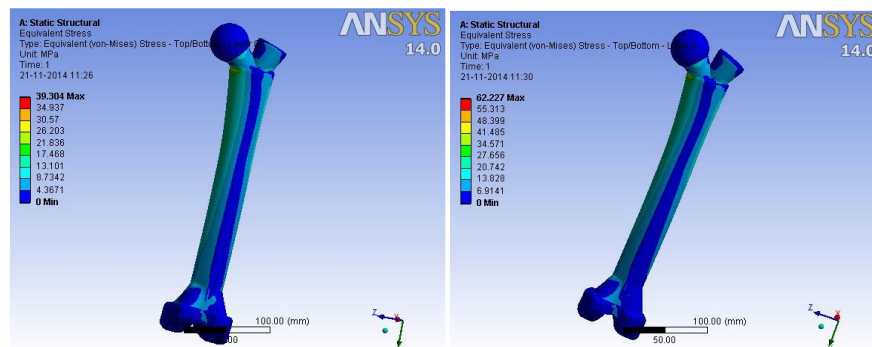
Figure 5-9: Total Stress developed during Jumping and Running

For gait, a force of 750N was imposed on the knee joint while the femoral head is pinned. The torque of the knee joint was set at 10000N-mm. The analysis showed that during normal walking the stress developed was 7.41 MPa.

During the jumps, an 850 N force was applied to the knee joint while the femoral head was pinned. Knee torque is considered to be 10000Nmm. The vertical trend developed during the activity was 8.73MPa. Similarly, during running, a 1410N force was applied to the femoral head, with the same torque on the knee joint. The vertical trends developed were 13.82 MPa. The effects of stress developed on activities are below the safety level of a healthy person's femur.

The results of the study are improved compared to previous research. There was a small variation in the numerical results of the trends due to deviations in modeling. This study focuses mainly on the reaction of the femur to the imposition of stresses during daily activities. The analysis did not apply the muscles that create additional tendencies in the bone, otherwise the tendencies would increase by 30%. The results of this research can be used to find the trends that will lead to a bone fracture. In addition it helps in the choice of the thickness and the type of material that will be used for the treatment of cracks and fractures in the bone. It can also help in the selection of materials for the creation of artificial bones.

The study (Baharuddin,et. al, 2014) proposed a new design process of the cementless femoral stem using a three dimensional model which provided more information and accurate analysis compared to conventional methods.

This complete design cycle began with morphological analysis, followed by femoral stem design, fit and fill analysis, and nonlinear finite element analysis (FEA). Various femur parameters for periosteal and endosteal canal diameters are measured from the osteotomy level to 150 mm below to determine the isthmus position.

Generally, the femur image of the patient is taken by standard radiograph and the template given by the implant's manufacturer was used to determine the implant's size. However, we proposed another method which was more efficient than the conventional methods. The first step was to acquire the computed tomography (CT) dataset of the femur, followed by the reconstruction of three dimensional (3D) morphological analysis. The 3D anthropometric dataset of 60 healthy subjects were then used to design a cementless femoral stem before performing a 'virtual surgery of hip arthroplasty' using the "averaged" femora based on our previous studies. The canal fit and fill were analyzed for the optimal implant, and finally the finite element model was analyzed to examine stress distribution, displacement and micro motion.
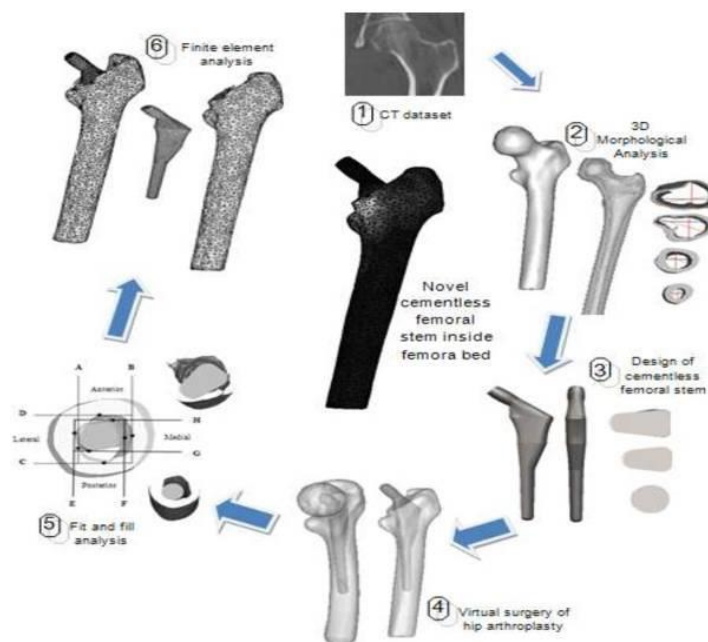
Figure 5-10: Summarize steps of designing the cementless hip arthroplasty.

A cross sectional study was carried out from January 2009 to December 2009 following approval from the National Medical Research Register (NMRR) and the local hospital ethics committee. We measured the femora periosteal and endosteal canal diameters of 60 healthy femora (30 male, 30 female). The average age for all subjects was 25.01 ± 5.18 years. The average weight was 70.76 ± 14.38 kg for male and 53.31 ± 13.11 kg for female. The average height was 170.96 ± 6.37 cm for male and 156.02 ± 6.17 cm for female. Subjects were excluded from this study if they were pregnant, had experienced prior femur injury or bone disease (osteoporosis, osteoarthritis, and rheumatoid arthritis), had abnormal body mass index (BMI), wore implants or underwent a computed tomography scan less than 6 months from the date of consent filling. This was verified by clinical examination and computed tomography (CT) images. The femora image was acquired using four row multi slices CT scanner (Somatom, Volume Zoom, Siemens) operating at 120 kV and 90 mAs. Other scanning parameters were set: 1.25 mm collimation, 3.0 mm thickness, 1.5 mm recon increment, 12.0 mm table feed per rotation and 512 x 512 pixel resolution. Subjects were asked to lay down in a supine position with their feet stabilized using the specially designed wooden jig to standardize foot position during image acquisition. Gonad shields were used and no contrast media was administered.

The "average" morphology of bone used as a guideline for the implant's design, which better addresses the population diversity. The assumptions made regarding size selection and implant design were based on this "average" femur provides the actual figure of the bone itself. The best fit and fill were considered to contribute to the fixation stability of the implant. Combining the parameters acquired from periosteal and endosteal canal, the stem design was done carefully. The implant width is in accordance with the femora endosteal canal diameter to achieve optimal fit and fill with the bone and promoting osseointegration between implant – bone.The implant length and distal

size did not exceed the position of the isthmus level or the isthmus canal diameter. The stem neck followed standard 12/14 taper. The optimal stem cross section geometry is according to the endosteal canal shape; wedge shape at the metaphyseal region, tapered at middle region, and cylindrical at distal. The medial and lateral curvature followed the actual femora proximal radius; lateral flares provide the "rest fit" for the implant, better physiological load and prevent subsidence distribution. The proximal region provides three contact points between the implant and bone for better primary fixation stability. The distal stem was designed straight with 1° taper to reduce strain distally.
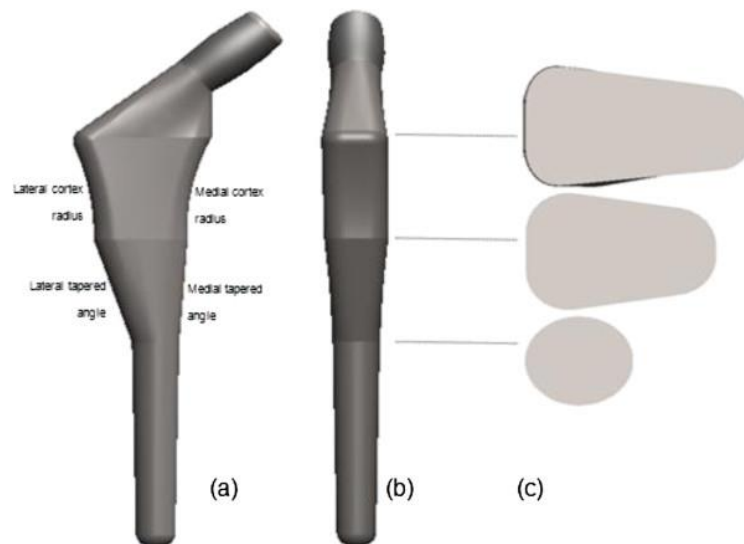
Figure 5-11: Cementless femoral stem design according to the femur morphology (a) mediolateral view (b) anteroposterior view (c) cross section view.

Virtual implantation was simulated in Mimics 12.1 software where the newly designed cementless femoral stem was aligned inside the "average" femur canal which was developed from the previous morphological study as shown in Figure 5. The femur neck was resected at the osteotomy level (20 mm above the center of lesser trochanter). The fit and fill were essential to the femoral fixation stability and determined the success of the implant. Fit was defined as 1 mm or less perpendicular distance between the implant and endosteal. The fit was determined by translating the contact between the implant and the endosteal canal into a straight line. The contact area was computed by trapezoid area, with fit acting as the base of the trapezoid, and the height from the cross section. In addition, fill was defined as the percentage of the implant area within the femur intra medullary from the anteroposterior view and mediolateral view for each cross section . The cross section was divided into three levels; proximal, middle and distal. The proximal represented the metaphyseal region, medial (the upper end of isthmus) and distal (10 mm above the stem's tip). The goal was to acquire the optimal fit and fill and as such, the stem should be within reasonable size, making it easier for the orthopedic surgeons without breaking the femur. The newly designed stem was then compared with other cementless stems.

Two static physiological loadings were simulated; normal walking and stair climbing. The result focused on three parameters; equivalent von Mises stress, micromotion and displacement. Two other parameters were observed in this study; total strain energy density and contact normal stress.
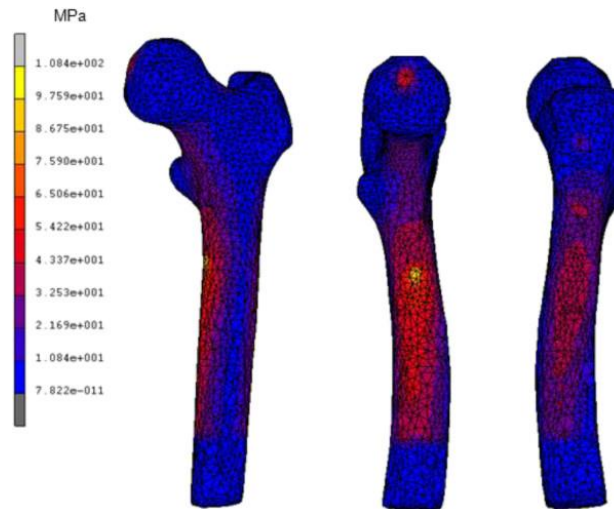
Figure 5-12: Contour plots of equivalent von Mises stress using stair climbing loading from frontal view, medial view and lateral view.
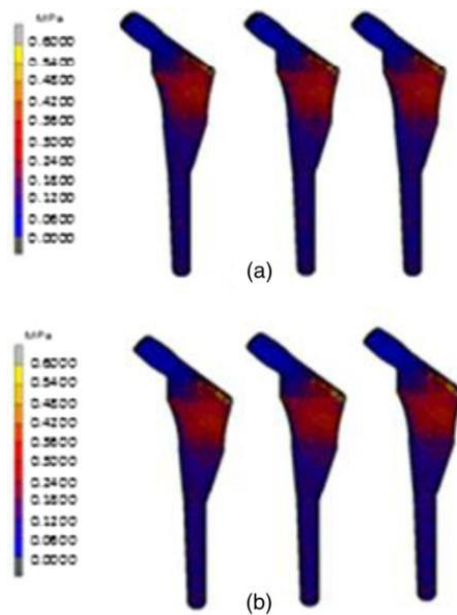
Figure 5-13: Contour plots of equivalent von Mises stress using normal walking loading and stair climbing loading

The results showed better total fit (53.7%) and fill (76.7%) canal, with more load distributed proximally to prevent stress shielding at calcar region. The stem demonstrated lower displacement and micromotion (less than 40 μm) promoting osteointegration between the stem–bone and providing primary fixation stability. This new design process could be used as a preclinical assessment tool and will shorten the

design cycle by identifying the major steps which must be taken while designing the femoral stem.

The article (Zameer,et. al, 2015) studied the mechanical strength of the femur in the imposition of trends that create daily activities, with the computer program ANSYS. Figure 5.14 shows the hip joint, which was modeled using the CATIA design program. Endoprosthesis and femoral design were performed separately and assembled using CATIA applications. For the construction of the joint model, the standard dimensions of the human femur based on experimental results were used. Optimizations for model restructuring have also been introduced in the design.

The dimensions of the hip implant are as follows, the diameter of the femoral head is 27mm, the inclination of the neck is 45 degrees, the outer radius of the prosthesis is 9.93mm, the inner radius is 8.04mm and the length of the neck is 172.25mm. The endoprosthesis form is that of a compressed cone, it also has a conical cross section designed to reduce the diffusion and relaxation of the endoprosthesis and increase the stability and fatigue resistance of the implant. Contact of data exists only if one surface element penetrates another element. For contact surfaces they are defined as fully connected.
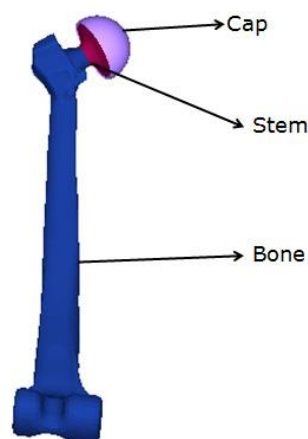
Figure 5-14: CATIA model of the assembled hip joint

The materials used were: UHMWPE / TiO2 Complex polymer, Cap, porous bone, cortical bone. In which the measure of elasticity, the Poison ratio and the leakage limit were defined.

The static analysis was performed with the computer program ANSYS11. In the measurements it was considered that the bone accepts all the weight of the body. The bone being examined is the right hip in an upright position. The boundary conditions were set: all the nodes at the bottom of the bone, ie the knee, were considered to be packed. The hip is subjected to a vertical force of 1304N on brisk walking, 1270N on normal walking, 431.9N when bending the knee and 1473N at the descent of stairs.

Also added is a 1937N force exerted on the bone by the muscle on the large trochanter at an inclination of 20 degrees.
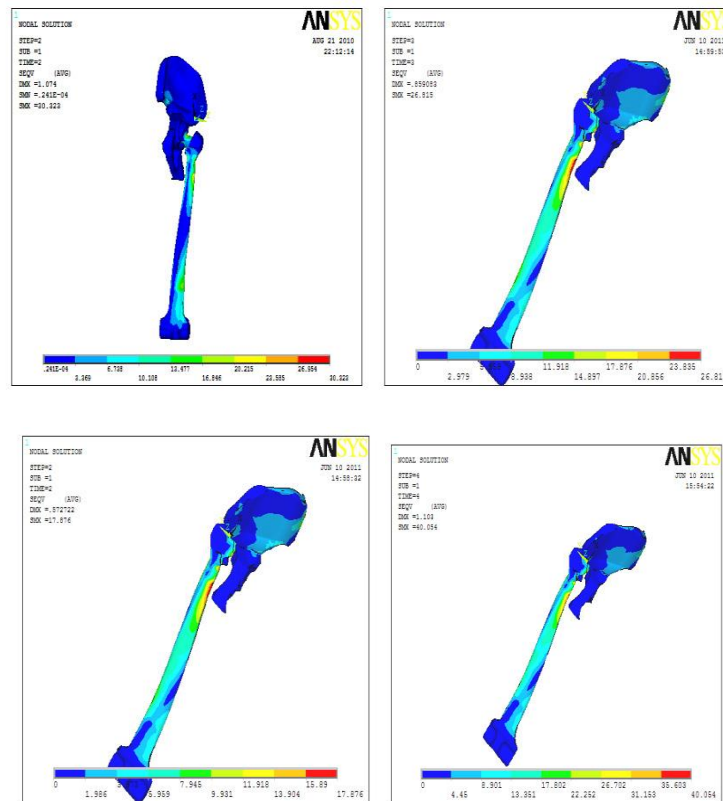
Figure 5-15: Distribution of Von Mises strains with 1270N, 1304N, 431.9N and 1473N power.

The maximum stress at normal walking is 45,485 MPa and the displacement is 1,611 mm. Maximum stresses were observed along the neck while reduced voltages were observed towards the thickened end. It was also observed that the maximum stress at brisk walking was 30,323 MPa and the displacement was 1,074 mm. During knee flexion, the maximum stress was 21,463 MPa and the displacement was 0.687 mm. Maximum stresses appeared in the area below the neck. On the descent of the stairs the maximum stress was 21.054 MPa and the displacement 1.103 mm. Maximum stresses occurred in the neck area.

The objective of the study (Abdullah,et. al , 2017) is to predict the risk of femoral bone fractures in total hip arthroplasty (THA) and resurfacing hip arthroplasty (RHA). Femoral bone fracture is one of the main causes for the failure of hip arthroplasties (HA). Being subjected to abrupt and high impact forces in daily activities may lead to complex loading configuration such as bending and sideway falls. A computed tomography (CT) based on finite element analysis was conducted to demonstrate damage formation in a three dimensional model of HAs.
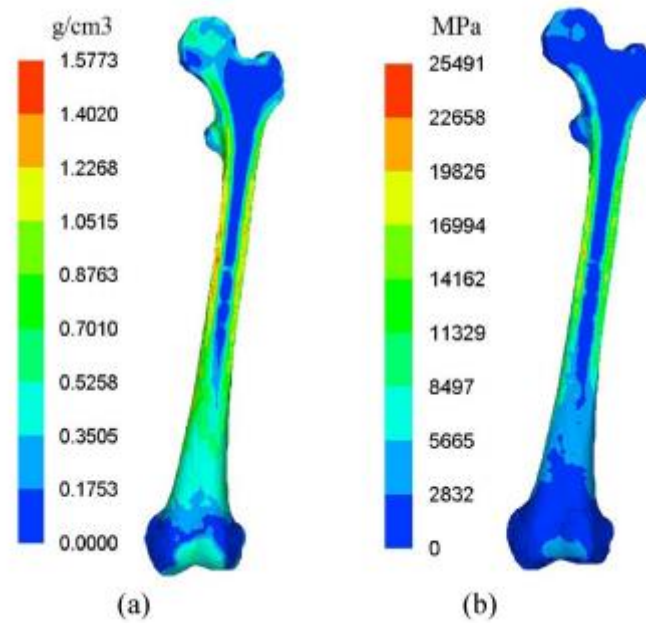
Figure 5-16: Distribution of (a) bone mineral density and (b) modulus of elasticity in inhomogeneous femur mode.

The geometry of the femoral bone was developed from a CT based image of a 79-year-old living female with hip osteoarthritis in the left joint. The data was provided by Kyushu University Hospital, Japan. The CT images were compiled and stacked into commercial biomedical software Mechanical Finder 6.1 (Research Center of Computational Mechanics Inc, Tokyo) to construct a three dimensional (3D) model using FE analysis. The total number of elements for the femoral bone in THA and RHA were 146,414 and 166,414 respectively. For femoral components, prosthesis and femoral ball were assigned with 23,349 elements while resurfacing implant had 37,484 elements. Automated mesh size of 2 mm was considered with tetrahedron elements for all models. In generating an inhomogeneous model, each element of the bone model was generated based on the basis of the linear relationship between 'apparent density' and gray value of the data in Hounsfield unit (HU). Material properties for the bone elements were computed based on the basis of the study by Keyak et al. to present the variation of bone mineral density and young's modulus for the femoral bone. The high values of Young modulus in outer part present cortical bones, while lower values indicate cancellous bones. The model was also assumed to be an isotropic material.

HA models were constructed by replacing the hip joint with different femoral component models. The 3D models of femoral components or implants were imported into the biomedical software to develop the THA and RHA models. The THA model was developed by replacing the hip joint with Titanium Alloy prosthesis stem and Alumina femoral ball. The femoral head was cut off and the prosthesis stem was aligned properly into the femoral canal. The difference in the RHA model is that the femoral head was resurfaced by implanting the Cobalt Chromium prosthesis pin. The connection between the implant and the bone is assumed to be perfectly bonded at the interface.

In this study, different configurations are examined to demonstrate the various loading directions and boundary conditions. Three types of isometric loadings were axial compression configuration (ACC), torsion configuration (TC) and lateral bending configuration (LBC). The consideration of loading was adapted from the well-established and validated testing protocol for periprosthetic femoral shaft fixation. In addition, the characteristic of stance (SC) and sideway fall (FCs) configurations were developed on the basis of the computational analysis of the proximal femur by Bessho et al.
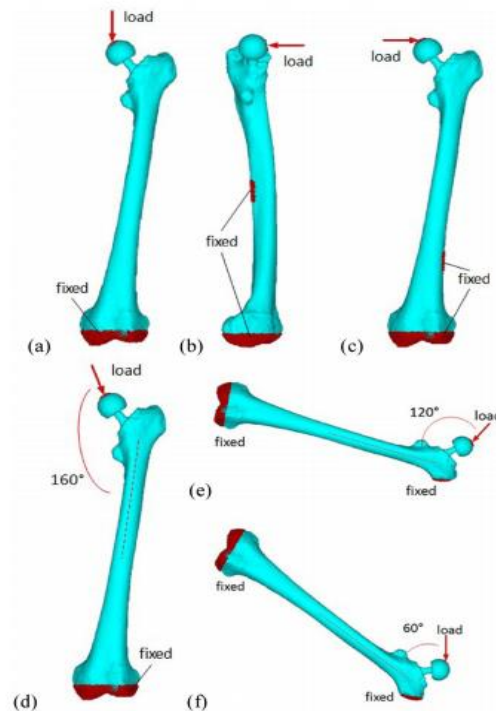
Figure 5-17: Loading and boundary conditions of (a) ACC, (b) TC, (c) LBC, (d) SC, (e) FC1 and (f) FC2.

Each configuration of falls displayed different angles of loading with 'α' degree in reference to the long axis of femur in frontal plane and 'β' degree in reference to femoral neck axis in horizontal plane. The loading magnitudes may vary in each individual and configuration. Therefore, the magnitude of the applied load was subjected to the patient's body weight (BW) at 60.0 kg and the load increments were ranged from 0.5 BW to 3 BW in predicting the fracture patterns and locations at different configurations. Experimental study conducted by Groe et al. suggested that the impact velocity and loading magnitudes were differed at different fall techniques. For instance, the application of martial art techniques during fall manages to reduce the impact from 3.9 BW to about 2.8 BW. FE analysis combined with a damage mechanics model was performed to predict bone fractures in both arthroplasty models and intact femur.
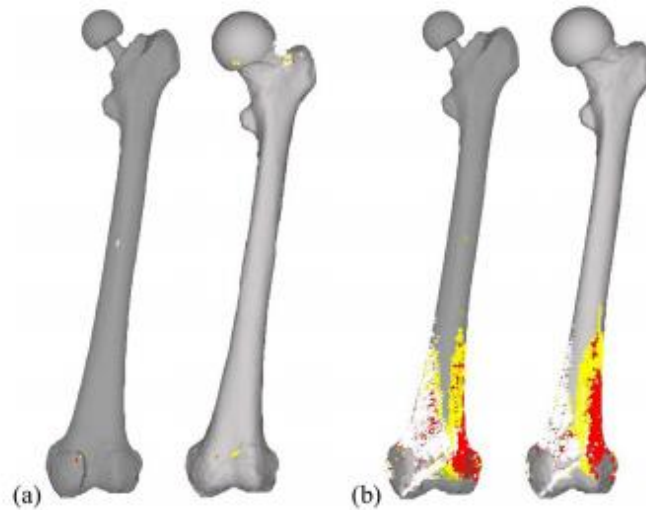
Figure 5-18: Prediction of failure elements in THA and RHA models for (a) ACC and (b) SC configurations at 3 BW loading.
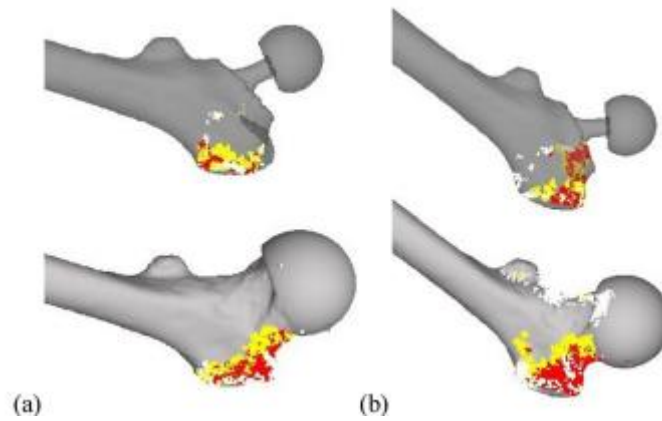
Figure 5-19: Fracture location in THA and RHA models at 3 BW loading for (a) FC1 and (b) FC2 configurations.
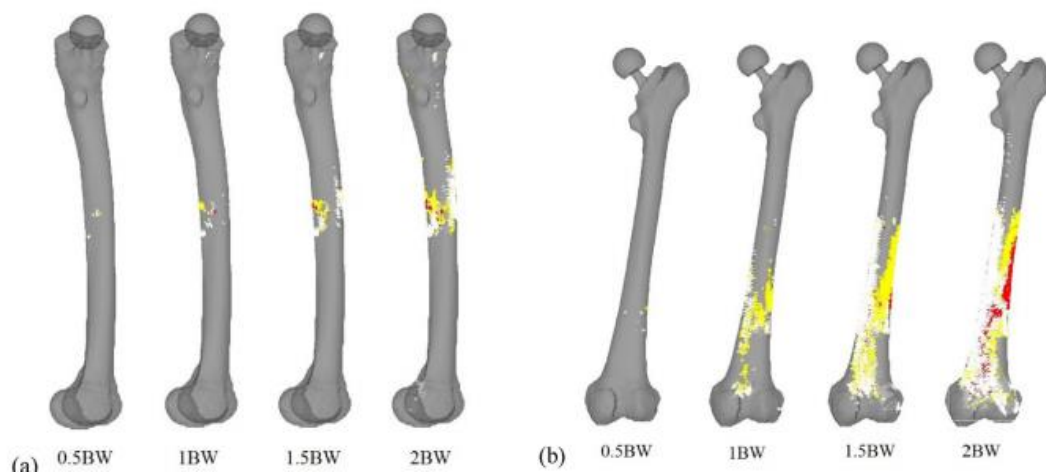
Figure 5-20: Patterns of damage accumulation in THA model for (a) TC and (b) LBC.
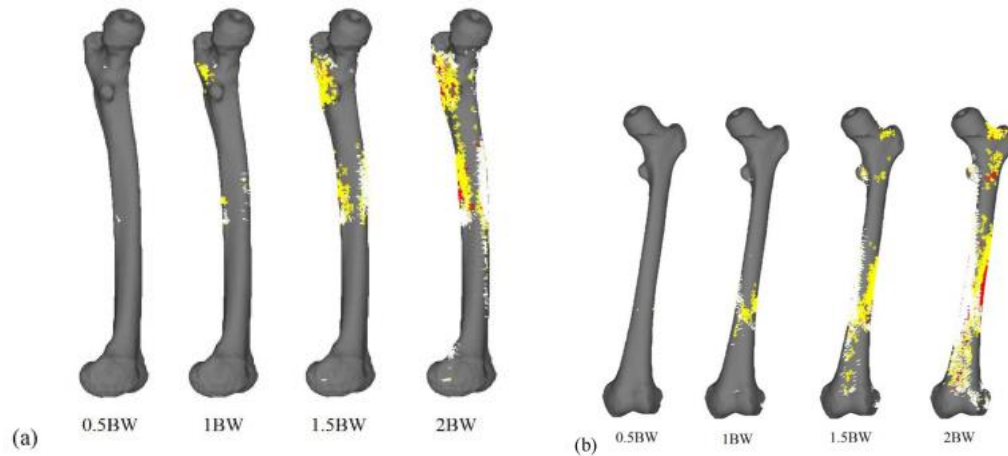
Figure 5-21: Patterns of damage accumulation (0.5 BW–2 BW) in RHA model for (a) TC and (b) LBC.

The results indicate that loading directions can forecast the pattern and location of fractures at varying magnitudes of loading. Lateral bending configuration experienced the highest damage formation in both THA and RHA models. Femoral neck and trochanteric regions were in a common location in the RHA model in most configurations, while the predicted fracture locations in THA differed as per the Vancouver classification.

The biomechanical study demonstrated the capabilities of CT-based FE analysis to predict damage formulation of femoral fractures in HAs. The presence of different femoral components in the femur had influenced the predicted fracture locations. The RHA model demonstrated a greater risk of femoral fractures compared to the THA model in all configurations. Different configurations applied in the analysis suggested the importance of loading and boundary conditions in simulating and predicting the fracture locations. TC and LBC demonstrated a large number of damage formation in both models at lower impact loading. Predicted femoral fractures in the RHA model focused on the neck and trochanteric region. The projection of fracture location in the THA model ultimately correlates with the Vancouver classification.

The aim of this preclinical study (Burchard,et. al, 2017) was to investigate if there are short-stem-design-depended differences of the stress shielding effects in each different type of short-stem THA implant. Using a previously validated data set, THA-stem dependent stress-shielding effects were analysed by virtual hip stem implantation within the framework of a finite element analysis (FEA).

The main objective of every new development in total hip arthroplasty (THA) is the longest possible survival of the implant. Periprosthetic stress shielding is a scientifically proven phenomenon which leads to inadvertent bone loss. So far, many studies have analyzed whether implanting different hip stem prostheses result in significant preservation of bone stock. The aim of this preclinical study was to investigate design-

depended differences of the stress shielding effect after implantation of a selection of short-stem THA-prostheses that are currently available.

Based on computerized tomography (CT), a finite elements (FE) model was generated and a virtual THA was performed with different stem designs of the implant. Stems were chosen by osteotomy level at the femoral neck (collum, partial collum, trochanter sparing, trochanter harming). Analyses were performed with previously validated FE models to identify changes in the strain energy density (SED).
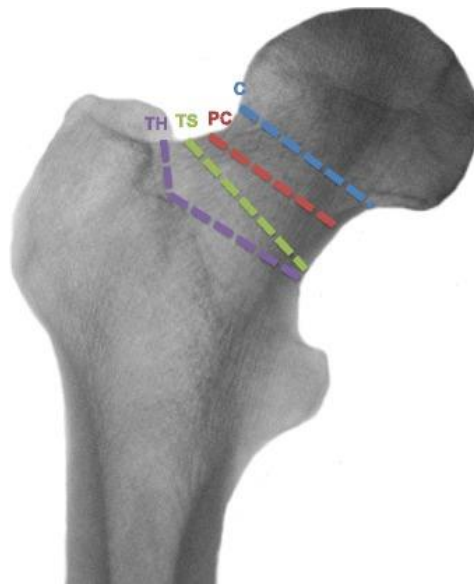
Figure 5-22: Osteotomy levels of the different stem types (collum (C), partial collum (PC), trochanter sparing (TS), and trochanter harming (TH)

A validated set of an in vivo scanned right femur of a female subject at the age of 75 was examined. The scanner setting (Somatom® Plus-4, Siemens, Erlangen, Germany) was 140 kV, 206 mA, 17 s, spiral algorithm with recalculated slice thickness of 2 mm and a 512×512 pixel resolution. The CT voxels were transferred to finite elements (FE) on a scale of 1:1 using the full information to generate the femoral model with an identical resolution of 0.66 m $\times$ 0.66 mm $\times$ 2 mm (FE and CT).

The different stem designs were realized through a virtual implantation using the FE software Ansys® (Ansys 14.5.7, Ansys Inc., Canonsburg, USA). A geometrical matrix of each stem was generated and an automatic algorithm selected all elements of the bony model that belong to the matrix information The elements were assigned to an elastic modulus value of titanium alloy (110,000 MPa). FEA was performed on the cluster of the University of Siegen which provides 272 Intel-Xeon®-CPUs, 6.4 TB Working Space and 40 TB physical space. Therefore, the usable peak performance was above 17 TFLOPs.

For stress analysis, a weight-dependent head force was applied with a magnitude of 347% of the bodyweight. The vertical axis (z) of the coordinate system was defined by the hip and knee joint centre and the frontal axis (x) by the dorsal aspect of the femoral

condyles. So the head force was multiplied by -sin(15°) to obtain the x-component, by -sin(13°) to obtain the y- and by cos(15°) to obtain the z-component. Because of their highly variable in vivo magnitude, simulation of additional muscle forces was disregarded.

The strain simulation process after applying the hip center force was performed with the gradient solver (default settings) of the FE software during the solution process. In addition, periprosthetic regions of interest (ROI) were defined according to Gruen et al. of each short-stem-type and according to the ROIs of a typical standard stem (CLS Spotorno®, Zimmer, Warsaw, USA).

Statistical analysis was done by a Z-Test according to Paternoster that compares regression parameters. The method estimates adequate fitting curves by different regression models. To find the best fitting curve we test for each type of prostheses a linear, quadratic, and cubic regression function and compare the resulting R2 values. The highest R2 value is equivalent for the best fit and shows the most adequate model for the underlying relationship.
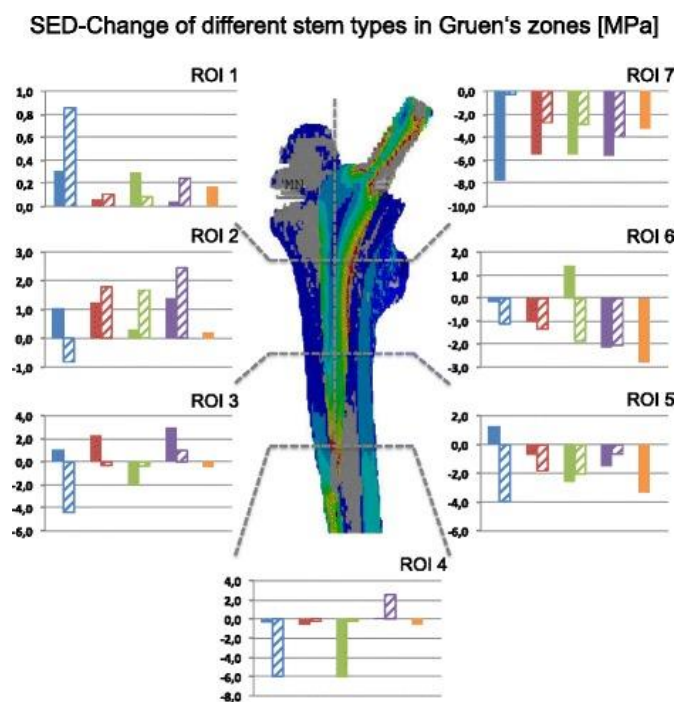
Figure 5-23: The different stem types (collum (*blue*), partial collum (*red*), trochanter sparing (*green*), trochanter harming (*violet*), and standard (*orange*)) were taken for stress analysis. ROIs were defined by stem type (populated) and geometry of the standard stem (hatched).

Based on the result of this study, we cannot confirm that the design of current short stem THA-implants leads to a different stress shielding effect with regard to the level of osteotomy. Somehow unexpected, we found a bone stock protection in metadiaphyseal bone by simulating a more distal approach for osteotomy. In the proximal bone only a collum THA-prosthesis could lead to this effect but so far there is no THA-implant on the marked that provides this kind of stem. Further clinical and biomechanical research

including long-term results is needed to understand the influence of short-stem THA on bone remodeling and to find the optimal stem-design for reduction of the stress-shielding effect.

A discussion about the type of design and the material that can be used for hip implants is taken place in the study (N, Zuber,et. al, 2019)

In this work, four shapes namely circular, ellipse, oval and trapezoidal are modeled with three different profiles. Finite element method is used to carry out static analysis is on all the twelve models using ANSYS R-19. Boundary conditions are considered according to the ASTM standards. Ti–6Al–4V and CoCr alloys are the widely used materials in the hip implant stems. Both materials are evaluated along with different designs to find the best suited materials which can be used for hip stems. The first part of the study involves the modeling and analysis of stems which is a basic component in total hip arthroplasty. Next a combination of stem, acetabular cup, femoral head and backing cup are analyzed to find the best suited complete hip implant.

Several types of designs are popularly used in the total hip arthroplasty. The shape and profile are the important parameter in the design of the stem. In this study, circular, oval, ellipse and trapezoidal shapes are considered in the analysis. Fig. 5.24 shows the changes in the cross sections of the stem and defined as profile 1, profile 2 and profile 3. In profile 1, a straight stem with radius on lateral side near the proximal end is considered. The arc length and diameter of the profile 2 is increased along with the total angle between the medial and lateral faces. In profile 3, a cornered shoulder replaces the radius on the lateral side. The neck and medial side dimensions are constant in all the three designs. In total, twelve designs are modeled using CATIA V-6 as non-modular implant stems. These models are subjected to static structural analysis using ANSYS R-19 to evaluate the von Mises stress, deformation in load acting direction and total deformation.
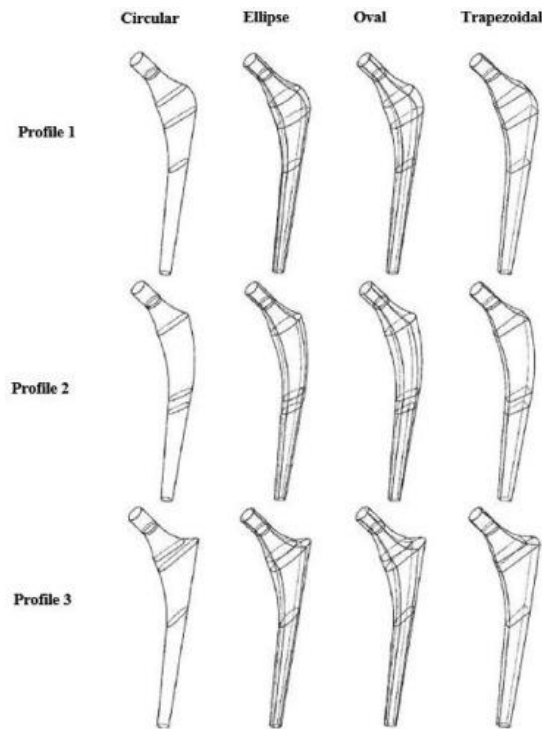
Figure 5-24*:* The different stem designs used for the study.

The models were meshed using unstructured mesh. The mesh independency study carried out resulted in the selection of optimal mesh size for the analysis. In this work, the circular shaped profile 1 stem was considered for mesh dependency. Several mesh size was developed by varying the mesh size from 5mm to 0.25mm.It can be seen that the stresses increase significantly as the mesh size is reduced 1mm from the initial size of 5 mm. Beyond the mesh size lesser than 1mm, there is no major changes in stresses for subsequent mesh size. Thus the mesh size of 1 mm was adopted for the analysis of all the models in this work. The total number of elements and nodes obtained in modeling of various implants were approximately 675, 000 nodes and 495,000 elements.

The boundary conditions are applied as per the ASTM F2996-13 and loading conditions are considered as per ISO 7206–4:2010(E). According to the standards, the modeled stems are bisected into three cross sections from the top surface of the stem. The hip stem is sectioned from the center of head as per the ISO 7206–4:2010(E) with the worst-case head/neck offset. This section from the center of head helps represent the stress distribution over the implant. A second section was made 10 mm below the first cut. The hip stem was constrained in all directions on all faces distal to the second cut. Constraining the stem in this manner ensures that excessive erroneous stresses are not generated at the region of interest due to the influence of rigid fixation. Static structural analysis is carried out for all the twelve designs by enforcing identical boundary conditions.

The commercially available implants are made of cobalt chromium (CoCr) or Ti–4Al–6V materials. The 12 designs are analyzed for the implants made of CoCr and Ti–4Al–

6V materials at uniform loading of 2300 N. It was observed that, profile two exhibited less deformation compared to other two profiles in all the four different shapes.
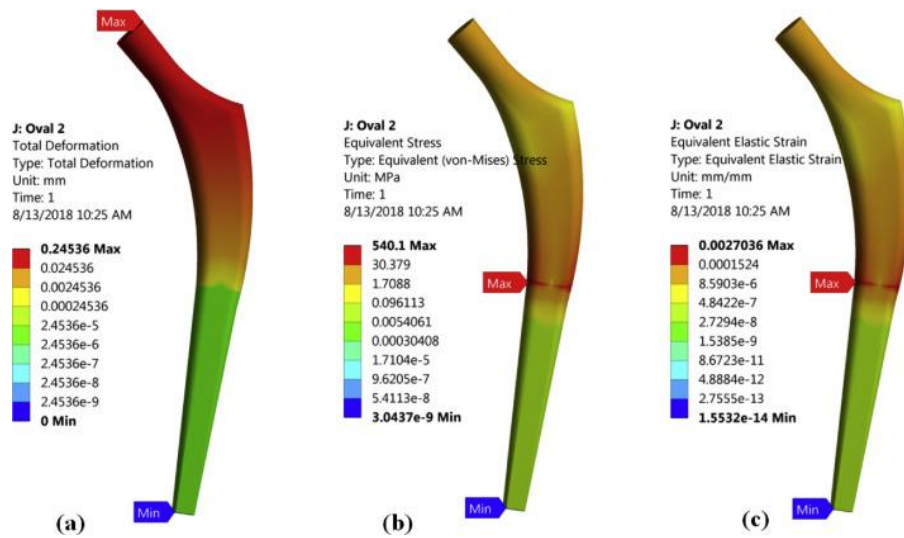
Figure 5-25*:* Oval Profile two: (a) Total Deformation, (b) von Mises Stress, (c) Elastic strain using CoCr alloy.
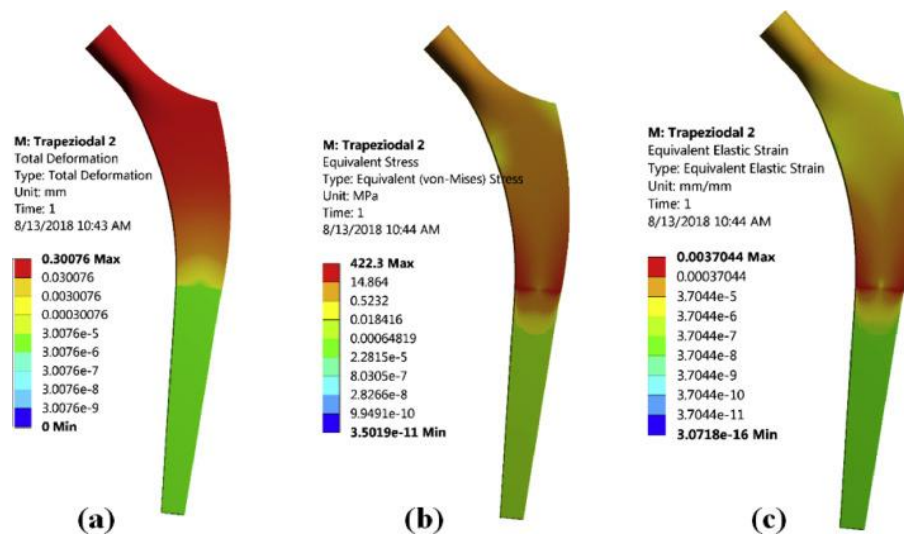
Figure 5-26*:* Trapezoidal Profile 2: (a) Total Deformation, (b) von Mises Stress, (c) Elastic strain using Ti–4Al–6V.

The next stage of analysis involved the combination of stem made of CoCr (along with its acetabular components. The acetabular cup is fitted to the head with a constant thickness of 4mm which is further covered with a metal backing cup having a thickness of 2mm.The material combination is defined as CoCr material for hip stem, femoral head, and backing cup (thickness of 2mm). The acetabular liner of thickness 4mm was investigated for 2 materials which are CoCr [CoC implants] and UHMWPE [CoPE implants]. Two different combinations of materials are considered for the study namely CoC (ceramic on ceramic) and CoPE (ceramic on polyethylene).
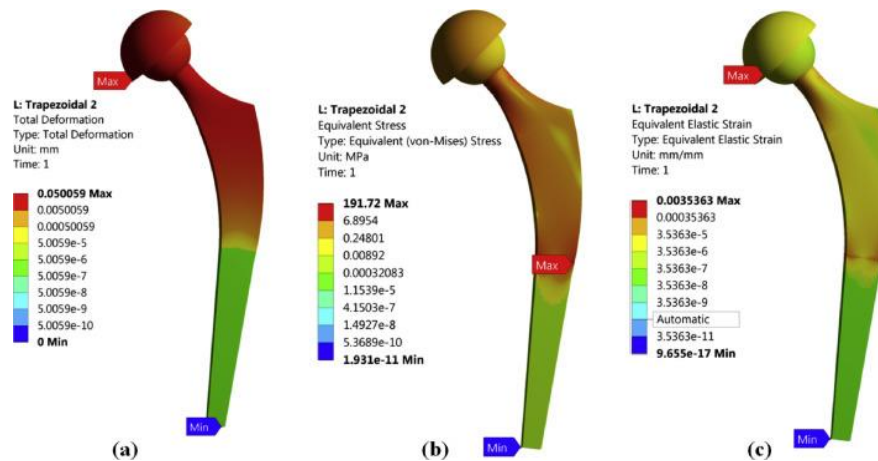
Figure 5-27: Trapezoidal Profile 2: (a) Total Deformation, (b) von Mises Stress, (c) Elastic strain using Acetabular cup made of CoPE
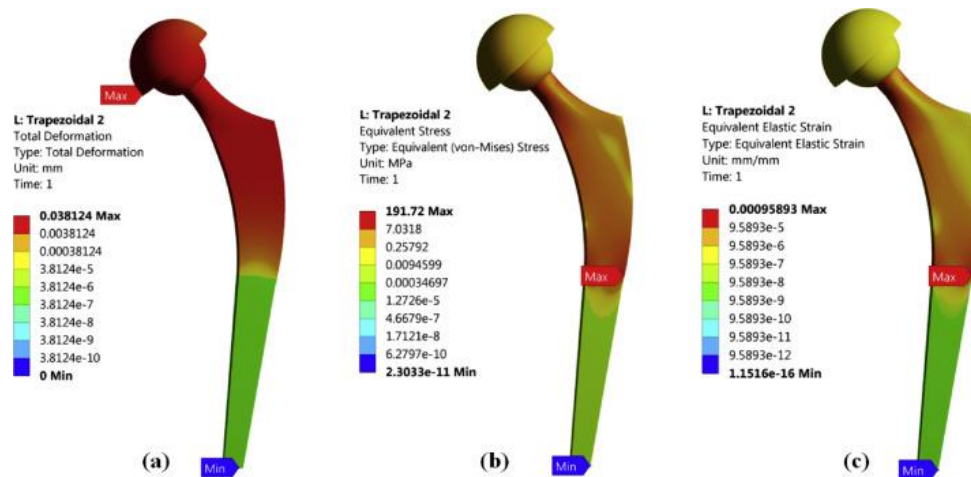
Figure 5-28: Trapezoidal Profile 2, (a) Total Deformation, (b) von Mises Stress, (c) Elastic strain using Acetabular cup made of CoC.

CoCr was found to be the preferred choice of material for stem design. It was also observed that, irrespective of material considered for the analysis profile 2 with trapezoidal stem showcased lesser deformation and von Mises stress over the other eleven models. For analysis involving acetabular cups, CoCr implants exhibited better mechanical properties over the conventional CoPE materials such as UHMWPE. It is inferred from the findings of this study that, the profile 2 with trapezoidal stem design made of CoCr material and acetabular cup made of CoCr material is best suited for hip joint implants.

In paper (Colic, et al., 2016) a numerical investigation of replacement implant for partial hip arthroplasty is presented. The long-term stability of hip implants depends, among other things, on the loads acting across the joint. Forces occurring in vivo can be much greater than the recommended test values, because a typical gait cycle generates forces up to 6–7 times the body weight in the hip joint. A finite element analysis (FEA) was

performed using 3-dimensional models to examine the mechanical behavior of the femoral component at forces ranging from 2.5 to 6.3 kN. This implant design was chosen for numerical analysis because stress concentration in femoral component lead to implant fracture.

Model was set up with adequate boundary conditions, including fixing of the implant bottom surface along all degrees of freedom, and the load was applied in the appropriate direction relative to the top of the femoral head of the prosthesis. FEM analysis of the prosthesis was performed using ABAQUS (Dassault Systèmes) software, for simulating slow walking on a flat surface for a model made of Ti-6Al-4V alloy. The most realistic models are considered those based on plasticity or viscoplasticity, in particular the HISS models, as they include other plasticity models as special cases. However, for evaluation of failure or ultimate loads the classical plasticity models are often used. In this part of the numerical investigation, three dimensional static idealizations are considered, and constitutive models were used for elastic-plastic behavior of biomaterial. Elastic-plastic von Mises conventional material model was used in this numerical analysis. For preliminary studies of mechanical behavior of hip implant presented in this paper, linear elastic behavior of a material was analyzed, as a function of two elastic constants - Young's modulus 120 GPa and Poisson's ratio 0.3.
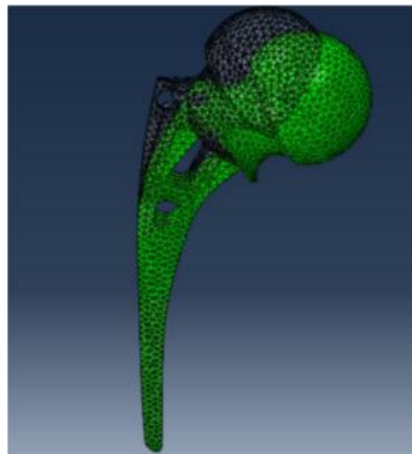
Figure 5-29*:* Comparative representation of the initial state and maximum load state of the implant

Analyses of three-dimensional stress states determined according to Von Misses criteria were performed, along with three dimensional displacement fields depending on the loads of the implant. Stresses were calculated in order to estimate the probability of prosthesis failure under the effect of maximum loads which can occur during a walking cycle.
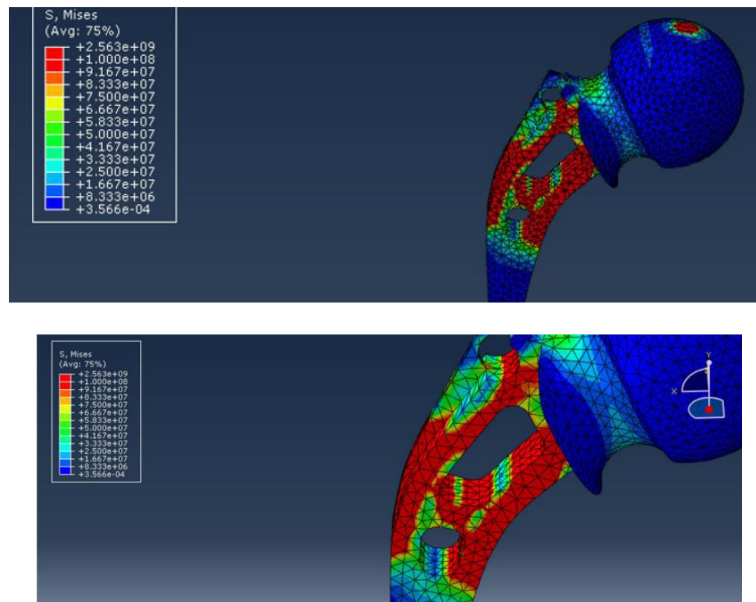
Figure 5-30*:* Von Misses stresses in the stem.
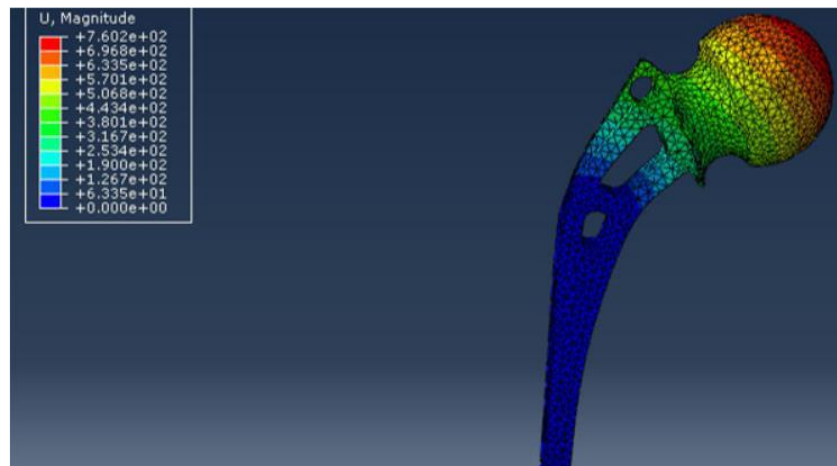
Figure 5-31*:* Total prosthesis displacement under the effects of maximum load.

Results show that the force magnitudes acting on the implant are of interest, and that they can cause implant stress field changes and implant stability problems, which can lead to implant failure.

Based on the results presented in this paper and obtained by applying the Finite Element Method, one can conclude the following:

FEM is reliable and powerful tool for stress-strain analysis of complex-shaped implants, like the artificial hip. Results of the numerical analysis show that the stress state in the implant cross-section with the hole corresponds to the location of the hole in the actual prosthesis, and it represents the location of critical stress concentration. Stresses caused by maximum static loading are still lower than the yield strength of Ti-6Al-4V and CoCrMo alloy, but higher than the yield strength of 316L stainless steel.

6   Computational analysis

The computational stage of the analysis consists of:

- Problem definition
- Selection of preferences
- Definition of type and format of finite elements (2D or 3D)
- Determination of material properties (Young's modulus of elasticity, Poisson's ratio, etc.)
- Establishing a model with appropriate dimensions
- Determination of mesh density
- Meshing establishment

The objective of the current thesis is the numerical evaluation of the effect of different loading conditions during various activities on a long bone of a patient who has undergone total hip arthroplasty.

The conditions of static loading which the stent and thigh bone have exposed to, are given below:

CT images have taken from a patient who is 59 years old and weights 57 kg. The CT images are used for the construction of the main body of the prothesis that has been used to the patient for the total hip arthroplasty. The actual prosthesis consists of acetabular (continuum: size 52), thigh stem (spotorno: size 13, 75) and ceramic head (size 36, 5(+3.5)).

The stent was then applied to the femur, which had previously been incised in the head region in agreement with the CT images of the total hip arthroplasty.

6.1   Geometry and stent material

6.1.1   Geometry

The system studied in this work consists of the bone and the stent, with the latter being made up of the sternum, neck and artificial acetabular. The stem, neck, and shell of the acetabular were made of titanium alloys (Ti6Al7Nb) while the head was of a ceramic system. For the purpose of this effort, the femur bone was firstly modeled precisely, with the help of a 3D reconstruction program (3D Slicer V19). The adopted approach took into special consideration the incision at the neck point, removing the head as it actually occurs during total hip arthroplasty and as seen in our patient's CT. The sternum, neck, femoral head and lining were then modeled. Additionally, the 3D Slicer program was also used to model the stem of the patient exactly as it was, right after the conclusion of the femur part.
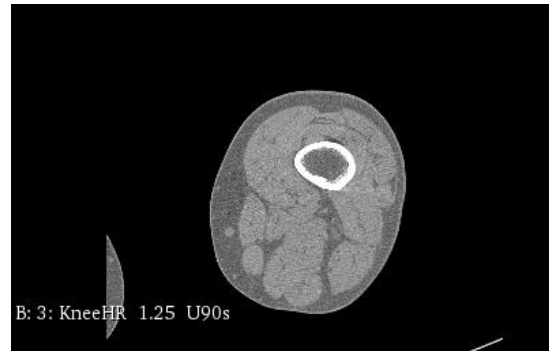
Figure 6-1: Ct image in 3D Slicer program
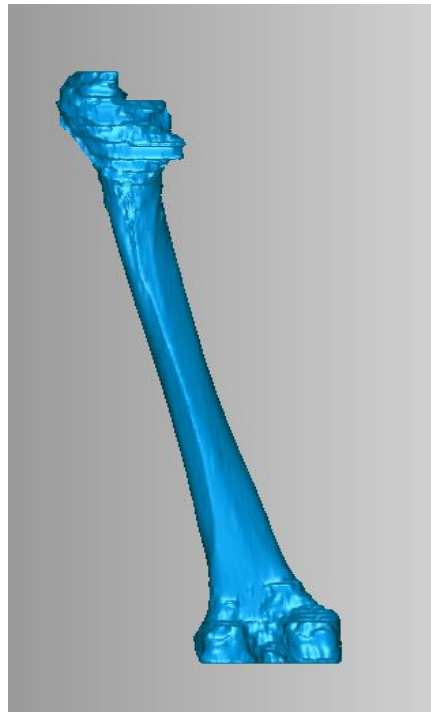
Figure 6-2: Bone's geometry

6.1.2 Stent materials

The materials identified for the stent parts and for the bone are considered linear elastic of isotropic behavior in order for appropriate calculations of the stresses and strains, imposed by the geometry, to be conducted. For the materials used, the modulus of elasticity (Young's modulus) and Poisson's ratio, were defined.

Poisson's ratio is defined as the ratio of the transverse to the longitudinal, that is, when a rod is tensed, its length increases while its other dimensions, perpendicular to the load, decrease. The elasticity measure E, i.e. the Young's modulus, is the slope of the straight section of the voltage-power curve. This measure can also be considered as the stiffness of the material or its resistance to elastic deformation.

Table 6-1: Material properties **(Smyris, et al., 2017)**

	Young 's Modulus(GPa)	Density (kg/m^3)	Poison 's ratio
Bone	16,7	1640	0.3
Prothesis	110	4510	0.31

Titanium alloy Ti6Al7Nb

Ti6Al7Nb is a titanium alloy with high strength, low weight ratio and excellent corrosion resistance. It is one of the most commonly used titanium alloys in a wide range of applications requiring low density and excellent corrosion resistance, as are industrial applications such as implants and prostheses. The alloy is composed of 6.2% Al, 0.10% Fe 0.2% O, 0.004% C, 0.005% Mo, 0.46 Ta, and titanium Ti.

Ceramic

Ceramic heads, unlike metal, are much less soiled when moving and their friction products are non-toxic. Ceramic heads are made of aluminum or zirconium oxide or a mixture of oxides of these metals. However, unfortunately, these materials are quite expensive.
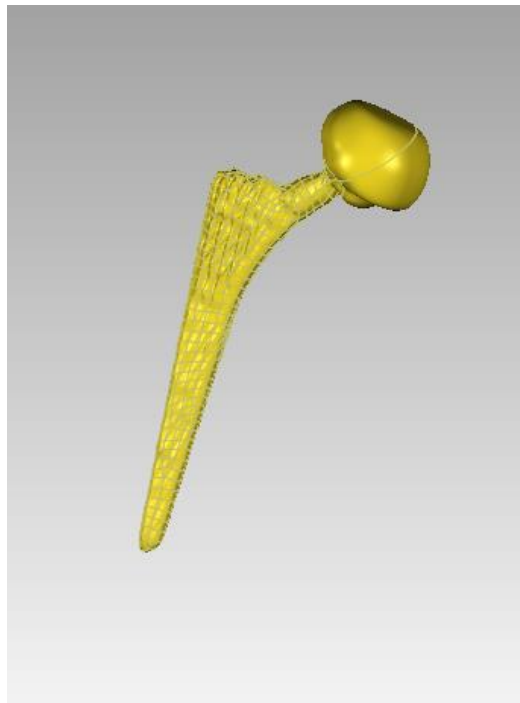
Figure 6-3: Stent's geometry

6.2   Creating a grid

The 3D bone geometry was transferred to the ANSYS finite element program. The appropriate mesh was created for the computational process after a coverage study that was performed. With the corresponding application (sizing) the grid was adjusted for each part of the geometry, that is, the grid was modified differently for the stent parts and for the bone. The mesh type/shape was a triangle while the size of the minimum triangle was 0.274240 mm. Finally, the number of the elements was 1005999 and of the nodes 1569294.
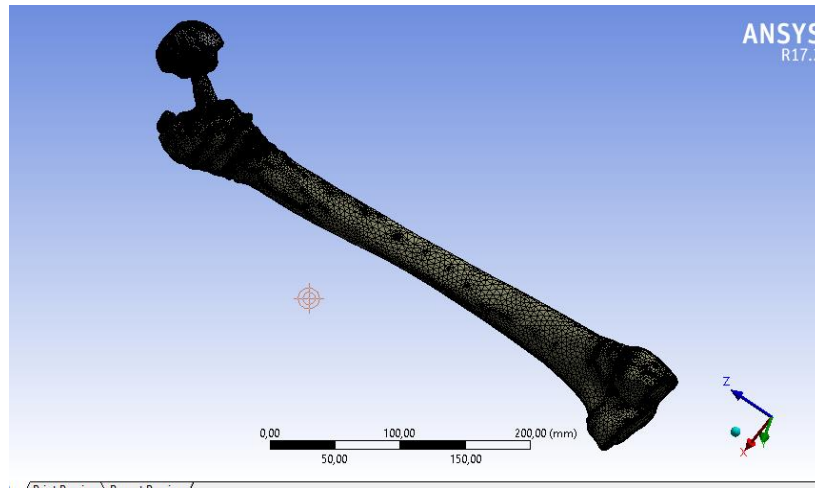
Figure 6-4: Grid of bone-stent

6.3   Boundary conditions

6.3.1   Fixed constrain

The boundary condition of the clamp prevents the movement or distortion of flat or curved surfaces, straight or curved edges as well as the movement of the peaks. In the case of the bone, this boundary condition was applied to the bottom, i.e. the knee, as shown in the Figure 6-5. This implies that the bone had rotation and degree of freedom equal to zero.
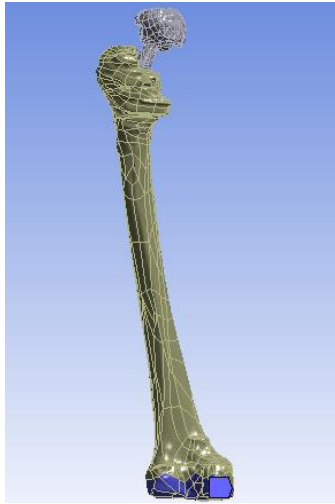
Figure 6-5: Fixed constrain boundary condition

6.3.2 Forces

During normal hip function, pressure is exerted on the surface of the femoral head by sucking it into the pelvic area. For the measurements, the components of the force F were defined as shown below (Figure 6-7), in three directions, in certain angle 13° and with measures presented in the following tables 6-2,3,4. Especially these measures of forces have been taken from diagrams that are presented below (Figure 6-8). (Bergmann,et. al, 2016). The components of the force exerted on the stent-bone system were defined as non-instantaneous, and as such the results depend on time and are specifically related to the load cycle.

Figure 6-6: Loading conditions of bone-stent
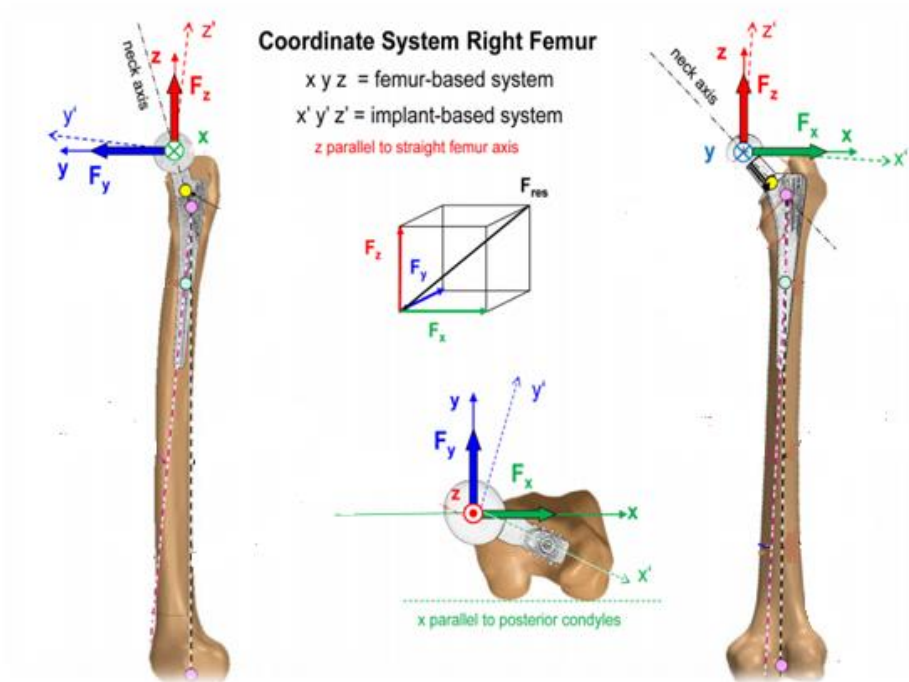
Figure 6-7*:* Direction of the forces that applied. (Bergmann,et. al, 2016)
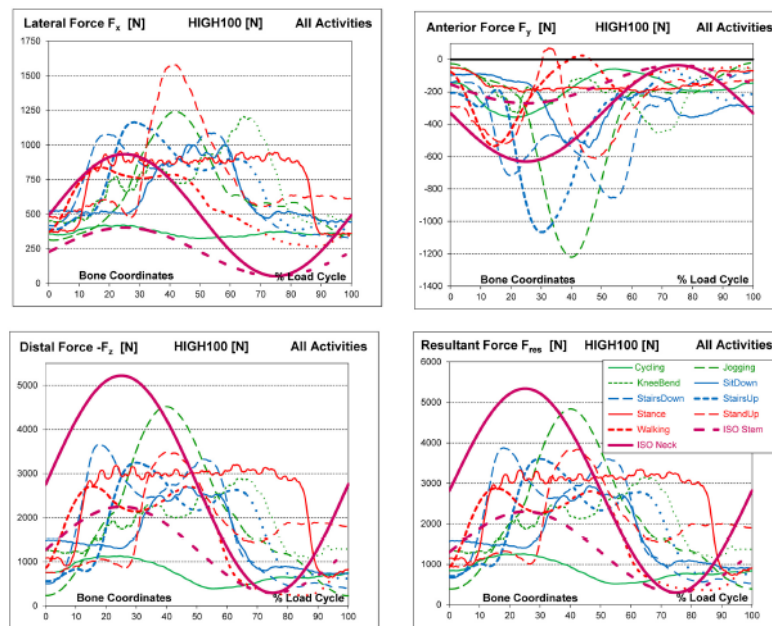
Figure 6-8: Diagrams of Fx, Fy, Fz during activities (Bergmann,et. al, 2016)

Table 6-2: Measure of the F_x component (Bergmann,et. al, 2016)

	0	25	50	75	100
cycling	350	370	330	300	350
sit down	510	500	950	500	480
stand up	480	500	1250	570	650
knee bend	450	650	850	750	450
walking	370	770	670	300	370
stance	370	870	870	950	350
stairs up	370	1170	850	500	400
stairs down	400	950	1050	400	370

Table 6-3: Measure of the F_y component (Bergmann,et. al, 2016)

	0	25	50	75	100
cycling	-150	-450	-50	-200	-180
sit down	-100	-150	-380	-350	-280
stand up	-300	-250	-590	-100	-100
knee bend	-50	-200	-200	-350	-50
walking	-80	-300	-100	-50	-50
stance	-50	-200	-190	-190	-50
stairs up	-210	-800	-300	-100	-210
stairs down	-150	-620	-800	-200	-100

Table 6-4: Measure of the -F_z component (Bergmann,et. al, 2016)

	0	25	50	75	100
cycling	800	1100	500	700	800
sit down	1500	1300	2500	900	700
stand up	550	570	2500	1500	1800
knee bend	1300	1750	2500	1900	1350
walking	800	2200	2700	250	600
stance	1100	3000	3100	3000	800
stairs up	510	3000	2250	1100	510
stairs down	520	3000	3300	510	500

7 Results

This study investigated the behavior of the hip joint of a patient who has undergone total hip arthroplasty during daily activities such as cycling, sitting down, standing up, knee bending, stance, walking, stairing up, stairing down. CT images of a patient helped us to construct the femur and prosthesis. The applied forces depend on time, and are specifically related to the load cycle. The simulation results are shown in the forthcoming Figures 7-1 to 7-24. They contain the necessary information for the deformation, the Von Mises's stress and the strain that are developed in the models for each daily activity.

7.1 Results of cycling
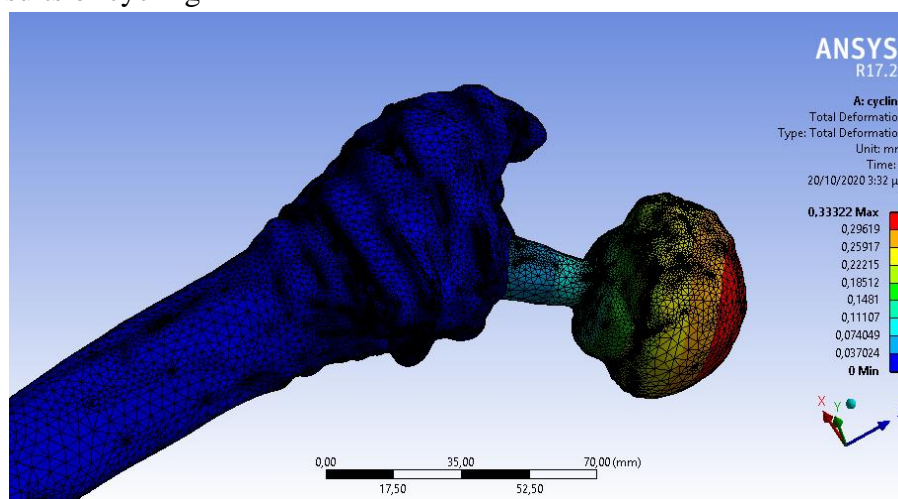
Figure 7-1: Deformation of cycling
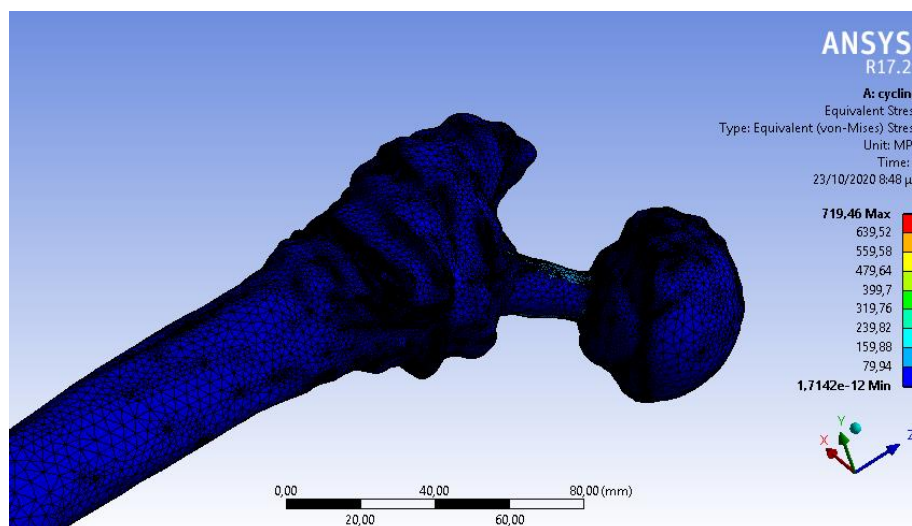
Figure 7-2: Stress of cycling
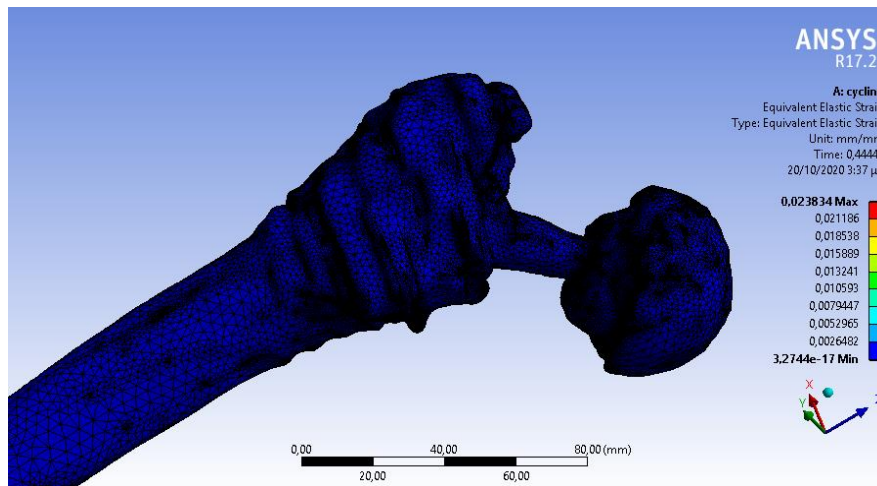
Figure 7-3: Strain of cycling

As it can be observed, the deformation of cycling ranges from 0.037024 mm to 0.33322 mm, while the strain ranges from 0.0016432 mm/mm to 0.014789 mm/mm. Moreover, the stress extends from 79.94 MPa to 719.46 MPa. It can also be noticed that the bone-stem pair has a relatively large strain.

7.2   Results of knee bending
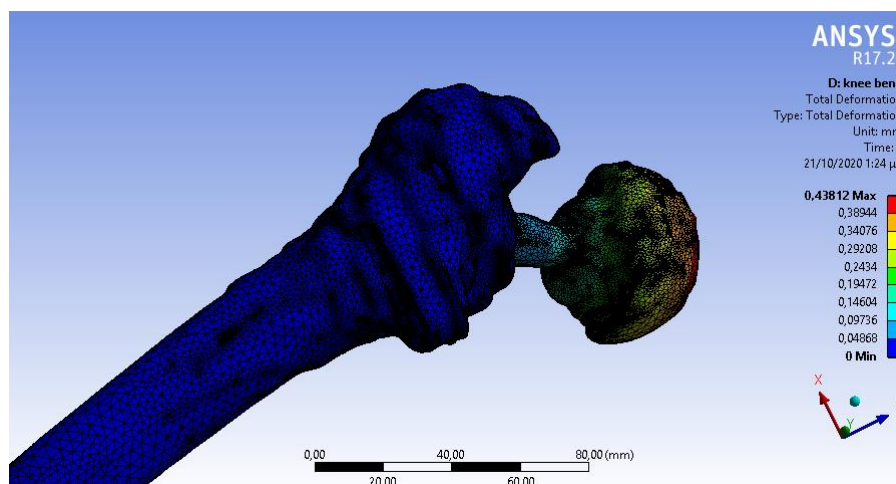
Figure 7-4: Deformation of knee bending
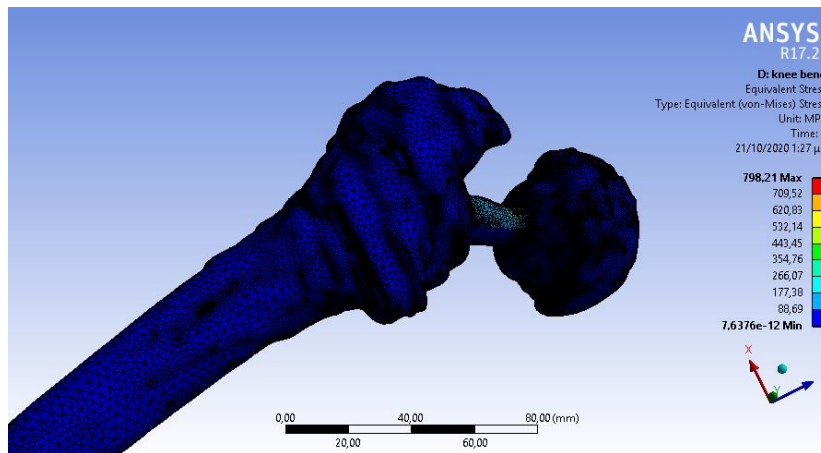
Figure 7-5**:** Stress of knee bending
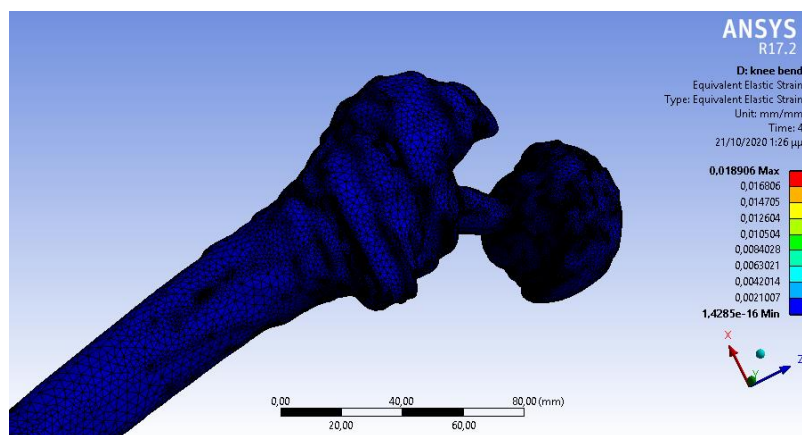
Figure 7-6: Strain of knee bending

Knee bending is an activity with a large deformation that ranges from 0.04868 mm to 0.43812 mm and a large stress of 798.21 MPa. The strain extends from 0.0021007 mm/mm to 0.018906 mm/mm. The pressure to the bone-stem is higher in the case of knee bending than in cycling and the patient must be more careful about impingement.

7.3   Results of sitting down
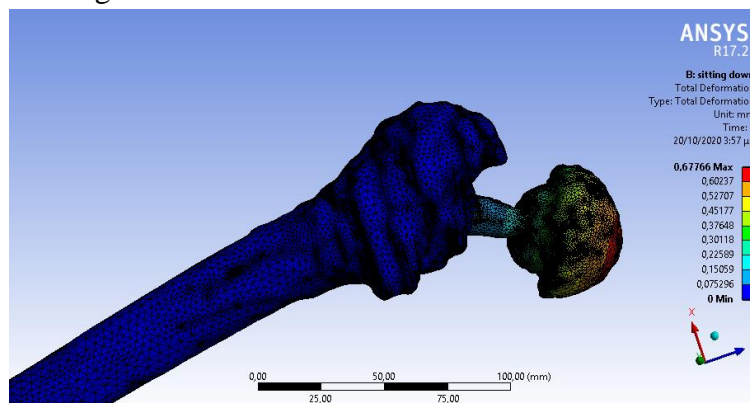
Figure 7-7: Deformation of sitting down
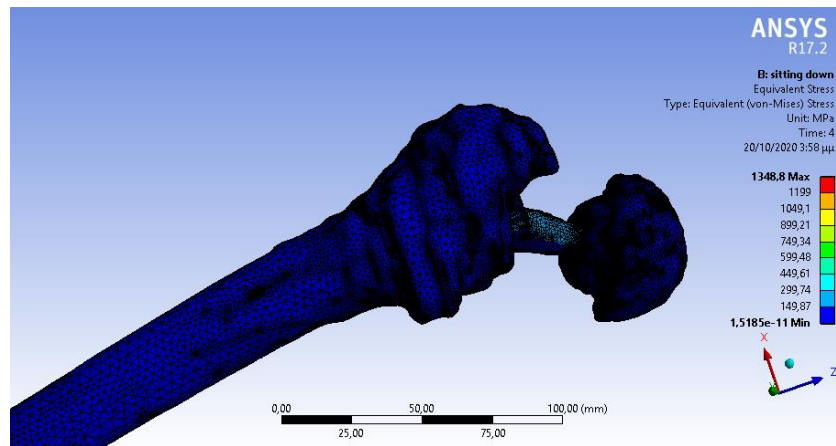
Figure 7-8: Stress of sitting down
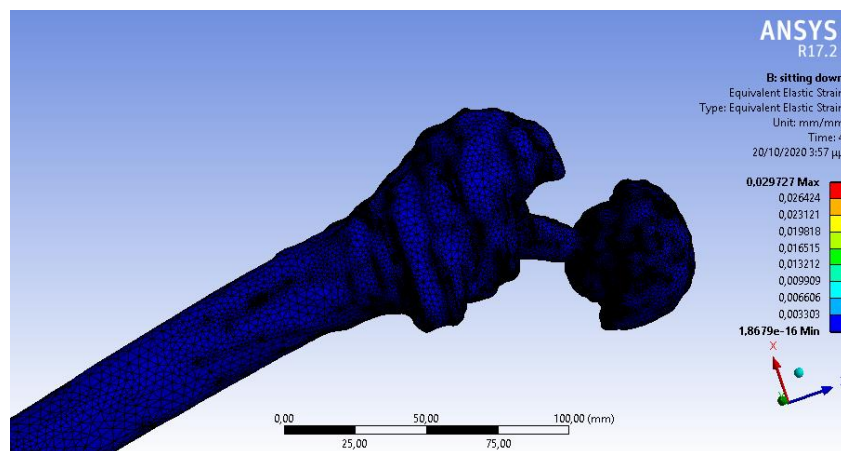
Figure 7-9: Strain of sitting down

The most painful activity for bone-stem system, is the sitting down process because as it can be seen in Figures below (Figure 7-7, 7-8, 7-9), large deformation and stress are developed. The deformation reaches 0.67766 mm while the stress has maximum value of 1348.80 MPa.

7.4 Results of standing up
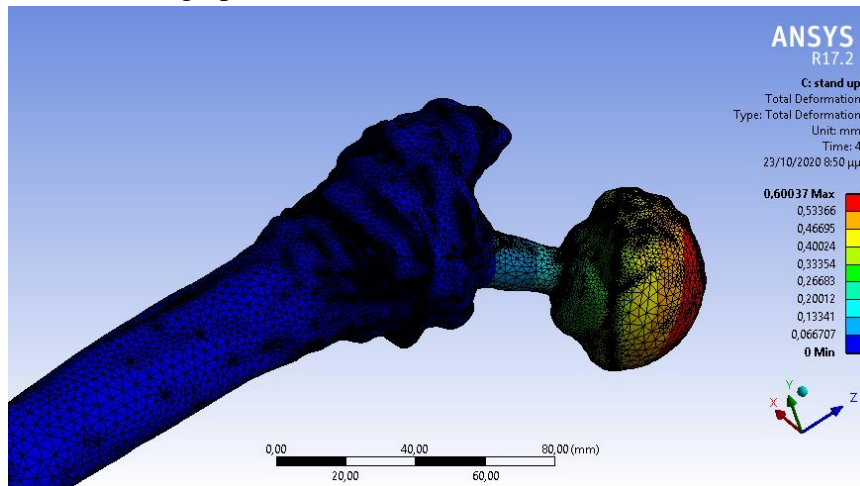
Figure 7-10: Deformation of standing up
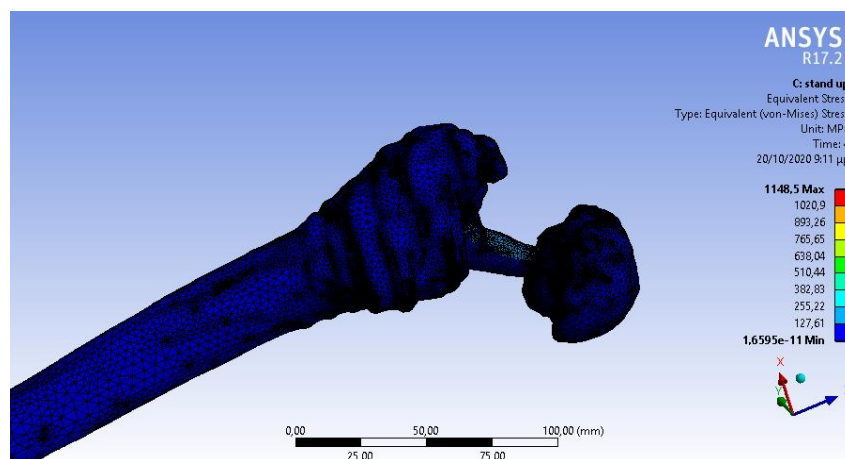
Figure 7-11: Stress of standing
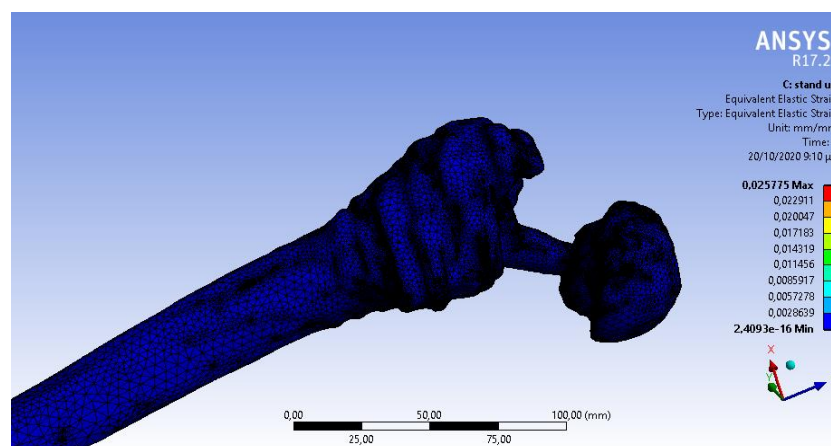
Figure 7-12: Strain of standing

The bone-stem is also suffered during standing up but in a lesser extent than sitting down. The deformation of the standing up activity ranges from 0.066707mm to 0.60037mm. As it can also be noticed, the strain is 0.025775 and stress is 1148.5 MPa.

Comparing to the previous activities, the standing up is the second more dangerous activity for impingement.

7.5   Results of stairs down
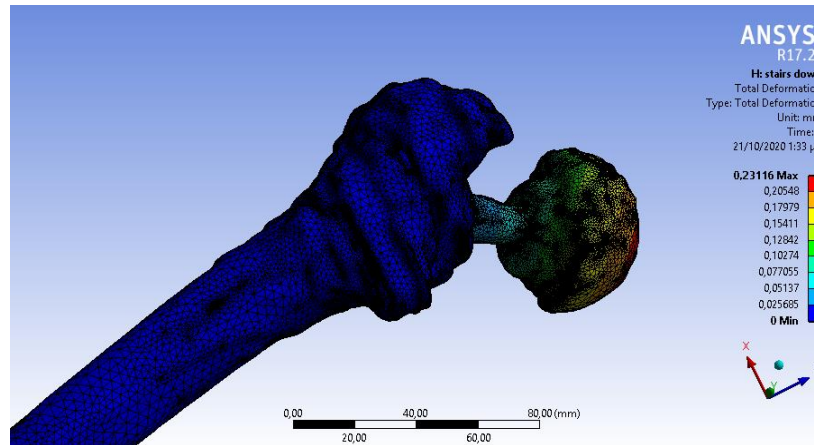
Figure 7-13: Deformation of stairs down
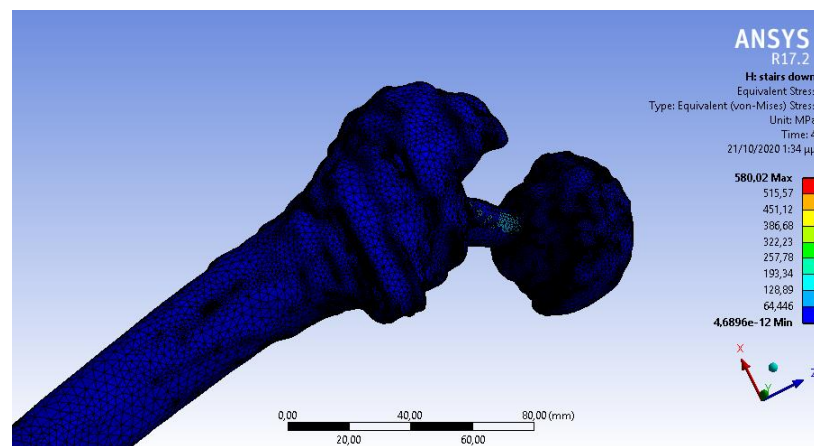
Figure 7-14: Stress of stairs down
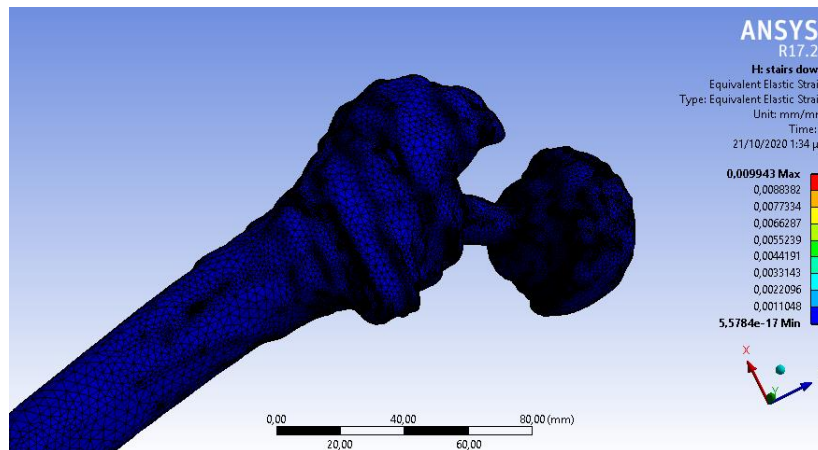
Figure 7-15: Strain of stairs down

Stairs down activity has a deformation of 0.23116 mm causing a small displacement for bone-stem system. The stress lays within the range from 64.446 MPa to 580.02 MPa that is not so severe for dislocation compared to the previous activities, especially to the sitting down one that has 1348.80 MPa stress.

7.6   Results of stairs up
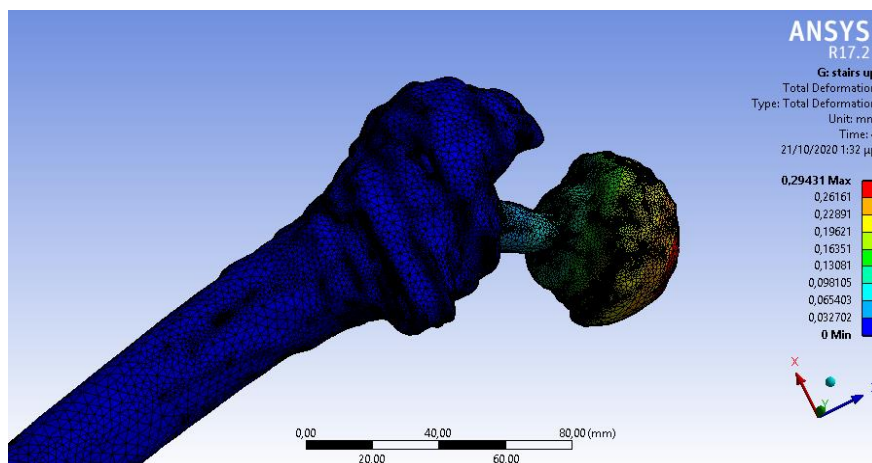
Figure 7-16: Deformation of stairs up
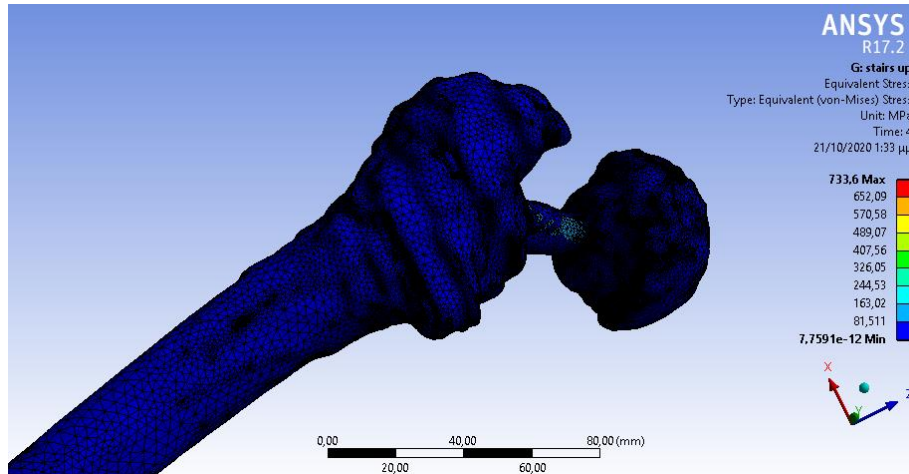
Figure 7-17: Stress of stairs up
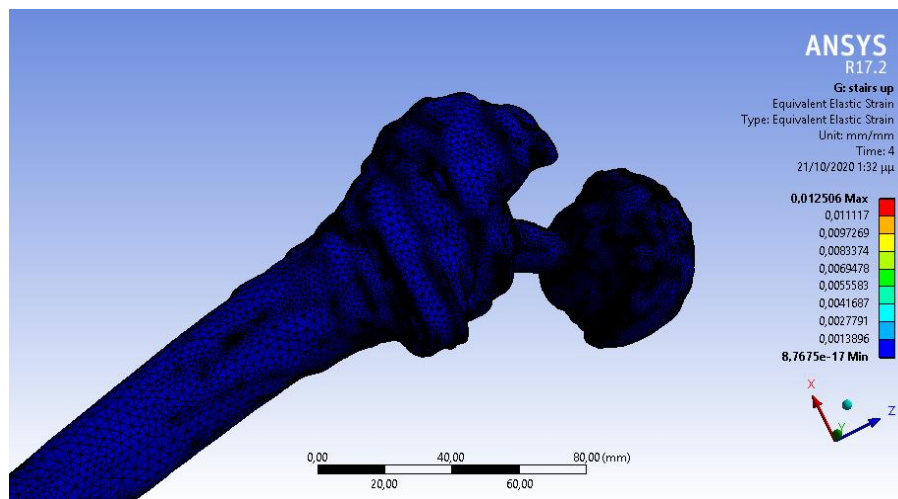
Figure 7-18: Strain of stairs up

By observing the above figures, it can be observed that the maximum value of the deformation during stairs up is 0.29431 mm, stress is 733,60 MPa and strain is 0,012506 mm/mm. Stairs down activity is less intensive and safer for the bone-stem pair than the stairs up.

7.7   Results of stance
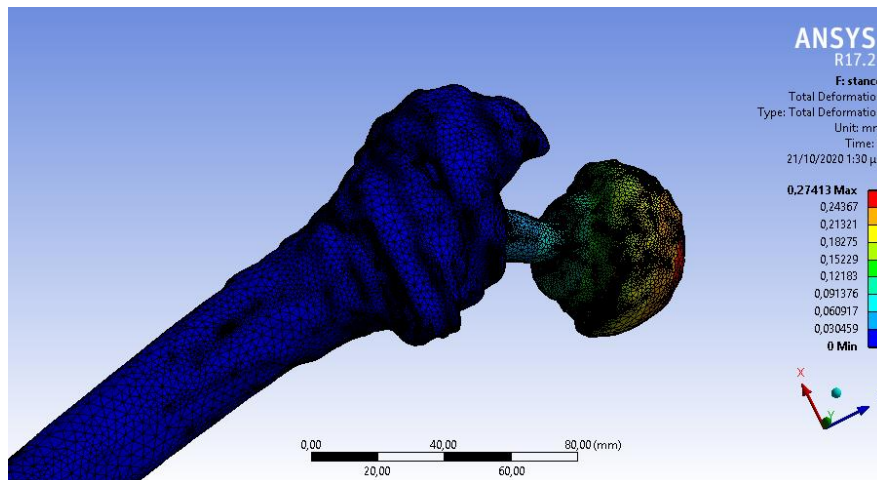
Figure 7-19: Deformation of stance
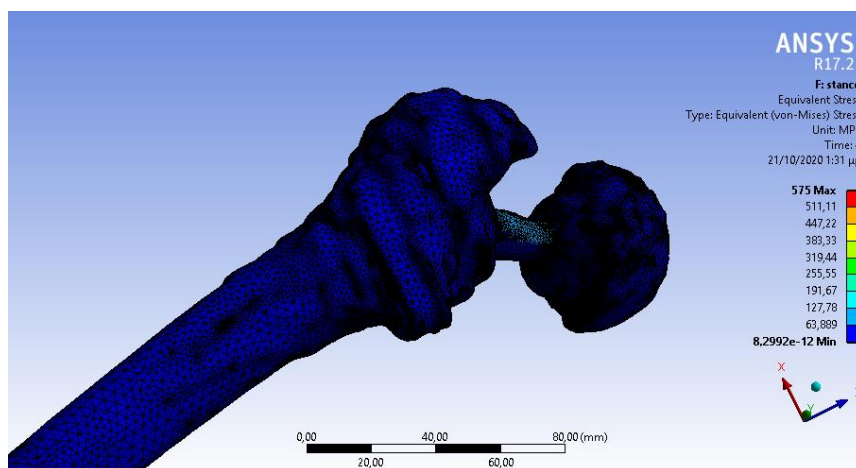
Figure 7-20: Stress of stance
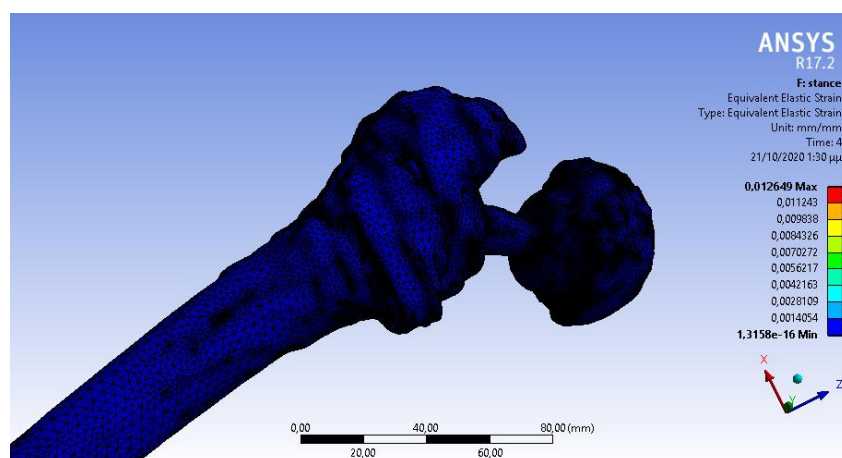
Figure 7-21: Strain of stance

Stance is a daily activity that always applies to the bone-stem system and is hardly to avoid it. However, it is an activity that a patient can do more safely because of the small value of deformation (0.27413 mm), stress (575.00 MPs) and strain (0.012649 mm/mm). It is the second less harmful activity for the bone-stem response, comparing to the activities previously mentioned.

7.8   Results of walking
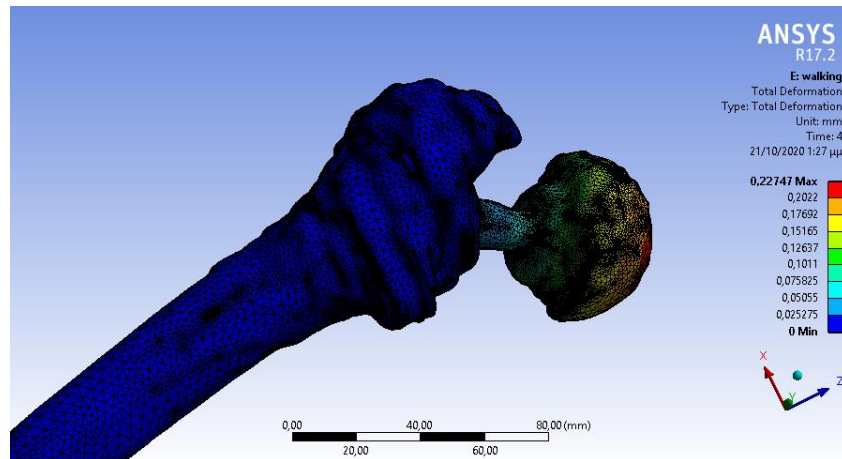
Figure 7-22: Deformation of walking
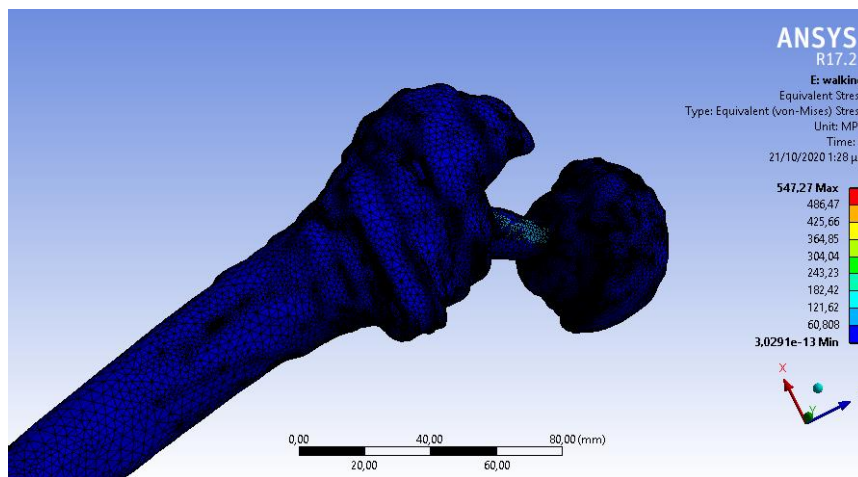
Figure 7-23: Stress of walking
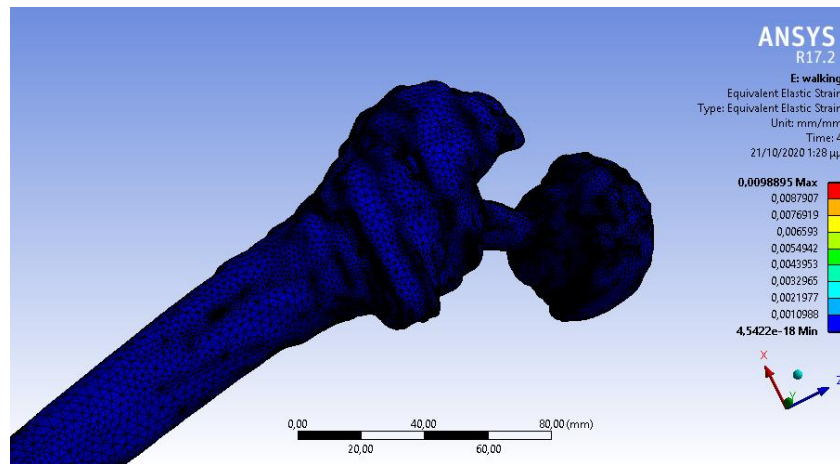
Figure 7-24: Strain of walking

Walking is also an activity like stance that cannot be avoided in daily life. Furthermore, one more similarity with the stance is that it also exerts reduced maximum values of stress (547.27 MPa), strain (0.009889 mm/mm) and deformation (0.22747 mm). These are actually the smallest values that were obtained among all eight activities.

Finally, as it can be seen in table 7.1, maximum displacement of 0.67766 mm was found for sitting activity, while maximum von misses stress distribution of 1348,8 MPa was obtained for the sitting activity, as well. In the case of walking, it was noticed that the examined patient has the minimum stress distribution of 547.27 MPa and this leads to receiving a minimum deformation of 0.22747 mm. A patient with total hip arthroplasty have to be more careful while sitting down, standing up and knee bending than walking and just stance.

Table 7-1: Results of deformation, stress and elastic strain during activities(maximum values)

	Deformation (mm)	Stress (MPa)	Elastic Strain (mm/mm)	Measuring position
Cycling	0.33322	719.46	0.014789	Acetabular
Sitting down	0.67766	1348.80	0.029727	Acetabular
Standing up	0.60037	1148.50	0.025775	Acetabular
Knee bending	0.43812	798.21	0.018906	Acetabular
Walking	0.22747	547.27	0.009889	Acetabular
Stance	0.27413	575.00	0.012649	Acetabular
Stairs up	0.29431	733.60	0.012506	Acetabular
Stairs down	0.23116	580.02	0.009943	Acetabular

8 Discussion

This study investigated the behavior of the hip joint of a patient during daily activities. Especially CT images were taken from a patient who has undergone total hip arthroplasty. The patient was 59 years and 57 kg. After this the geometry of the bone and stem was made by using the appropriate program. When the geometry was ready, finite element method was used, Ansys to simulate eight daily activities, walk, stand up, sit down, stance, knee bend, stairs up, stairs down. The bone model and the prothesis model were introduced exactly as they are placed in the patient according to the CT images. The appropriate properties of the materials were set and the grid of the bone and stem were made. After the boundary conditions were applied: fixed constrain and the other forces at an angle 15° in three dimensions.

After the simulation, results for each activity were obtained. The different values of deformation; stress and strain of these eight daily activities are presented in the graphics below (Figure 8-1, 8-2, 8-3).It is obvious that walking has the smallest deformation and stress while on the other hand sitting down activity has the bigger deformation and stress. The results showed that in the sitting position the change of the acetabular prefix was the biggest. This has to do with the relationship between the spine and the pelvis. It has therefore been shown that depending on how stiff the spine is in a sitting position, because the inclination of the pelvis changes, we may have a dislocation. This happens because along with the pelvis, the orientation of the acetabular changes substantially.
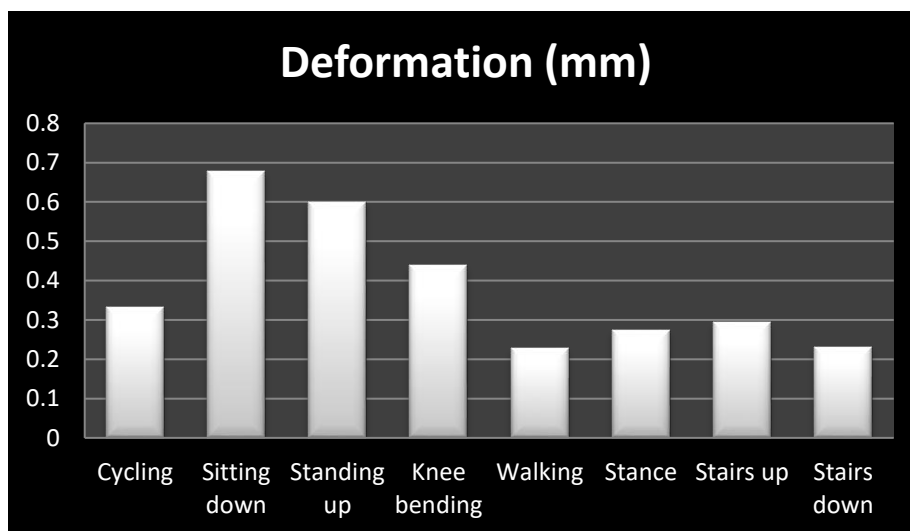
Figure 8-1: Comparative table of deformation of daily activities.
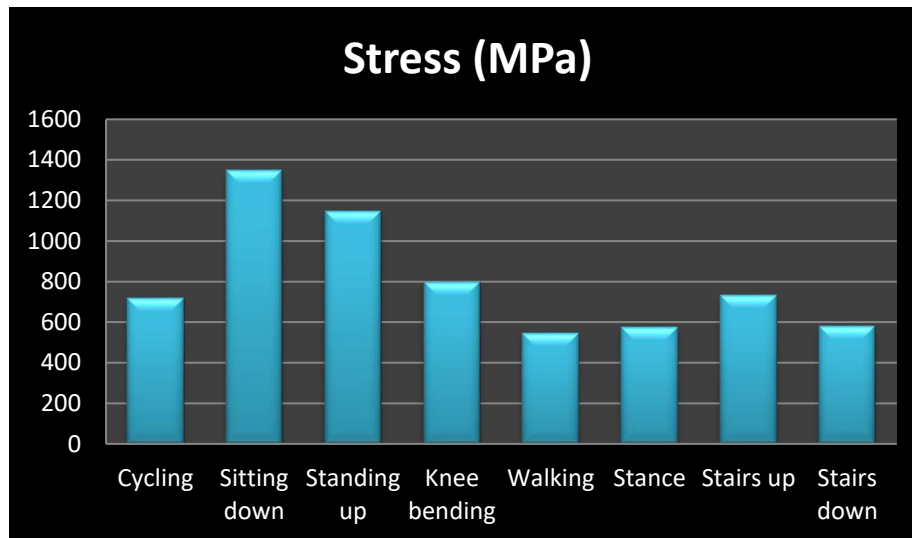
Figure 8-2: Comparative table of stress of daily activities
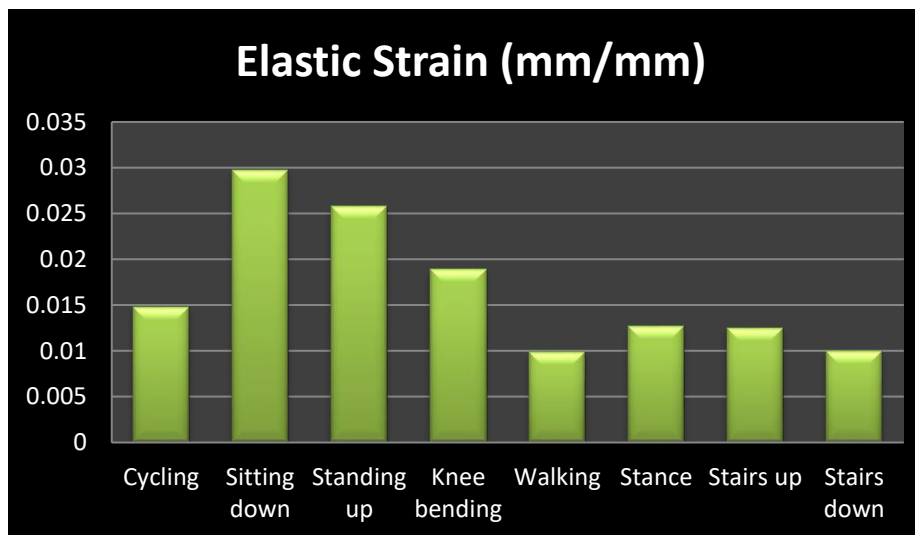
Figure 8-3: Comparative table of strain of daily activities

Moreover, in order to validate the results, a comparison with previously studies has to be done. Especially, in the study, (Chethan,et. al, 2018) femur bone of two humans of different lengths (tall femur and short femur) were subjected to static structural loading conditions to evaluate their load-bearing abilities using Finite Element Analysis. The 3D models of femur bones were developed using MIMICS from the CT scans which were then subjected to static structural analysis by varying the load from 1000N to 8000N. The von Mises stress and deformation were captured to compare the performance of each of the femur bones. The tall femur resulted in reduced Von-Mises stress and total deformation when compared to the short femur. However, the maximum principle stresses showed an increase with an increase in the bone length. In both the femurs, the maximum stresses were observed in the medullary region.

Additionally, in the study (Mishra,et. al, 2011) the three dimensional FE model of femur bone generated from CT data have become interest because of their high Potential in clinical practice. It may be noted that only static load applied on femur. The results depend on the accuracy of FE model with reference to real conditions. This study investigates stress distribution, total deformation and fatigue failure of femur for a weight of 75 Kg male during normal position.

Furthermore, in this analytical study of femur (Chethan,et. al, 2019) circular, oval, ellipse and trapezoidal-shaped stem designs are considered .The load condition of 2300N was applied. The human femur is modeled using Mimics. CATIA V-6 is used to model the implant models. Static structural analysis is carried out using ANSYS R-19 to evaluate the best implant design while walking.

One more study (Andreaus,et. al, 2008) perform finite element investigation of the mechanical behavior of a prosthesized human femur during walking and stair climbing. Such activities are in fact encountered with the highest frequencies during daily living. In order to numerically analyze the stress shielding of the femoral bone with an artificial hip replacement, the strain and stress distributions both in the femur and in the stem were evaluated using the finite element method. From a set of CT images the geometry of the femur was recovered and meshed.

Moreover, in this study (Kumar, et. al, 2015) a three dimensional virtual femur bone is modeled using Solid Edge V19 and the bone is analyzed for hip contact stresses/forces during normal walking, standing, running and jumping activities while load of 705N were applied. The stress analyses were carried out using ANSYS 14.0 in order to investigate the behavior of the femur bone during these activities.

 Last but not least, the loads acting on the hip joint are repetitive and fluctuating depending on the various activities, which may leads to failure of Hip joint. In this study (Zameer,et. al, 2015) analysis of Hip joint model was carried out using finite element software Ansys while brisk walking, normal walking and bending the knee. The load conditions were F=1270N (brisk walking), F=431.9N (normal walking), F=1473N (bending the knee). Stress analysis took place for the hip joint design. The results for stress, strain and deformation of each study are shown below. (Table 8-1, 8-2, 8-3) The outcomes of the present work are in good agreement with other similar studies because both the size range and the vales are very close.

Table 8-1: Deformation in mm for different loading condition

	Type of study / Type of loading	Measuring position	Deformation in mm for different loading conditions							
			Cycling	Sitting down	Standing up	Knee bending	Walking	Stance	Stairs up	Stairs down
This work	Numerical/ sinusoidal	Acetabular	0.33322	0.67766	0.60037	0.43812	0.22747	0.27413	0.29431	0.23116
Chethan K.N[1]	Numerical/ constant	Acetabular	-	-	-	-	0.16031	-	-	-
Chethan K.N[1]	Numerical/ constant	Acetabular	-	-	-	-	2.441	-	-	-
RaJI Nareliya[2]	Numerical/ constant	Acetabular	-	-	-	-	0.23496	-	-	-
Syed Zameer[6]	Numerical/ constant	Acetabular	-	-	-	0.687	1,611	-	1.103	-
Chethan K.N[3]	Numerical/ constant	Acetabular	-	-	-	-	0.24536	-	-	-
Ugo Andreaus [4]	Numerical/ constant	Acetabular	-	-	-	-	0.33	-	0.60	-
Ugo Andreaus[4]	Numerical/ constant	Acetabular	-	-	-	-	0.44	-	0.57	-

Table 8-2: Stress in MPa for different loading conditions

	Type of study / Type of loading	Measuring position	Stress in MPa for different loading conditions							
			Cycling	Sitting down	Standing up	Knee bending	Walking	Stance	Stairs up	Stairs down
This work	Numerical/ sinusoidal	Acetabular	719.46	1348.80	1148.50	798.21	547.27	575.00	733.60	580.02
Chethan K.N[1]	Numerical/ constant	Acetabular	-	-	-	-	218.78	-	-	-
Chethan K.N[1]	Numerical/ constant	Acetabular	-	-	-	-	122.53	-	-	-
RaJI Nareliya[2]	Numerical/ constant	Acetabular	-	-	-	-	310.87	-	-	-
Syed Zameer[6]	Numerical/ constant	Acetabular	-	-	-	21.463	45.485	-	21.054	-
Chethan K.N[3]	Numerical/ constant	Acetabular	-	-	-	-	540.1	-	-	-
Ugo Andreaus [4]	Numerical/ constant	Acetabular	-	-	-	-	21.0	-	33.0	-
Ugo Andreaus[4]	Numerical/ constant	Acetabular	-	-	-	-	31.0	-	44.0	-
Nithin Kumar KC[5]	Numerical/c onstant	Acetabular	-	-	-	-	35.211	28.859	-	-

Table 8-3: Strain in mm/mm for different loading conditions

	Type of study / Type of loading	Measuring position	Strain in mm/mm for different loading conditions							
			Cycling	Sitting down	Standing up	Knee bending	Walking	Stance	Stairs up	Stairs down
This work	Numerical/ sinusoidal	Acetabular	0.014789	0.029727	0.025775	0.018906	0.009889	0.012649	0.012506	0.009943
Chethan K.N[1]	Numerical/ constant	Acetabular	-	-	-	-	0.0029163	-	-	-
Chethan K.N[1]	Numerical/ constant	Acetabular	-	-	-	-	0.0027036	-	-	-
Ugo Andreaus [4]	Numerical/ constant	Acetabular	-	-	-	-	0.00130	-	0.0330	-
Ugo Andreaus [4]	Numerical/ constant	Acetabular	-	-	-	-	0.00120	-	0.0314	-

This work is subjected to specific limitations such as the bone was considered as a linear elastic, isotropic and homogenous medium. In fact, even at the microscopic level, bones have a highly complex internal structure made up of different parts of their structure. Moreover a fixed constraint was considered at the lower surface of the femur (femur-knee surface), this means that the forces at the femur-knee surface don't appear. Furthermore, the examined loading conditions were derived from the literature and the patient specific profile and characteristics have not been considered, as well as the material properties were derived from the literature and do not correspond to the femur material properties of the patient used to develop the 3D geometry.

On the other hand, the novelty of this work compared to the current state of the art is based on the loading conditions that were applied in three dimensions(x, y, z).The forces applied also depend on time specifically related to the loading cycle.

9   Conclusions

The objective of this thesis is the numerical evaluation of the thigh bone's mechanical environment during gait after total hip arthroplasty. Additionally, different loading conditions are evaluated and compared to the numerical findings of gait analysis such as cycling, sitting down, standing up, knee bending, stance, stair up and stair down. The results showed that in the sitting position the change of the acetabular prefix was the biggest. This has to do with the relationship between the spine and the pelvis. It has therefore been shown that depending on how stiff the spine is in a sitting position, because the inclination of the pelvis changes, we may have a dislocation. This happens because along with the pelvis, the orientation of the acetabular changes substantially. So many surgeons where possible do anteroposterior and lateral radiographs of the lumbar spine and below and even do it in a sitting position.

10 Future work

In the future, a numerical evaluation of the effect of different loading conditions during various activities to more patients that have undergone total hip arthroplasty can lead to more accurate conclusions. Finite element analysis of different lengths of stem to a patient that have undergone a total hip arthroplasty is also a good idea for future research. Furthermore, a future work that must take place is actual measurements and finite element analysis to a patient with a total hip arthroplasty bone with loading conditions from gait analysis. Finally, another important issue for future work is to repeat the current work with less limitations adopted in the present effort

Bibliography

❖ Andreaus, U., & Colloca, M. (2008). Mechanical Behaviour of a Prosthesized Human Femur: a Comparative Analysis Between Walking and Stair Climbing By Using the Finite Element Method. Biophysics and Bioengineering Letters, 1(3).

❖ Lunn, D. E., Lampropoulos, A., & Stewart, T. D. (2016). Basic biomechanics of the hip. Orthopaedics and Trauma, 30(3), 239–246.

❖ Kumar, K. C. N., Tandon, T., Silori, P., & Shaikh, A. (2015). Biomechanical Stress Analysis of a Human Femur Bone Using ANSYS. Materials Today: Proceedings, 2(4–5), 2115–2120.

❖ Knight, S. R., Aujla, R., & Biswas, S. P. (2011). 100 Years of Operative History Er Ci Us E on Er Al. Orthopaedic Reviews, 3, 2–4.

❖ Bergmann, G., Bender, A., Dymke, J., Duda, G., & Damm, P. (2016). Standardized loads acting in hip implants. PLoS ONE, 11(5), 1–23.

❖ Chethan, K. N., Shyamasunder Bhat, N., Zuber, M., & Satish Shenoy, B. (2019). Finite element analysis of different hip implant designs along with femur under static loading conditions. Journal of Biomedical Physics and Engineering, 9(5), 507–516.

❖ Howard Community College. (2016). Human Anatomy and Physiology I Laboratory Manual. 187–207.

❖ Burchard, R., Braas, S., Soost, C., Graw, J. A., & Schmitt, J. (2017). Bone preserving level of osteotomy in short-stem total hip arthroplasty does not influence stress shielding dimensions - A comparing finite elements analysis. BMC Musculoskeletal Disorders, 18(1), 1–7.

❖ Origin, E. (2017).Bone. Encyclopaedia Britannica Web, 1–14.

❖ J. Houcke1, V. Khanduja, C. Pattyn1,E. Audenaer. (2018). The History of Biomechanics in Total Hip Arthroplasty. Indian Journal of Orthopaedics.52(may), 161–169.

❖ Nareliya, R., & Kumar, V. (2011). Biomechanical analysis of human femur bone. International Journal of Engineering Science and Technology, 3(4), 3090–3094.

❖ Bennett, D., & Goswami, T. (2008). Finite element analysis of hip stem designs. Materials and Design, 29(1), 45–60.

❖ ANSYS. (2009). Theory Reference for the Mechanical APDL and Mechanical Applications. Knowledge Creation Diffusion Utilization, 3304(April), 724–746.

❖ Abdullah, A. H., Todo, M., & Nakashima, Y. (2017). Prediction of damage formation in hip arthroplasties by finite element analysis using computed tomography images. Medical Engineering and Physics, 44, 8–15.

❖ Baharuddin, M. Y., Salleh, S. H., Zulkifly, A. H., Lee, M. H., Noor, A. M., A Harris, A. R., Majid, N. A., & Abd Kader, A. S. (2014). Design process of cementless femoral stem using a nonlinear three dimensional finite element analysis. BMC Musculoskeletal Disorders, 15(1).

❖ K.N., C., Zuber, M., Bhat N., S., Shenoy B., S., & R. Kini, C. (2019). Static structural analysis of different stem designs used in total hip arthroplasty using finite element method. Heliyon, 5(6), e01767.

❖ Colic, K., Sedmak, A., Grbovic, A., Tatic, U., Sedmak, S., & Djordjevic, B. (2016). Finite element modeling of hip implant static loading. Procedia Engineering, 149(June), 257–262.

❖ Etchels, L., Wang, L., Al-Hajjar, M., Williams, S., Thompson, J., Isaac, G., Wilcox, R., & Jones, A. (2019). Computationally efficient modelling of hip replacement separation due to small mismatches in component centres of rotation. Journal of Biomechanics, 95, 109296.

❖ https:/www.ansys.com

❖ States, U. (2019). Common Causes of Hip Pain. Common Causes of Hip Pain, 1–14.

❖ Smyris, A. F., Potsika, V. T., Farmakis, I. I. K., Tachos, N., Fotiadis, D. I., Xenakis, T. A., & Pakos, E. E. (2019). The effect of the hip joint endoprosthesis length after a total hip arthroplasty: A biomechanical study. Journal of Orthopaedics, Trauma and Rehabilitation, 26(1), 61–66.

❖ Saputra, E., Anwar, I. B., Jamari, J., & Van Der Heide, E. (2013). Finite element analysis of artificial hip joint movement during human activities. Procedia Engineering, 68, 102–108.

❖ Merola, M., & Affatato, S. (2019). Materials for hip prostheses: A review of wear and loading considerations. Materials, 12(3).

❖ Chethan K.N., Mohammad Z., Shyamasunder Bhat N., Satish Shenoy B.,[a,*] an Chandrakant R. i (2019). Static structural analysis of different stem designs used in total hip arthroplasty using finite element method. Heylion.5(6)

❖ Raju V., Mayank C., Abhishek V.(2013). Bone cement. J Clin Orthop Trauma. 4(4).157–163.

❖ Zameer, S., & Haneef, M. (2015). Fatigue Life Estimation of Artificial Hip Joint Model Using Finite Element Method. Materials Today: Proceedings, 2(4–5), 2137–2145.

❖ Beer, F., Johnston, & McGraw, D. (1992). Mechanics of materials. McGraw-Hill. 978-0-07-338028-5.

❖ Enderle, J., Bronzino, J., & Blanchard, S. M. (2005). Introduction to Biomedical Engineering. Academic Press. 9780080473147.

❖ Maquet, P. G., & AywailleBelgium. (1985). Biomechanics of the Hip. Springer-Verlag Berlin Heidelberg. 978-3-642-50960-5

❖ Kojic, M., & Filipovic, N. (2008). Computer Modeling in Bioengineering.Jour.1(446)

❖ Rapp, B. E. (2017). Microfluidics: Modelling, Mechanics and Mathematics.Elsivier. 978-1-4557-3141-1

❖ Kapandji, A. (2010). The physiology of the joints. Churchill Livingstone. 9781455725205

❖ Γούλας Δ. (2005). Εισαγωγή στην εμβιομηχανική Γλωσσάρι εμβιομηχανικής. Κλειδαριθμο.

❖ Δ. Μακρής. (1967).Η ιστορία και η εξέλιξη της ολικής αρθροπλαστικής του ισχίου. Η ιατρική σήμερα . 35–38

❖ Ε. Δ. Κατρίτση, Α. Κελέκη. (1387). Στοιχεία φυσιολογίας. Ίδρυμα Ευγενίδου. 978-960-337-072-7.259